FORENSIC APPLICATIONS OF ASSOCIATING HUMAN SCALP HAIR MORPHOLOGY AND PIGMENTATION ANALYSIS AT THE MICROSCOPIC AND MOLECULAR LEVEL

by

Wesli Kay Stubbs

A Thesis

Submitted to the Faculty of Purdue University

In Partial Fulfillment of the Requirements for the degree of

Master of Science

Department of Forensic and Investigative Science

Indianapolis, Indiana

August 2017

THE PURDUE UNIVERSITY GRADUATE SCHOOL
STATEMENT OF COMMITTEE APPROVAL

Dr. Susan Walsh, Chair
Department of Biology
Dr. Nicholas Berbari
Department of Biology
Dr. Christine Picard
Department of Biology

Approved by:
Dr. John Goodpaster
Head of the Graduate Program

Dedicated to my parents, my two amazing sisters, and my best friend Chelsea. Without your support none of this would have been possible.

TABLE OF CONTENTS

LIST OF TABLES

LIST OF FIGURES

LIST OF SYMBOLS

SNP - Single Nucleotide Polymorphism

CODIS - Combined DNA Index System

GWAS - Genome Wide Association Studies

°C - Degree Celsius

® - Registered

™ - Trademark

ng- nanogram

uL- microliter

Rpm- rotations per minute

qRT-PCR- Quantitative Real-Time Polymerase Chain Reaction

RFU- Relative Fluorescence Unit

HKG- Housekeeping gene

ABSTRACT

Author: Stubbs, Wesli Kay. MS
Institution: Purdue University
Degree Received: August 2017
Title: Forensic Applications of Associating Human Scalp Hair Morphology and Pigmentation Analysis at the Microscopic and Molecular Level
Major Professor: Susan Walsh

Criminal investigation and the science behind evidence analysis is an ever-growing niche, and forensic DNA phenotyping (FDP) is no exception. For years the only information given to authorities regarding DNA found at a crime scene was STR analysis and matching to a comparative DNA sample from a known source. However, what happens when there is no suspect to compare DNA profiles, or the case involves a missing person where the only available piece of evidence is a biological sample found at the scene? Before FDP, not much could be done with the DNA sample and the investigation would be stalled. Now it is becoming possible to statistically predict an individual's visual characteristics using FDP. Currently, with the use of Irisplex, HIrisplex, and HIrisplex-S, statistical analyses and predictions can be done for categorical eye, hair, and skin color by looking at specific genes and their associative SNPs, such as *HERC2* and *OCA2.* The more that is understood about trait-determining genes and their functional significance with regards to our physical traits, the more phenotypes can be added to these prediction tools.

In an effort to discover additional genes associated with human phenotypes, this study looked at thirty-two pigmentation-associated candidate genes, and eleven hair structure and morphology associated genes in owl monkey pelage samples. Although the samples were not of human origin, it is important to point out the high conservation between humans and their non-human primate relatives. The owl monkeys used in this study were helpful for tracking expression levels of genes controlling different pigmentation and hair structure types, because each monkey had intra-individual variation in thickness and in coat color which allowed the generation of potential candidate genes for human investigation. Of the 43 total candidate genes analyzed, 36

had successful amplification, and 28 showed a significant difference in expression when comparing the different samples.

The second part of this study was to compare quantitative characteristics of human hair in physical samples and two-dimensional (2D) photos. A test set of 45 individuals had 3-5 hairs from the vertex of their head plucked and analyzed, and a 2D photograph was taken of their scalp hair. The idea was to be able to make quantitative phenotypes in hair (such as hair width, amount of curl) from 2D imagery, when physical samples are not available for analysis. This is due to the fact that the majority of genotype-phenotype databases consist solely of photographic imagery, and seldom have hairs that can be microscopically prepared for analysis. Defining measurable phenotypes from 2D photos that strongly correlate with their physical counterparts allow for the generation of a more accurate phenotype for future genome wide association studies (GWAS) within and outside this laboratory that study hair thickness and hair curl. Three different quantitative phenotypes were compared between the microscopic and 2D photo-analysis.

CHAPTER 1. INTRODUCTION

1.1 Purpose and Goals of this Research

Traditionally during an investigation, DNA analysis uses STRs (short tandem repeats) to compare an individual to an evidentiary DNA sample [1]. STR analysis has been the primary form of DNA analysis in crime scene investigation for the past three decades [2]. However, when this analysis fails to match the unknown DNA profile to an individual, a different approach needs to be available for use in order to gather any relevant information from the DNA collected from a crime scene. With the ability to use DNA phenotyping, it is possible to statistically predict certain physical characteristics of the person that the DNA originated from [3]. Although using this type of analysis cannot link the DNA to any one person, it can be used as a 'biological witness' by providing the analysts and investigators with an individual's most statistically probable physical appearance profile [3]. To predict the physical features of an individual using a DNA sample, knowing which genes correlate to specific physical traits is imperative; however, this is not a trivial task due to the enormous complexity in genotype-phenotype connections. Phenotypes are not the results of a single gene, but multiple genes interacting in a compounding manner to influence a specific trait. This makes it harder to pin point which genes interact with each other to give rise to a specific phenotype. An example would be understanding the myriad of genes that control hair pigmentation and morphology which would lead to the possibility of predicting the type of hair a person, whose DNA sample was found at a crime scene, has. Current phenotyping research is also being done on skin and eye pigmentation [3, 4]. As of right now, the only method for predicting hair morphology is on a categorical scale (straight, wavy, or curly). The problem with this method is, even if the group of genes that control hair morphology are studied, reviewed, and put into a prediction model, it still leaves a lot of ambiguity as to how curly or straight the individual's hair actually is. This ambiguity can by fixed by using quantitative values that capture the complex nature of the trait instead of using simple categorical terms, such as straight, wavy, or curly.

The first part of this thesis investigates the expression of a candidate list of genes in non-human primates, more precisely, owl monkeys (*Aotus Nancymaae*). Owl monkeys are a nocturnal genus of primates that are native to much of tropical South America that have different pelage color depending on the body region of the monkey [5]. As seen in Figure 1.1, owl monkeys have an orange belly, a striated brown/gray back, and the distal portion of the tail is completely black.

Figure 1.1: The Aotus Nancymaae owl monkey. This species can be found in the Rio Amazonas

Although forensic DNA phenotyping pertains primarily to humans, it is important to note that much of the research on the genotype-phenotype relationship between complex genes is often performed on non-human primates, such as macaques, orangutans, and the owl monkey [6]. Using non-human primates, such as the owl monkey, that have different hair colors allows us to compare intra-individual variation in gene expression related to pigmentation genes. Bradley *et al* (2012) analyzed seven different key pigmentation genes in non-human primates based on the fact that the gene and its function are conserved in melanin deposition in humans [7]. There are nine owl monkeys in our collection, with RNA sequencing having been performed on four of the monkeys to create a candidate list of genes, which was produced using bioinformatic approaches outside the scope of this thesis. From here, the aim was to confirm the differential gene expression patterns on the other five monkeys in our collection using quantitative real-time polymerase chain reaction (qRT-PCR) analysis. By doing this, it can be visualized whether any/all of the thirty-two candidate genes are truly differentially expressed in hair with lighter/darker pigmentation within this particular primate species.

This study also examined the use of quantitative morphological methods to measure the owl monkey hair at the microscopic level to assess the physical variation found in the formation of the hair follicle and its pigment distribution. This would help define phenotypes that may correlate with the gene expression values seen in the owl monkey, thus enabling the development of hypotheses as to why both humans and non-human primates differ/are similar at the phenotypic and genotypic level. Due to the fact that hair color is usually associated with hair thickness [8], the comparison of hair colors within the owl monkey led to the comparison of hair structure and hair shaft thickness at different parts of the owl monkey's back, belly, and tail.

During an additional bioinformatics search on the same four owl monkey samples that underwent RNA-sequencing, another candidate list was proposed that focused on hair thickness between the three regions/colors within the owl monkeys analyzed. Again, qRT-PCR was used to confirm the gene expression of the candidate list of 11 genes associated with hair thickness in the remaining owl monkeys. It is envisioned that the laboratory will also perform a similar check on these confirmed hair structural candidate genes in human hair samples in the future.

The second part this thesis specifically focused on human scalp hair follicles and their morphological structure. In this section hair phenotypes (such as the amount of curl and thickness of hair) are defined in a subset of 45 individuals, and all quantifiable measurements are linked to photos taken of the same individuals who gave hair samples. The goal was to use this test set to optimize the structural categories that are possible through imagery alone as the majority of genotype-phenotype databases simply consist of hair images. Therefore the ability to gain quantifiable information from these images would be a significant advantage in future genome wide association studies (GWAS) performed by the laboratory. Hair curliness is theorized to be linked to the individual's ancestry as well as hair thickness [9]. Having the ability to link quantifiable measurements using microscopy practices to physical photos of the individual's hair will further examine this theory.

1.2 The Owl Monkey

Owl monkeys, also referred to as night monkeys, are the only nocturnal primates found in the New World [10]. A notable characteristic of this genus is the large size of their eyes which have evolved as an adaption to their nocturnal lifestyle [11]. Although there is an ongoing dispute about the speciation of the *Aotus* genus, there are currently ten recognized species of owl monkeys within the genus that are split into two major groups:

the gray-necked which are found North of the Amazon River (*A. lemurinus* and its subspecies, *A. hershkovitzi, A. trivirgatus, and A. vociferans*) and the red-necked which are found South of the river (*A. miconax, A. nancymaae, A. nigriceps, A. azarae* and its subspecies) [11].

1.2.1 Owl Monkey Morphology

Aside from having either gray or red fur on the sides of their necks, the Aotus genus has a common pelage coloring across all species and subspecies [12]. They have pale orange pelage on their bellies and underside of arms and legs, light gray/white markings around their eyes, their backs are band with light to dark brown as well as gray and orange colored fur, and the distal part of their tail ranges from dark brown to black. Depending on the location and the color of the hair, the owl monkeys coat ranges in thickness and density. The region of which a specific species of owl monkey lives also plays a factor as to how thick their coat is, with those living in high altitudes having thicker coats [11].

This intra-individual variation in the owl monkey's pelage makes them the perfect non-human model to analyze gene expression in genes that are known to play a part in hair pigmentation, particularly as the pelage also displays both eumelanin and pheomelanin characteristics as described in the next section, that mirror the composition and variation of human hair color. This model animal also allows us to compare expression results to those of the concurrent human study on gene expression on hair pigment genes.

1.3 Pigmentation and Melanogenesis in Humans

To better understand why certain candidate genes were chosen to track for expression in hair samples that varied in pigment; it is important to know what melanogenesis is and how it works. Melanogenesis is the process of which pigment producing cells, called melanocytes, create and store pigment molecules known as melanin in lysosome-like organelles called melanosomes. Melanocytes are found throughout the skin, hair, eyes, inner ear, bones, heart, and brain [13], and require specific proteins to mature and catalyze melanogenesis. Tyrosinase (TYR) and Tyrosinase-related Protein 1 (TYRP1) are examples of two proteins that affect the quality and amount of melanin that is created in the melanocytes. Other proteins, such as PMEL17 and OCA2 are important in the sorting and distribution of the melanosomes, and therefore the distribution of melanin [14]. Melanocytes are located in the basal layer of the epidermis next to a cluster of keratinocytes. When enough melanin has been formed and stored inside the melanosomes, they are distributed among the neighboring keratinocytes via the dendrites of the melanocytes. Figure 1.2 below shows a melanocyte located in the middle of a cluster of keratinocytes in the basal layer of the epidermis.

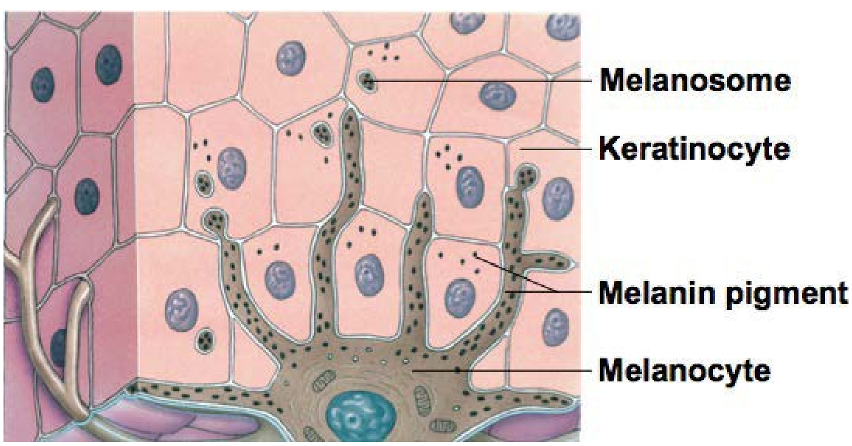

Figure 1.2: A melanocyte transferring melanin pigment granules to the neighboring keratinocytes via its dendrites. Image adapted from http://www.lephysique.com/prevent-sunburns-easily/

There are two types of melanin that can be synthesized in a melanocyte: eumelanin and pheomelanin; eumelanin are the larger, brown-black pigment granules where tyrosine is synthesized to L-dopachrome, and pheomelanin are the smaller, yellow- red pigment granules whose synthesis are dependent on the amount of cysteine in the cell [15]. Eumelanin is the major pigment type found in individuals with darker skin, hair, and eye color, while individuals who predominately have pheomelanin tend to have much lighter skin and red hair [13]. Of course, individuals do not have just one type of pigment or the other; they have a combination of both. It is this ratio of light to dark melanin that controls the color of an individual's skin, eye, and hair color.

1.4 Biology of Hair: Stages of Growth and Morphology

There are three distinct layers in the shaft of a human hair: the cuticle, cortex, and medulla. The cuticle is the outermost layer of the hair and has a scale pattern that makes it distinct from other animals [16]. Humans have an imbricate (flattened) scale pattern, while other hair bearing animals have a myriad of other patterns such as coronal (crown-like) and spinous. The cortex, or middle layer, is where the pigment granules are found. Hair color is dependent on the type and density of melanin cells found in the cortex [17]. During melanogenesis, the melanocytes are moved to keratinocytes that are found in the cortex. The medulla is found at the very center of the hair shaft. The ratio of medulla diameter to hair shaft diameter is called the medullary index (MI), and is typically found to be much smaller in humans at less than ¼ versus other animals at around ½ [18]. Even more perplexing is that often the medulla is completely absent or nearly invisible in human hair. There is still speculation as to the primary function of the medulla [19]. Figure 1.3 below shows the different layers of a hair.

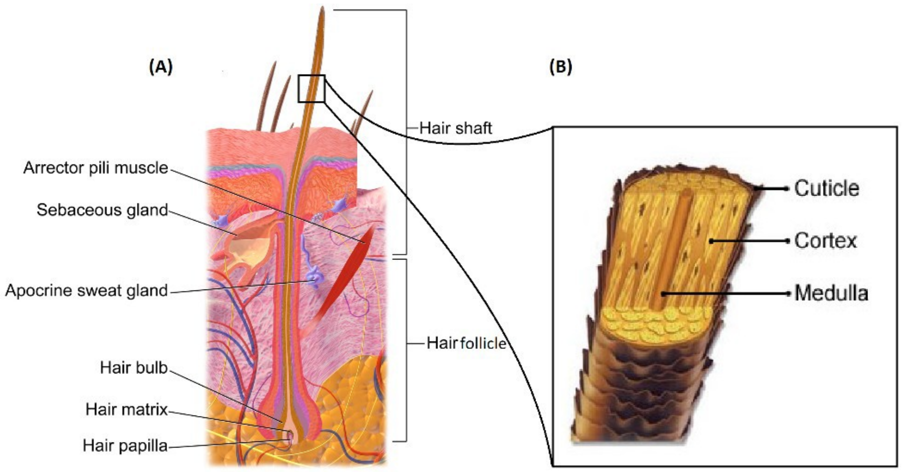

Figure 1.3: (a) The various parts of the hair and surrounding structures in the dermal layer of skin. (b) The three layers found within the hair shaft. Image adapted from http://www.peoples.bm/blog/anatomy-hair/

Human hair goes through four stages of growth in its lifetime. The first phase in the hair life cycle is the anagen phase, or “growth” phase. This phase lasts between 2-6 years and it is during this time that melanogenesis occurs in the hair [20]. During anagen, active melanocytes found in the hair bulb transfer pigment granules to neighboring pre-cortical keratinocytes that move into the shaft and become the main cells of the cortex. [21]. The next phase in the hair cycle is the catagen phase, which lasts about ten days and is when the hair’s growth stops and the follicle starts to separate from the dermal papilla. During this time, melanogenesis is also turned off [20]. The third stage is the telogen phase which lasts two to three months. During this phase, the follicle becomes completely detached from the dermal papilla, making room for a new hair to form. The last phase of a hair’s life cycle is exogen, which is the shedding phase. This is when hair sheds naturally. As exogen occurs the follicle refreshes and returns to the anagen stage with a new hair. When taking human hair samples for this study, hairs pulled that were found to be in the anagen phase were used for this study. This is because these hairs are in the height of growth and melanogenesis occurs in this stage.

1.5 Pigmentation Analysis

Coat color variation and the genes that control them are a very prominent aspect of phenotypic diversity within and among different mammalian species. With this in mind, previous studies have looked at different variations in primate pelage as well as rodent pelage [7, 22, 23] in order to try and pin point which genes are responsible for the different variations in coat coloring within a taxa.

One such paper that focuses on pelage pigmentation in rodents is the Steiner *et al* (2007) study that focused on the relative gene expression levels of *MC1R* and *Agouti* using qRT-PCR in two subspecies of the *P. polionotus* mouse. Each subspecies had a different wild-type coat color; *P.p. leucocephalus (*beach mouse) had white, while *P.p. subgriseus* (mainland mouse) had brown. Also included was the sister species *P. maniculatus* (deer mouse) that also had brown pigmentation to see if expression patterns of both genes are derived or ancestral [22].

Their results showed that *Agouti* expression was upexpressed in tissues from beach mice (white coat color) than in mainland mice (brown coat color) or in deer mice (the ancestral relative also having brown pigmented fur). The expression of *Agouti* being lower in both mainland and deer mice show that the difference in expression is derived and not ancestral. The *MC1R* gene did not show any significant difference in expression levels in any of the tissue samples from all three species. Figure 1.4 below shows the expression levels of both the *Agouti* and *MC1R* qRT-PCR data.

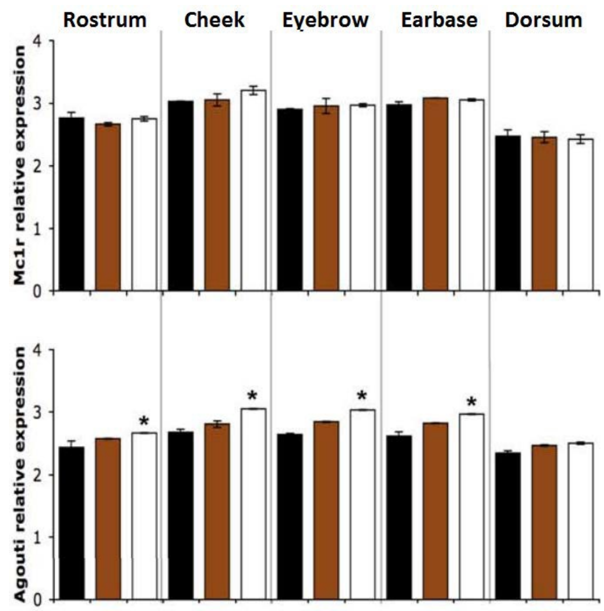

Figure 1.4: qRT-PCR Expression levels of MC1R and Agouti in beach mouse (white), mainland mouse (brown) and deer mouse (black). A * denotes significant difference in expression. The five difference sections are different areas on the mice that tissue samples were taken. Image adapted from Steiner et al paper [8].

Other studies such as the Bradley *et al* and Manceau *et al* studies [7, 22] have tracked the expression levels of the *Agouti* gene in both rodents and non-human primates. *Agouti* has shown to cause melanocytes to synthesize pheomelanin and in turn cause a lighter pigmentation. *MC1R*'s function in melanogenesis has been extensively studied in rodents, non-human primates, and humans [7, 23, 24]. The fact that this particular gene has been conserved across multiple species, and even more so between humans and non-human primates, shows why it is so relevant to test these genes in animals prior to testing in humans. This high conservation allows us to use animal models when human samples are not available and reliably correlate the results of these genes to their human homolog.

There has not been much analysis of comparative gene expression in non-human primate pelage; however, a study performed by Bradley et al (2012) focused on the relative gene expression levels of *MITF, MC1R, MGRN1, ATRN, SLC24A5, TYRP1,* and

DCT using qRT-PCR in different pigmented pelage samples in rhesus macaques (*Macaca mulatta*) [7]. They found no significant difference in the level of expression between light, medium, and dark hair colors in any of these target genes to conclude that they do not have a significant effect on the amount of hair pigmentation in the macaques. The relative expression levels of these genes can be seen in Fig 1.5. All P values for each gene were estimated using the $2^{-\Delta\Delta C_T}$ method and ranged: 0.13–0.98. The final results for this study indicated that coat color variation was not due to expression differences in these seven target genes. This study also used the $2^{-\Delta\Delta C_T}$ method using the samples plucked from the Tail region (dark pigmentation) as the reference sample. This method allowed us to set the other two samples (light and medium pigmentation) fold change relative to the tail samples.

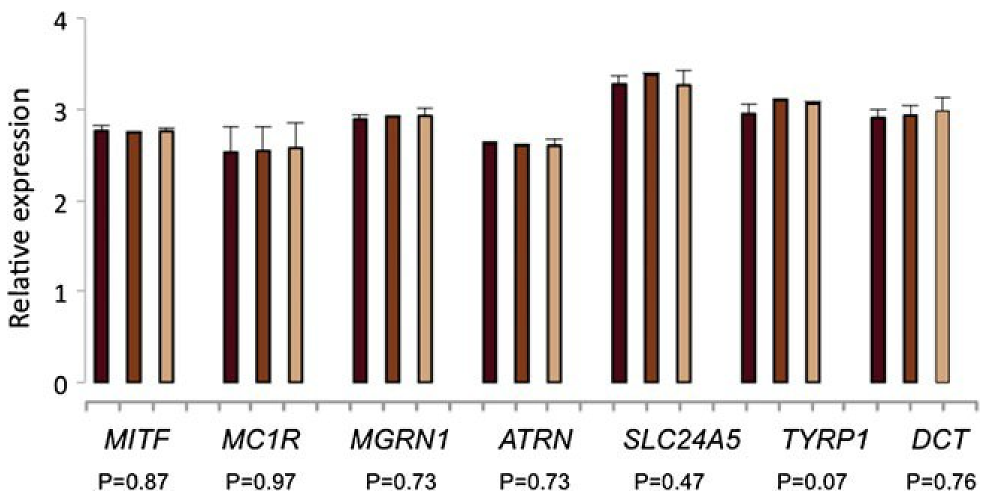

Figure 1.5 Relative expression of candidate genes in dark (black bars), intermediate (light brown bars), and light (white bars) hair tufts from rhesus macaques. Relative expression values are based on qRT-PCR data, normalized with beta-actin and calculated following Steiner et al. study [7].

Something particularly notable about the Bradley et al (2012) study is that they had a gene of interest that failed to amplify during qRT-PCR. The gene in question that they could not get quantifiable PCR results for was *ASIP*, agouti signaling protein, gene.

It was stated that this failure could be due to custom primer design and PCR conditions, or that the expression levels of the *ASIP* gene was too low to quantify in the hair samples that they used. This shows there can be difficulty in designing the right area within the gene of interest to create a custom qRT-PCR primer/probe set with the right conditions to give quantifiable results. Following in the steps of Bradley *et al* (2012), this part of the research focuses on the difference in expression in genes that can be associated with hair pigmentation.

To fully study melanogenesis and the genes that are associated with this process, a candidate list was provided using RNA sequencing data that was aligned to the human transcriptome due to the absence of a published and reliable owl monkey genome. Candidate genes that showed significant difference in expression between the three body regions: head, back, and tail, of the owl monkey was produced from the analysis of 4 owl monkeys.

Table 1.1: Candidate Genes for Pigmentation Analysis. Gray genes are up-expressed in tail, orange genes are up-expressed in belly

GPR143	**TRPM1**	**KIT**	**KITLG**	**MLANA**	**PLXNC1**	**TMEM50B**	**SLC2A8**
VAT1L	**SLC16A9**	**SLC30A1**	**SLC7A5**	**SLC6A14**	**SLC16A1**	**PMEL**	**TYR**
TYRP1	**MIR29B2**	**TMEM139**	**C19orf44**	**SLC25A23**	**BCORL1**	**PPFIBP1**	**IRF2**
SLIT3	**SNX1**	**IRF2BP2**	**C10orf11**	**PLXNB1**	**VAMP2**	**SLC1A2**	**SLC43A2**

The RNA-sequencing data not only generated a candidate list of genes to test for pelage pigmentation, but also the level of expression patterns in the three body regions. As seen in Table 1.1, 17 genes on the candidate list have been bioinformatically hypothesized to have increased expression in the tail/dark hairs compared to the back/brown and belly/orange hairs. The other 15 genes have been bioinformatically hypothesized to have higher expression in the back and belly samples compared to the tail.

Many of these genes have been previously studied and play a role in pigmentation in hair in other species of animals and humans. For example, Tyrosinase (*TYR)*, Tyrosinase Related Protein 1 (*TYRP1)*, Transient receptor potential cation channel subfamily M member 1 (*TRPM1)*, G Protein-coupled receptor 143 (*GPR143)*, Pre-melanosome protein *(PMEL)*, KIT proto-oncogene receptor tyrosine kinase (*KIT)*, KIT Ligand *(KITLG)*, Plexin C1 (*PLXNC1)*, and Solute Carrier Family 16 Member 1 (*SLC16A1)* have been previously associated with pigmentation and the melanogenesis pathway. *TYR* is one of the most important enzymes in the melanogenesis pathway, whose disruption can cause loss of pigmentation and silenced mutation can cause albinism. *TYR* and its stabilizing chaperone-like protein, Tyrosinase Related Protein 1 (*TYRP1)*, work to hydroxylate tyrosine to L-3,4-dihydroxyphenylalanine (*DOPA)* which is then converted DOPAquinone [25]. *TRPM1* encodes for a cation channel expressed in melanosomes [26]. *GPR143* is involved in intracellular signal transduction and that is activated by L-DOPA and functions in the pigmentation pathway [27]. *PMEL* is a melanocyte-specific transmembrane glycoprotein, and has been previously been associated with silver pelage in mice [28]. *KIT* is a transmembrane tyrosine kinase receptor has been shown to be allelic with the white spotting locus on mice[29], and *KITLG* controls the survival of *KIT* expressing melanocytes by regulating melanin migration, melanocyte proliferation, and differentiation as well as activates keratinocytes to produce promelanogenic factors [30, 31]. *PLXNC1* is a *SEMA7A* receptor which regulates dendrite extension in melanocytes [32]. A previous study also showed that *PLXNC1* was upregulated in individuals with graying hair compared to those who had dark brown hair [33]. Although its function in the pigmentation pathway is not fully clear, *SLC16A1* has previously shown to be down regulated in chickens with lighter plumage compared to those with darker [34]. The function of *MLANA* isn’t completely clear, however, it has been widely studied and has been associated as a melanoma-specific antigen and a melanosome-specific marker [35]. *SLC16A9* is in the same family as *SLC16A1* and can have a similar association with melanogenesis as *SLC16A1*. Solute carrier family 2 (facilitated glucose transporter), member 8 (*SLC2A8*) belongs to the solute carrier 2 family and is a glucose transporter with an unusual and still researched tissue-specific gene expression [36]. *SLC30A1* is a zinc transporter, *SLC7A5* is a glycoprotein associated amino acid transporter, *SLC6A14* is a sodium and chlorine dependent neurotransmitter symporter, *SLC34A2* is a type-II sodium/hydrogen phosphate co-transporter, and *SLC1A2* is a glutamate and neutral amino-acid transporter [37]. Upregulation in *SLC1A2* has been associated cytotoxic damage to neurons. This association was found in patients with schizophrenia [38]. Transmembrane Protein 139 (*TMEM139)* is proposed to be involved in intracellular kidney anion exchanger 1 trafficking [39], however its role in the pathway of melanogenesis is still unknown. Chromosome 6 open reading frame 11 (*C10orf11)* is a melanocyte differentiation gene localized in melanoblasts. A previous study showed that a mutation in *C10orf11* causes albinism in humans [40]. Interferon Regulatory Factor 2 (*IRF2*) has not been extensively studied, however, it belongs to the same family as Interferon Regulatory Factor 4 (*IRF4)* has been investigated in pigmentation. Downregulation of *IRF4* has shown to be associated with lighter hair colors [41]. Although not seen in the pigmentation pathway, a previous study has shown mice lacking the Slit Guidance Ligand 3 (*SLIT3)* gene developed congenital diaphragmatic hernia, which causes mortality in infants. *SLIT3* is predominately expressed is the mesothelium during embryonic development [42]. *SNX1* functions as an endosome to Golgi-apparatus transporter [43]. *VAMP2* is associated with vesicle docking and fusion. MicroRNA 29b-2 (*MIR29B2*) functions as a tumor suppressor and induces apoptosis [44]. Transmembrane protein 50b (*TMEM50B)* is an intracellular membrane protein expressed in the brain during development and has been shown to over-express during cerebellar development in mice models with Down syndrome [45]. Not much is known about Vesicle Amine Transport Protein 1 Like (*VAT1L)* except for that it has been proposed to participate in the oxidation reduction process [46]. Solute Carrier Family 25 member 23 (SLC25A23) has not been extensively studied, but its paralog *SLC25A25* functions to catalyze the electroneutral exchange of adenine nucleotides [47]. BCL6 corepressor like 1 (*BCORL1)* is involved in the repression of E- cadherin, a known CtBP target, however its full function in repression is yet to be known [48]. Interferon Regulatory Factor 2 Binding Protein 2 *(IRF2BP2)* interacts with the C-terminal of *IRF*-2 and is a co-repressor with IRF2BP1, however its full biological function is still unknown [49].

1.6 Hair Structure Analysis

Hair morphology is one of the most distinct physical traits among human populations [50]. Among the European population alone, approximately 45% individuals have straight hair, 40% have wavy hair, and 15% have curly hair [9]. The problem, however, is that there has not been a significant amount of research performed to clarify exactly which genes control the different types of hair morphology, particularly quantitative measures of morphology. Between human populations, there have been a few genes that stand out, such as the *EDAR* and *FGFR2* genes associated with thick, straight hair in Asian populations [51]. However, the research for determining the expression levels of known hair morphology associated genes between individuals with straight, wavy, or curly hair in European populations is still very novel. Previous studies have focused on the macro- and microscopic differences in hair structure and morphology, such as diameter, shape of cross-section, and level of moisture [52, 53]. While understanding the physical differences between individual's hair morphology is important, this part of the study focuses more on the molecular differences in genes that can be associated with hair structure and morphogenesis.

One such gene of interest is the Trichohyalin (*TCHH*) gene. *TCHH* is expressed in the inner root sheath of the hair follicle and parallels the distribution of the EDAR variant in Asian populations. It functions as an intermediate filament protein between the inner root sheath and cortex of the hair shaft during the anagen phase [54]. It forms multiple crosslinks with itself and other structural proteins, such as keratin intermediate filaments, to give strength to the hair [55]. Medland et al (2009) performed a GWAS study that found *TCHH* to account for approximately 6% of variance in hair morphology in Europeans [56]. With *TCHH* displaying 6% variance within European populations, qRT-PCR analysis was performed to track gene expression with samples of different hair thickness and morphology.

When microscopically analyzing the owl monkey hairs, it was determined that the tail/dark hairs were significantly thicker in diameter than the orange/belly hairs. Concurrent RNA-sequencing data analysis performed on the same owl monkey samples by the laboratory highlighted several genes that showed significant gene expression differences depending on the location and thickness of the hairs. To propose novel candidate genes for hair structure association investigation in humans beyond those mentioned in the previous paragraph, qRT-PCR analysis was performed on the hair structure candidate gene list on additional owl monkey samples to confirm their significance. These genes are: Caspase 14 (*CASP14),* Cytoskeleton Associated Protein 4 (*CKAP4),* Calponin 1 (*CNN1),* Keratin 8 *(KRT8),* Keratin 32 *(KRT32),* Keratin 73 *(KRT73),* Keratin 78 *(KRT78),* RAS oncogene family member 29 *(RAB29),* Serine Proteinase Inhibitor Clade B Member 7 *(SERPINB7),* and Solute Carrier family 7 member 11 (*SLC7A11). CASP14* is found in keratinocytes but its true function between keratinocytes and the epidermis or hair follicle is still unknown [57]. *CKAP4*, otherwise known as *p63*, is a protein transporter between the rough endoplasmic reticulum and the Golgi apparatus [58]. *CNN1* is an actin filament- associated regulatory protein and shown to be up-regulated in smooth muscle tissues during development [59]. *KRT8* and *KRT78* are type II epithelial keratins that form filaments in epithelial cells and plays a role in maintaining cell structure [60]. *KRT32* and *KRT73* are type I hair keratins that are expressed in the inner root sheath of hair follicles and are responsible for the structural integrity of the hair [61]. *RAB29* is co-located with *TYRP1* and is hypothesized to be involved in the intracellular transport of the *TYRP1* protein [62]. *SERPINB7* participates in tissue integrity by maintaining extracellular matrix homeostasis and loss of expression is hypothesized to lead to loss of cell adhesion and integrity [63]. Lastly *SLC7A11* is a major genetic regulator of pheomelanin and controls the production of the pigment directly [64].

1.7 Microscopic Analysis of Human Hair Morphology

Human hair analysis has been exploited by criminal investigators as evidence for over 50 years [50]. Although many microscopic features can be deduced by using microscopic practices, it usually cannot be identified as exclusively belonging to one person [50]. Regardless, microscopic analysis provides researchers and investigators alike with valuable information. This type of research has emphasized the variability in hair phenotypes between human ethnic groups, as well as linking the amount of curl an individual's hair has to the thickness of the hair shaft [15]. Much analysis has gone into ranking hair thickness and curliness [9, 65-67]. There are currently five different parameters to measure an individual's hair curliness [9, 66]. The current quantifiable measurements that can be taken of an individual's hair is: hair thickness (diameter), curl diameter, curl index, wave count, and twist count. These are further mentioned in the methods section for microscopic hair analysis.

The first parameter is the measure of thickness of the hair shaft. This is done by measuring the width of the hair shaft using a microscope. The second parameter uses a CD meter to measure the curl diameter. Using a curve diameter (CD) formula first used by Bailey and Schliebe [65], the CD of the hair can be measured. Loussouarn *et al,* came up with a simplified CD arch meter to place on a transparency to measure hair [9]. Figure 1.6 is what the CD arch meter looks like. If the hair's curl fits within one of the arches the hair falls into the I-IV category of hair. If the hair's curl is small enough to fit in the blue half- circle then the 2-4 parameters are used to figure out if the hair is category V-VIII.

Figure 1.6: The CD Meter showing ranges I-IV. Anything fitting in the blue region falls under ranges V-VIII

When CD is measured, if the hair fits within the CD meter, then the hair is ranked I-IV according to which arch it fell under. If it fits in the blue shaded region of the CD meter, then the third parameter, which is the curl index (*i*), is used. This denotes the ratio of the length of the hair fully stretched to 6 cm to its length at natural rest.

All hair samples that are measured in the third parameter are also measured using the fourth parameter. The fourth parameter is the highest number of waves (*w*) when the hair is pulled to four-fifths its full length. Using these methods to further understand the differences between hair morphologies, as well as the genes that control them, enhances our understanding of the genotype-phenotype relationship between these genes and the physical characteristics they control. Understanding these differences can provide further research to improve the already used statistical modeling tools for phenotype prediction, such as the use of FDP for criminal investigation.

CHAPTER 2. MATERIALS & METHODS: OWL MONKEY ANALYSIS

2.1 qRT-PCR Materials and Methods

2.1.1 Owl Monkey Sample Collection

Hair tuft samples were collected from five owl monkeys housed in a sanctuary funded by MD Anderson. For each owl monkey, samples from many different regions of the body were taken. The three regions of interest for the course of this study were the back, belly, and tail region. The importance of these areas is due to the fact that owl monkeys have different pelage pigmentation depending on the area of the body hair is sampled from. Just like the rhesus macaques, owl monkeys have a light orange coloring on their bellies, an intermediate or light brown coloring on their backs, and a dark black coloring on the distal end of their tails. This allows us to analyze the gene expression levels of all the target genes within a single monkey. Each body region gave three hair tuft samples in order to make sure there was enough sample for duplicates during qRT-PCR analysis as well as the consequential color classification and RNA extraction. All hair tuft samples were stored in sterile microtubes containing RNAlater solution (Ambion).

2.1.2 Color Classification and Quantification via Spectral analysis

Initial color phenotype classification was done visually in order to avoid excess handling of samples prior to RNA extraction. After RNA extraction was completed, the hair tufts from all samples could be handled directly, without worrying about RNA degradation. RNA-later does not affect the hair shaft’s pigment or its hair structure, so working with the samples after extraction had occurred did not cause worry that the hair tuft's physical characteristics were changed during extraction. More qualitative phenotyping was performed microscopically to see if there are any significant color and structural differences between the three regions tested. In order to quantify the hair color phenotype, the reflectance of each sample was measured using the Konica Minolta spectrophotometer and the CM-SA Skin Analysis Software. For each sample, the tufts of hair were gathered in a bundle and placed on a clean white background. All samples were measured at the same time and under the same lighting conditions. Five independent spectral measurements along the hair shafts were taken for each sample.

Each measurement captured the transmission values between 400-700 nm, and the reflectance was calculated as the normalized sum of the area under the curve [7]. Average reflectance values were then calculated for each region/color phenotype (Belly/Light, Back/Intermediate, Tail/Dark). Once the averages were calculated, an analysis of variance (ANOVA) was performed to check for significant differences among all three regions, and a Tukey's HSD (honest significant difference) post hoc test was performed to check for significant differences in reflectance between each region (Back-Tail, Belly-Tail, Back-Belly).

2.1.3 Selection of Target Genes for Pigmentation and Hair Structure Analysis

In a concurrent study in our lab, RNA-sequencing data gathered from four owl monkeys had been compiled to examine the transcriptional profile of each of the different body regions among each Owl Monkey. From this expression data, a list of candidate genes was generated for both hair pigmentation and structure. In total 43 genes were assessed for this study using qRT-PCR, 32 for pigmentation analysis and 11 for hair structure analysis. (See Appendix A for details on all targets and their primers/probes).

Based on previous RNA-sequencing data, 17 pigmentation genes showed increased expression in the tail/black samples, and 15 pigmentation genes showed increased expression in the belly/orange samples. For the hair structure RNA- sequencing analysis, four genes showed increased expression in the belly samples, and six genes showed increased expression in the tail samples. In addition to the ten genes chosen from the RNA-sequencing data, trichohyalin (*TCHH*) was also chosen to run confirmatory qRT-PCR analysis for hair structure based on previous studies [56]. Confirmatory qRT-PCR analysis was performed on these 43 genes in an additional set of five owl monkey samples, using hairs from three separate sites on the body. These samples were not involved in the previous RNA sequencing analysis.

2.1.4 Primer Design for Taqman™ Primers and Probes

Primers for each candidate gene was custom designed (synthesized by Metabion) based on conserved regions in human, chimpanzee, and marmoset. The following guidelines were used when designing the custom primers and probes to ensure PCR efficiency: 1) A GC content between 45-60%; 2) similar temperature range for forward and reverse primers, and the corresponding probe had a melting temperature 4-8° higher than the corresponding flanking primers; 3) for every gene, one of the primers was designed to span an exon-exon junction to minimize the possibility of genomic DNA being amplified; 4) primers and probes avoid runs of 3 or more G’s or C’s at the 3’ end, and 5) the probe did not interfere with the primers by being too close to the flanking primers. Once the primer and probe sequences were identified, they were BLAST searched against a custom-made database using owl monkey sequences that were created in house. Lastly, all primers and probes of each gene were checked to see if they would dimerize to themselves or to other primer/probe sets (AutoDimer). This last check is particularly important, because each gene was put in a duplex reaction with a housekeeping gene.

2.1.5 Selection of a Housekeeping Gene as an Internal Standard

As well as performing quantitative analysis on the designated genes for this project, a housekeeping gene, which has stable expression that allows quantification of the gene expression of target genes, must also be quantified and analyzed. The ideal control should have a constant transcription level under different conditions and is sufficiently abundant across different tissues and cell types [7]. For this project, the housekeeping gene chosen was the TATA-Box binding protein (*TBP*) gene. In a recent study, Life Technologies tested multiple housekeeping genes on multiple samples of human and mouse to test their variant expression levels. From their data, the housekeeping genes with the lowest standard deviation and shown across most tissues and cell types were *TBP* and 18S (Eukaryotic 18S ribosomal RNA). The smaller the standard deviation, the lower the variability across all the samples tested. To assess if *TBP* could be used as a viable housekeeping gene with the owl monkey samples, the conservation of *TBP's* sequence was assessed by BLAST searching its transcripts across the in-house owl monkey genome. This analysis showed that *TBP* was well conserved in owl monkey genome. As well as being highly conserved in the owl monkey genome, *TBP* is also present in all cell types in both the owl monkey and the human genome. This ensures that regardless of which type of cells are analyzed, *TBP* should have a constant rate of expression.

2.1.6 RNA Extraction

Before the RNA extraction was done, each hair tuft was transferred from its original tube containing RNAlater solution to a new, labeled 2 ml tube using sterilized forceps. After transferring the hair tufts, the RNeasy® Micro Kit (Qiagen, NV) was used to isolate RNA from the follicles. The manufacturer's instructions were closely followed, with the exception of the following modifications: after adding 350 µl of buffer RLT and 5 µl of Proteinase K to the tubes in step two of the Qiagen manufacturer's protocol, the hair was homogenized by crushing/stirring the hair tufts with a sterile glass rod and vigorously vortexing the hair/solution mixture for 15 seconds. After doing so, the mixture was centrifuged for 3 minutes and the supernatant was carefully removed into a new, sterile 1.5 ml microtube. After being transferred into a new tube, the procedure continued on step 4 of the manufacturer's protocol. To minimize the risk of amplifying genomic DNA in the qRT-PCR reaction, a DNase digestion step was performed as recommended in the RNeasy® Micro Kit. After extraction, the RNA was eluted in 17 µl of RNase-free water. To assess the concentration of the RNA, 1 µl of the extracted RNA was used on a Qubit 3.0 Fluorometer (ThermoFisher). After the concentration for each sample was taken, all samples were normalized to 1 ng/µl. Normalizing all samples to the same concentration reduces stochastic differences between samples.

2.1.7 cDNA Synthesis

First strand cDNA synthesis was then performed on the extracted RNA using qScript XLT cDNA Supermix (Quanta Biosciences, MD). For each cDNA synthesis, 4 µl of each RNA template was used, 4 µl of qScript reaction mix, and 16 µl of water for a total of 20 µl/reaction. The following amplification conditions were used for synthesis on an Eppendorf Mastercycler Nexus GX2: 25°C for 5 minutes; 42°C for 60 minutes; 85°C for 5 minutes.

2.1.8 Quantitative PCR and Relative Expression

The cDNA templates were then amplified using real-time quantitation PCR (qRT-PCR). To normalize gene expression for all the candidate genes, a housekeeping gene (TATA-box Binding Protein, also known as TBP) was also amplified along with the candidate genes in a duplex reaction.

The qRT-PCR reaction mixture (10 µl total volume) was the same for all loci and contained: 5 µl TaqMan® Multiplex Master Mix (ThermoFisher), .5 µl of both TBP and the candidate gene's primers (750 nM), 1 µl of both TBP and the candidate gene's probe (250 nM), and 1 µl of cDNA template. Amplification conditions on the ABI 7500 Real-Time PCR system (Applied Biosystems) were as follows: a temperature hold at 50°C for 2 min, denaturation at 95°C for 10 min, followed by 40 cycles at 95°C for 15 sec and 60°C for 1 min. All qRT-PCR reactions were performed in duplicates with results being consistent across the replicates. Each run also contained multiple negative controls (no cDNA template) to ensure no outside contamination occurred during reaction set-up.

2.1.9 qRT-PCR Data Analysis

All qRT-PCR data was analyzed following similar studies of gene expression in Macaques [6]. For each sample, the average threshold cycle (C_T) for all duplicates was calculated. All C_T values of the target genes were then normalized using the average C_T value of the housekeeping gene (TBP): $\Delta C_T = C_T$ (Target gene) – C_T (TBP). Lower C_T values represent higher expression levels. Next the $\Delta\Delta C_T$ was calculated using the following formula: $\Delta\Delta C_T = \Delta C_T$ (Back/Belly) – ΔC_T (Tail). For all calculations, normalized expression values were measured relative to the tail region due to it being the darkest phenotype (black). To better represent the amount of expression in all three regions, the $2^{-\Delta\Delta C_T}$ method was used [68].

Statistical significance was assessed by first evaluating the data for normality using the Shapiro-Wilk's Test and homogeneity using the Levene's Test. All genes either violated homogeneity or normality; therefore, violated the assumptions of a one- way ANOVA. A Kruskal-Wallis analysis of variance for nonparametric data followed by Dunn's Post Hoc tests with a Bonferroni correction was performed on all data (adjusted alpha = 0.05). This was all performed using R v.3.2.2 [75] with an alpha level of $p<0.05$.

2.2 Owl Monkey Hair Microscopy Analysis

For each sample, three hairs were mounted on a slide and observed under a Polarization Leica DM4 P Microscope (Leica, Germany). Quantitative and qualitative observations were made for each body region of the monkeys. All samples were observed, photographed, and hair shaft width was measured using the ocular scale divisions (OSD) that are superimposed on the eye piece of the microscope.

To guarantee that all measurements made using the OSDs were accurate, each objective on the microscope was calibrated using a glass slide with a micrometer ruler on it, and measuring how many OSDs it took to reach a certain length on the slide. Table 2.1 shows the measurement lengths for one OSD for each objective on the microscope. For example, if a hair observed under the 40x objective is 32 OSDs across, then the width of the hair is 80 µm long (32 OSD x 2.5 µm/OSD = 80 µm).

Table 2.1: Scale used for each objective when measuring the width of the hair shaft for each sample

Objective Size	4x	10x	20x	40x
µm/OSD	25 µm/OSD	10 µm/OSD	5 µm/OSD	2.5 µm/OSD

To ensure the truest color from the pictures taken of each hair sample, the ChromaCal datacolor calibration system was used (Chromacal Inc, CA). For this to work correctly, the program should be downloaded and used on the same computer system that is connected to the microscope camera. The calibration instrument first scans the ambient light in the room where analysis is taking place to make sure that the room isn't too bright or dark when taking pictures. This is to avoid glare on the glass slides that the samples are on. Next, a color calibration slide is placed under the microscope. This is the first picture taken. Once a picture of the color grid on the slide is taken, the following pictures are of the hair samples. One thing to note is that once the settings on the microscope have been set for the color slide (such as light intensity, angle, and which objective is used) all pictures of subsequent samples must be used in the exact same settings. This lowers the chances of light variation that could affect the color output of the samples. After pictures of all samples have been taken, the Chromacal's datacolor software is run, and each sample picture is calibrated according to the color calibration slide picture that was taken first. An example of a before and after can be seen below in Fig 2.1.

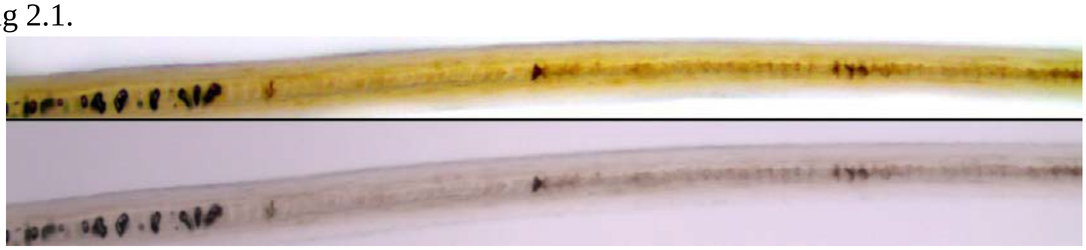

Figure 2.1: The photo on the bottom is a belly hair from an Owl Monkey before photo calibration, and the photo on the top is the same belly hair after photo calibration. There is a stark difference in the color of the hair shaft, the uncalibrated lacks almost all orange pigmentation, while the calibrated photo shows the bright orange pigmentation in the hair.

CHAPTER 3. MATERIALS AND METHODS: HUMAN SCALP HAIR STRUCTURAL MORPHOLOGY

3.1 Microscopic Analysis

3.1.1 Volunteers and Sampling

For this part of the study, volunteers were needed for hair pigmentation and structural morphology phenotyping. All study participants gave their informed consent for this study (IRB 1409306349). The only criterion for this specific study was to have hair without any perm, straightening, or relaxing treatments, as well as artificial dyes. For the people who volunteered for this study, approximately 5-10 hairs were pulled from the vertex of the head. This is to be done carefully, so as to not pull the root off the hair and to keep it intact. The hair samples are carefully bagged and logged for each individual. Gloves and a sterile pair of tweezers were used to obtain the hairs. The samples were stored in sterile zip-lock bags without any buffers and were stored at room temperature, in order to ensure the integrity of the hairs were intact for microscopic analysis.

3.1.2 Hair Structure Morphology Analysis

Three hairs were taken from the sample the volunteers previously gave. After a protocol of washing, rinsing, and drying the hairs were cut 6 cm from the root [9]. This is to get rid of any hair products that may affect the natural structure of the hair. After cleaning and cutting the hair, four parameters [9, 65, 67] were used to measure each hair on their amount of curliness for the microscopic hair structure analysis [9]. For this study 8 categories of curliness were used. Rank 1 being the least curly (or just straight) and Rank 8 being the curliest (or very kinky) [9, 65].

The first parameter used a CD meter to measure the curl diameter. The first step was to lay the cut hair on a glass plate without any outside or mechanical stress. This was done to best maintain the hair's natural shape. Then a second glass plate was carefully placed on top of the hair to keep it two-dimensional. Once the hair was placed between both plates, the CD was measured [9]. Measurements from three hairs per person were taken to get an average curve diameter. To make this a little easier, Loussouarn's CD arch meter was used by placing a transparency that had a pre- determined CD meter on it to measure the hair on the glass plates [66].

After the CD was measured in parameter 1, then the second parameter, which is the curl index (*i*), was used. This denotes the ratio of the length of the hair fully stretched to 6 cm to its length at natural rest. Past studies have only measured the curl index (*i*) if the hair fell inside the blue circle in the CD meter; however, for this study all hairs were measured in both the first and second parameter. This way there are at least three different measurements for all hair, and four measurements for very curly hair. To get the measurements for (*i*), the hair was laid on the glass plane that was used from the CD meter to sit at its natural "at rest" length. The distance to both ends were measured and that length was divided by 6 cm, which is the length of the hair full stretched out. After all three hairs from each person was measured, an average curl index was taken. The closer the curl index is to one the straighter the hair, and vice versa with the hair being curlier the closer the curl index was to zero.

All hair samples that fell inside the blue circle for the CD meter were also measured using the third parameter. The third parameter is the highest number of waves (*w*) when the hair is pulled to four-fifths its full length of 6cm. To get these measurements, the top glass plate was removed and the hair was taped on both ends of the bottom plate. The distance between both pieces of tape is fixed at 4 cm. The cover plate is replaced and the wave crests formed by the hair were counted [9, 65].

After the sample was measured using the first three parameters, the hair was measured using the fourth and last parameter, which is measuring the thickness of the hair shaft using a microscope. A single hair from each individual was placed on a clean glass slide and placed under a compound light microscope. Just like the width was observed for the Owl Monkey hair samples, the human hair samples were all measured under the same objective on the compound light microscope and the width of the hair shaft was recorded using the OSDs on the microscope. Three hairs were measured in the middle of the hair shaft and the average of all three hairs was recorded. Then using a Leica DMC4500 camera (Leica-Microsystems) that has been placed on the microscope, a picture of the hair was uploaded to the computer. To ensure the most accurate color depiction in the photos of each sample, the ChromaCal (Scientific Datacolor, CA) color calibration system was used on the pictures to ensure the color was as true as possible.

3.1.3 Color Calibration and Hair Microscopy Photos

The same type of calibration used on the Owl Monkey hair samples was performed on the human scalp hair samples. Figure 3.1 below shows an example of the difference between a human scalp hair before and after calibration

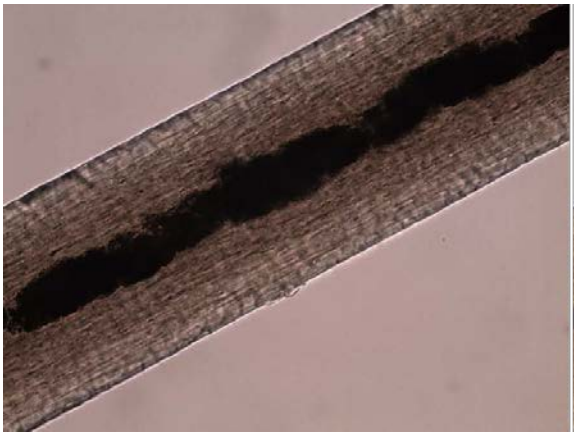

Figure 3.1a: Before Calibration

Figure 3.1b: After Calibration

3.2 Hair Structure Photo Analysis

All 45 individuals who gave a hair sample also had a photograph taken of their hair falling naturally on their head. The purpose of this was to compare the microscopic results of the hair (thickness and curliness) to the macroscopic observations in the photo. If a consistent correlation between both micro and macroscopic observations can be found, this set of 45 can work as a training set that allows us to classify an individual’s hair morphology when only a photo is available.

In order to perform macroscopic analysis on the hair photos of the individuals, a hair analysis computer program is needed. For this study, the ICY© bioimaging analysis software was used (icy.bioimageanalysis.org).

3.2.1 Recording Hair Width with ICY©

To start, the image of the individual was uploaded to the ICY© Bio-imaging software. Only one image can be opened at a time, so as to not over work the software. Once the image was opened, the following was performed on the pictures. All images in the training set also had an ID tag with a pre-determined length and width, to use as a scale to measure the width of the hair.

1. Set the scale of measurement for the picture by measuring the width of the ID tag in the picture and writing the known distance down in the measurement tool. The width of the ID tag is 25,400 µm and the length is 66,600 µm. This can be seen in figure 3.2.

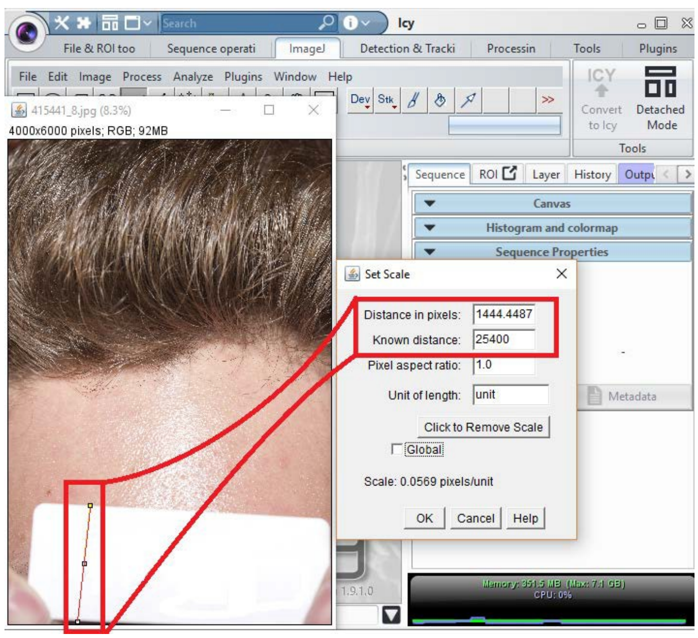

Figure 3.2: The red boxes show the measurement line made on the tag and where to set the known distance in the set scale box

2. After setting the scale, zoom in on the hair in the picture and find hairs that are by themselves and still have enough resolution to make a measurement.

3. Draw a line across the hair, click on the analyze button, then click measure. A small box will appear with the length of the line that was drawn across the width of the hair. Do this three times with multiple hairs to get an average hair width for the individual in question in the photo. Once you get three measurements, click the summary option in the measurement box to get the average hair width. Figure 3.3 below shows the results from the photo in figure 3.2.

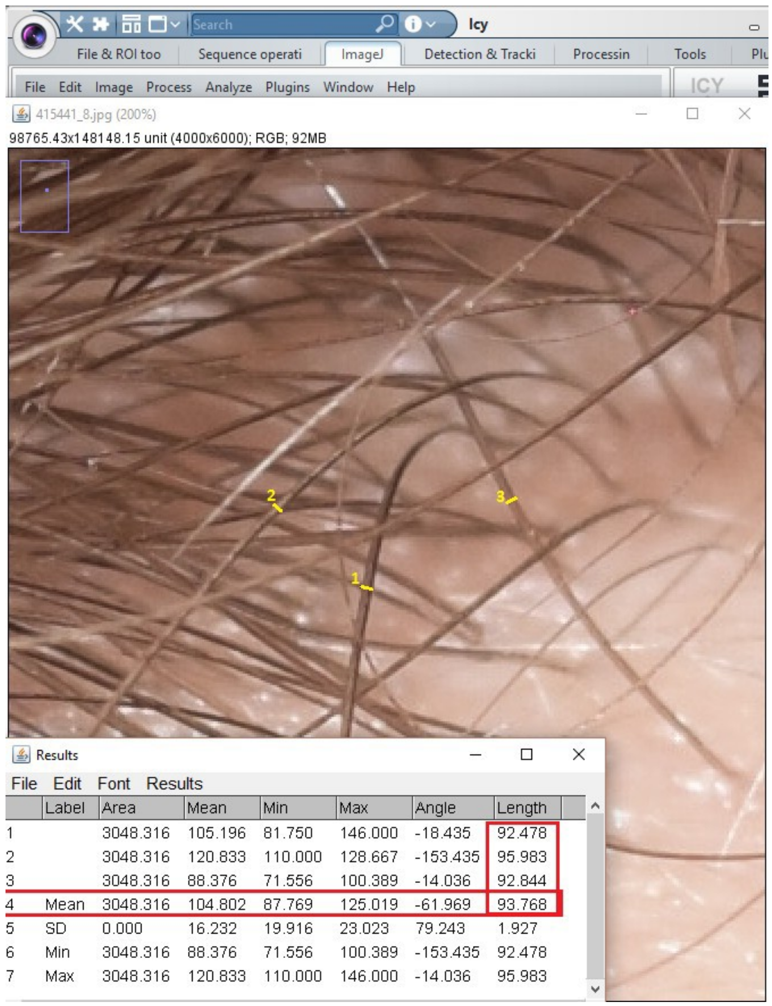

Figure 3.3: The yellow lines and numbers indicate which measurement responds to the reading in the results box on the bottom. The red box on the right shows the measurements and the long red box in the middle is the average width for all three hairs.

4. Once the measurement for hair width is taken, save the results and move on to the next picture.

3.2.2 Recording Curl Diameter for Individuals with Curly Hair

For individuals with naturally curly hair, the diameter of the curl was measured using the ICY bioimaging analysis software©. This proved to be more difficult, because only a small number of people from the 45 individuals in the training set had naturally curly hair that was not straightened, weaved, or had permanent relaxers in it. Those with any of the aforementioned treatments to their hair could not be used in photo-analysis due to the fact that it was not their natural hair. However, those who did have naturally falling curls during the time of collection were used in the training set. Just like measuring the width of the hair, the picture was opened in the ICY bio-imaging software© and the measuring scale was set using the ID tag as a reference. The difference, however, is how the hair was measured. If the curl of the hair fell in waves, then the measurements went from the top of one wave to the bottom of the next on the same hair. If the curl of the hair was in tight rings, then the diameter of the rings was measured. Figure 3.4 shows both an individual with waves comparted to an individual with tight rings and how the measurements were taken for both.

Figure 3.4: On the left is an individual with naturally wavy to curly hair, and the right is an individual with naturally very curly to kinky hair. The measurements on the left start from the top of one wave and end at the bottom of the next wave, and the measurement on the right goes straight across the ring of curl

3.2.3 Statistical Analysis to Link Microscopic and Photo Hair Observations

Once measurements for the training set of 45 individuals for both microscopic analysis and photographic analysis were completed, the next step was to see if the measurements correlated enough to have the ability to use one measurement or the other when only one type of analysis is available. This was done by taking the average hair width for both the physical sample and the photograph, then running a Pearson's R correlation test on all the samples in the test set, as well as a t-test to see if there was a significant difference between the width measured in the photo and the width measured under the microscope. Pearson's R was chosen for analysis, because it measures the strength of linear relationship between two independent variables. The two variables in this instance being the average width recorded from microscopic analysis, and the average width recorded from the photo-analysis. When using Pearson's R correlation, the coefficient can range from 1 to -1. The closer the coefficient is to 1 or -1 the stronger the correlation. If the correlation coefficient is positive then there is a positive correlation between the two variables and vice versa if the coefficient is negative. The closer the coefficient is to 0, the less correlated the two variables are to each other. For this study, the two variables needed to have a high correlation coefficient to give confidence when only one type of measurement is available. A high correlation between the micro and photographic hair width measurements will allow further studies that only have photographs to confidently gather quantifiable data from hair pictures. All statistics were generated using R v.3.2.2 with an alpha level of $p<0.05$.

3.2.4 Statistical Analysis to Link Micro and Photo Curly Hair Observations

Just as the physical hair samples from the test set were measured for their shaft width, three other parameters were also measured to assess the individual's curliness. The purpose of this was to see if one of the parameters could be linked to any quantifiable measurements taken from the photos of the individuals who have curly hair.

The first parameter for curl measured was the curl diameter. Loussouarn's CD arch meter was used, as seen in Figure 3.1, to measure the curl diameter for each individual [9]. For each individual, all three hairs consistently fell in the same CD arch, making it easier to make observations for everyone. The second parameter was also measured for all individuals in the test set who gave physical samples. Of the 45 individuals, only 5 people had hair curly enough to use the third parameter (*w*), so the wave count was not helpful as a quantifiable observation for the test set. The tables in Appendix I show the results for all the individuals in the test set and their microscopic measurements for the CD meter, curl index, and wave count.

After both microscopic and photographic analysis for curl was completed, the individuals with curly hair were run through a Pearson's R correlation and T-test to see if a there is a strong enough correlation between the both measurements. Of the 45 individuals in the test set, 15 people had naturally curly hair that was not chemically altered in any way that could affect the results. The first correlation test was between the ICY© photographic curl and the CD meter measurements. The second correlation test was between the ICY© photographic curl and the curl index measurements.

CHAPTER 4. RESULTS AND DISCUSSION: OWL MONKEY ANALYSIS

4.1 Color Classification Using Spectrophotometry

Spectral measurements showed to be consistent with the initial visual phenotyping of the hair tufts. Each hair tuft had its reflectance measured five times to ensure a proper estimate of each sample was recorded. The reflectance values differed significantly across all three classes ($F = 22.8$, $df = 24$, $p<0.001$) mean and standard deviation: light=14.86±1.29; intermediate=11.33±1.12; dark=9.44±1.03). This can be seen in Fig 4.1 below.

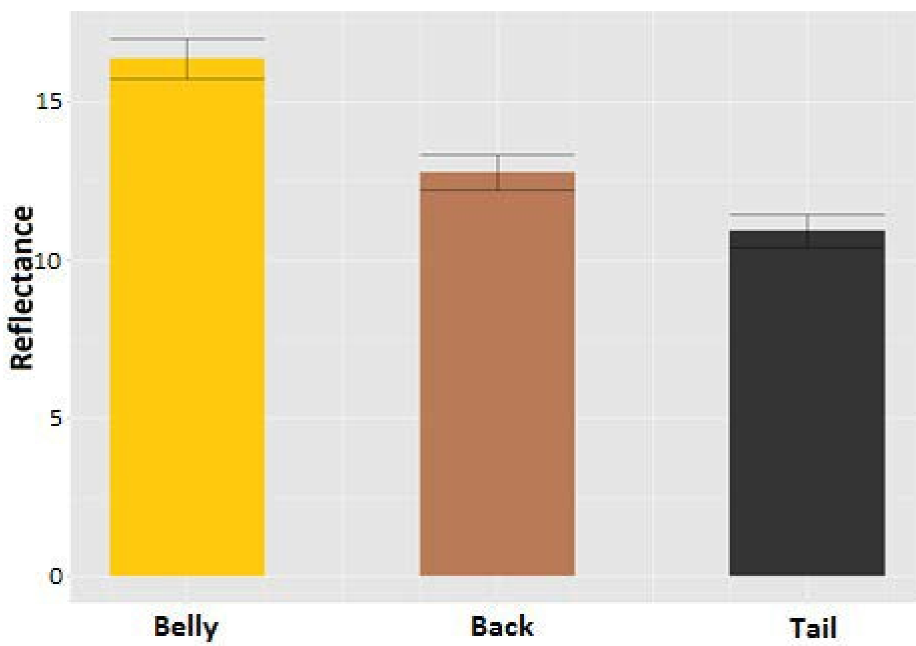

Figure 4.1: Measurements of Reflectance of each body region. This was quantified using a spectrophotometer to correspond to each of the phenotypic categories: Belly (Light coloring), Back (Intermediate coloring), and Tail (Dark coloring)

Other studies on pelage pigmentation of different non-human primate species have used similar color classification techniques to further characterize novel primate species and subspecies [11, 69]. Notably, one previous study performed a similar spectral analysis of reflectance on rhesus macaques [7]. The results observed with the owl monkey samples corroborated with the results observed in a previous study that was performed on macaques; however, where they had a significant difference between all three regions in the macaques, the owl monkeys show a significant difference only between the Back and Belly ($p < 0.05$) and Belly and Tail ($p < 0.05$). When comparing the spectral measurements between the Tail and Back, there no significant difference in the reflectance of the two regions ($p = 0.1041$). One postulation is that the intermediate pelage in Macaques is a lighter shade of brown giving it a higher reflectance in comparison to the darker region in the macaques, whereas the back/brown region in the owl monkeys is banded with different shades of brown, black, and orange. This banding and different shading in the back region could cause the reflectance measurements to highly depend on where exactly on the shaft of the hairs the measurements are taken. In this case, the measurements were taken in darker regions that resembled the tail/black region more than the belly/orange region.

4.2 qRT-PCR Analysis of the Pelage Pigment Genes

All samples consistently amplified the housekeeping gene (*TBP*), which gave confidence that sufficient mRNA was successfully extracted from the hair tufts and reversed transcribed into cDNA. Of the 32 candidate genes tested, 26 showed high qRT-PCR success rates (shown in Table 4.1). Of the 6 that did not, 3 did not amplify at all in the back and belly samples while amplifying with high success in the tail samples. Due to this, an accurate relative quantification to the tail samples could not be performed. The 3 candidate genes that had this issue were: *TYR*, *TYRP1*, and *KIT*. It is possible that they are not expressed to a high enough degree in the lighter samples of the owl monkey hairs to pass the C_T threshold during qRT-PCR analysis, however, the Bradley *et al* (2012) study showed success in *TYRP1* in all three hair types in the macaques. Performing expression analysis on these three genes with different owl monkeys would help determine and confirm if owl monkeys do not essentially express them in lighter pigmented hairs. The other 3 genes that were not included in the analysis (*GPR143*, *TRPM1*, and *MLANA*) only amplified in some samples while not in others, as well as having vastly different C_T values. The results from these three genes were too spotty and unreliable to give an accurate analysis on them. Because the primers worked for some samples and not others, it is possible that there was stochastic variation in the cDNA synthesis between the samples due to using random oligos when performing cDNA synthesis.

Table 4.1: Genes that amplified successfully and were assessed for relative gene expression in pigmentation. (*) denotes significant difference in gene expression.

KITLG *	**PLXNC1 ***	**PMEL ***	**SLC16A1 ***
SLC2A8 *	**SLC30A1 ***	**SLC6A14 ***	**SLC7A5 ***
TMEM50B *	**VAT1L ***	**BCORL1 ***	**C10ORF11 ***
C19ORF44 *	**IRF2 ***	**IRF2BP2 ***	**MIR29B2**
PLXNB1 *	**PPFIBP1**	**SLC1A2 ***	**SLC25A23**
SLC34A2 *	**SLIT3 ***	**SNX1 ***	**TMEM139**
VAMP2 *	**SLC16A9 ***		

The issue with these 6 genes could also be that there was a problem in the primer design. Without a published reference genome of using the owl monkey when initially designing the primers/probes, one possibility is that the primers/probes did not properly align to the owl monkey cDNA. Another explanation that could have caused the primers/probes not annealing to the cDNA during qRT-PCR is the preferential amplification in the cDNA synthesis step. The area of the mRNA that carried these genes could have had spotty cDNA synthesis and therefore not have enough product for the primers/probes to anneal to in the qRT-PCR step. Repeating the cDNA synthesis on these samples could possibly fix this issue.

TBP (housekeeping gene, HKG) was multiplexed with every set of genes for all analyses. The average C_T was calculated for *TBP* for each hair region and all amplification data was normalized with the C_T of the *TBP* of the same region. This new normalized number is called the ΔC_T. For example, the average C_T for the *TBP* in all belly samples is 31.237, so if *PLXNB1* had a C_T of 34.544 in one of the owl monkeys then ΔC_T=34.544-31.237. *PLXNB1's* ΔC_T = 3.307. This was done for all genes in all three regions. Relative fold change data was generated using the $2^{-\Delta\Delta C_T}$ method. All fold change values were assessed for significant difference in comparison to the tail/black samples.

In comparing the back, belly, and tail hair tufts, it was found that 22 of the 26 successful candidate genes confirmed a statistically significant difference in gene expression. Ten genes showed significantly higher expression in belly and back regions compared to the tail, and twelve genes showed significantly higher expression in the tail compared to the belly and back regions. Figure (4.2) shows the expression levels of all 26 genes with an asterisk (*) denoting those that have a significant difference in expression. As seen in fig 4.2, it has been separated by genes that were hypothesized to have higher expression in the tail region and by genes that were hypothesized to have higher expression in the back and belly regions. The hypothesis as to which genes should express higher in which region comes from the RNA sequencing data in the laboratory's concurrent study on Owl Monkeys. Comparisons for each gene break down can be seen on Table C.1 Appendix C. The overall *p* value and significance in expression between each region was done using a Kruskal-Wallis non-parametric test as well as a Dunn's Post-Hoc test with a Bonferroni correction.As seen in the table, the back and belly regions did not show significant differences between each other. However, when looking at back-to-tail and belly-to-tail comparisons, significant difference in expression can be seen.

Of the 26 successful genes that amplified, 4 did not show any significant difference in expression levels. This could due to lack of statistical power because there is only four samples of each color/region, or simply because there isn't a significant difference in expression between these genes in any of the different samples and those candidate genes could not be confirmed in this analysis.

Eleven genes that successfully amplified (and that were previously hypothesized to have higher expression levels in the tail hairs versus back and belly hairs) showed a significant difference in expression in favor of the tail hairs. Those genes were: *KITLG, PLXNC1, PMEL, SLC16A1, SLC16A9, SLC2A8, SLC30A1, SLC6A14, SLC7A5, TMEM50B* and *VAT1L.*

As previously stated *KITLG* is associated with *KIT* and controls the proliferation, migration, and survival of *KIT* expressing melanocytes. In both mice and fish studies, the loss of *KITLG* produces white pigmentation, while the heterozygous reduction of *KITLG* causes selective loss in pigmentation [30, 31]. The results from this study can be correlated with the results from the studies with both fish and mice. *KITLG* had high expression in the darkest pigmented samples, while it had significantly lower expression in the back and belly samples which had much lighter pigmentation. The results here and in the Miller *et al* study (2007) suggest that changes in the *KITLG* locus have been selected in multiple species, and that its regulation on pigmentation has been conserved [30]. *KITLG* seems to have a strong association with dark pigmentation and the degree of dark to light pigmentation is dependent on the levels of its expression as well as the expression of *KIT*. Interestingly *PLXNC1* has been previously shown to have higher expression in individuals with graying hair compared to their darker pigmented counterparts, however for this study, it was upregulated in darker hairs compared to their lighter counterparts. It is also relevant to note that *PLXNC1* negatively regulates *SEMA7A* which promotes dendritic extension in melanocytes. The increase in *PLXNC1* could have a negative effect on dendrite formation and extension in melanocytes, and therefore less melanosomes and melanin granules carrying pheomelanin can be transferred to the keratinocytes that give rise to pigment in hair and skin. Research on *PLXNC1* show be continued to extrapolate its functional role in the melanogenesis pathway, both in owl monkeys and in humans. *PMEL* has been previously been associated with silver pelage pigmentation [28], while the data from this study suggests it plays a larger role in darker pigmentation. *PMEL* is a melanocyte-specific transmembrane glycoprotein, so it could be hypothesized that the higher the expression of *PMEL* leads to more eumelanin is transferred out of the melanocyte and into the keratinocytes. The difference in expression data for *PLXNC1* and *PMEL* not being in lighter pigmented samples as seen in previous studies could also be that more samples are needed to fully suggest its role in melanogenesis with confidence. Although the study number was low at only 5 owl monkeys, there are strong indicators for hypotheses, however, it does need replication in a larger set of samples to confirm these hypotheses. It could also be that the owl monkey's *PLXNC1* and *PMEL* genes have a somewhat different role in melanogenesis compared to that of other species. *SLC16A1's* functional role in the pigmentation pathway has not been elucidated, however, another study showed that chickens with lighter plumage had a down regulation of *SLC16A1* [34]. *SLC16A1*, as well as its genetic relative *SLC16A9*, are both monocarboxylate transporters that may both play a role in regulating the acidity in melanocytes [34]. The level of acidity within the melanocyte may influence the formation of either eumelanin or pheomelanin. *SLCs 2A8, 30A1*, *6A14*, and *7A5*, and their functional role in pigmentation or melanogenesis, remain vague. However, just as *SLC16A1* and *16A9*, all of these *SLCs* play a vital role in the transportation of different important factors in keeping a cell healthy; such as zinc, glucose, and sodium. Because these particular *SLCs* showed to have significantly increase expression in owl monkey samples with darker pigmentation, they may play a role in regulating the health and structure of melanocytes and its surrounding cell structures.

Of the 15 other genes that successfully amplified, (and that were previously hypothesized to have higher expression levels in the back and belly hairs compared to tail) ten showed a significant difference in expression in favor of the back and belly hairs. The following genes had a significantly higher expression in the orange/belly and brown/back pigmented samples compared to the black/tail samples: *BCORL1*, *C10ORF11*, *C19ORF44*, *IRF2*, *IRF1BP2*, *PLXNB1*, *SLC34A2*, *SLIT3, SNX1,* and *VAMP2*. One gene, *SLC1A2*, was significantly higher in the tail hairs compared to the back and belly, which contradicts the original hypothesis.

It is important to note that although melanocortin 1 receptor (*MC1R*) has been shown to be associated with red hair pigmentation in humans [70], it did not show up in the RNA sequencing data for the owl monkeys. For this very reason, *MC1R* was not included in the analysis of red pigmentation gene expression. Although the owl monkeys have light red/orange hairs on their belly, they must have other genes that control this pigmentation. This could be potentially be attributed to convergent evolution between the owl monkeys and humans. The candidate gene list for orange hair expression that was created from the RNA sequencing data were found in both owl monkeys and humans, however, their function in human melanogenesis is still unknown. Due to their expression being significantly higher in orange/belly hairs than black/tail hairs in the owl monkeys, and being conserved in the human genome, their functionality in the human pigmentation pathway can be further studied to create a proper theory as to what they actually do during melanogenesis.

BCORL1 was previously stated to be associated with the repression of E-cadherin, however, the extent of its function in the pigmentation pathway is still unknown [48]. E-cadherin is a known adhesion molecule that is primarily responsible for the adhesion of melanocytes to keratinocytes [71]. It can be postulated that the increased expression of *BCORL1* has a negative effect on the expression of E-cadherin. The less E-cadherin there is, the harder it is for melanocytes to adhere to keratinocytes and transfer melanosomes and melanin granules properly. If melanin cannot be transferred to keratinocytes, then the surrounding hair will lack pigment. *C10orf11* is a known melanocyte differentiation gene in melanoblasts. Due to its affinity to lighter pigmented samples, its increased expression may lead to more pheomelanin pigment granules being led to the surrounding keratinocytes. *IRF2BP2* interacts with the c-terminal of *IRF2* however their biological function is still unknown. Both may play a role is regulation of other transcriptional factors in the pigmentation pathway, such as *TYR* or *TYRP1* who both increase the production of eumelanin. The increase of both *IRF2BP2* and *IRF2* may negatively regulate either these factors or others to decrease the production of eumelanin and increase the production of pheomelanin. *SLC34A2* mediates the transport of inorganic phosphate into epithelial cells that has previously been associated with increased expression in breast cancer tissues [72]. Perhaps the increase in *SLC34A2*, and therefore the increase in inorganic phosphates, cause proliferation of melanocytes and disrupt melanogenesis before melanosomes reach keratinocytes. Therefore, it may not be that it increases the amount of pheomelanin in the surrounding tissues, but decreases the total amount of melanin in general to reach the proper tissues that express pigmentation. *SNX1* is an endosome to Golgi-apparatus transporter, while *VAMP2* is associated with vesicle docking and fusion. Both work in the transportation of molecules in and out of the cell and were both seen in the owl monkeys to have an increased expression in lighter pigmented samples compared to the dark. This increase in expression could help with the transportation of pheomelanin out of the melanocyte and into keratinocytes.

Further investigation of all these genes, would either further prove their functional importance in the pigmentation pathway in both humans and non-human primates, or would shed some light as to their actual role in melanogenesis. If the functionality of these genes can be associated with pigmentation, then further research into the predictive SNPs within these genes can be studied in both the owl monkey and human samples. This in turn would increase the confidence in current Forensic DNA phenotyping prediction in additional causal predictors. The more that is understood not only in hair pigmentation as seen in these owl monkey samples, but in humans as well, the more useful information that can be extrapolated from a DNA sample of an unknown source.

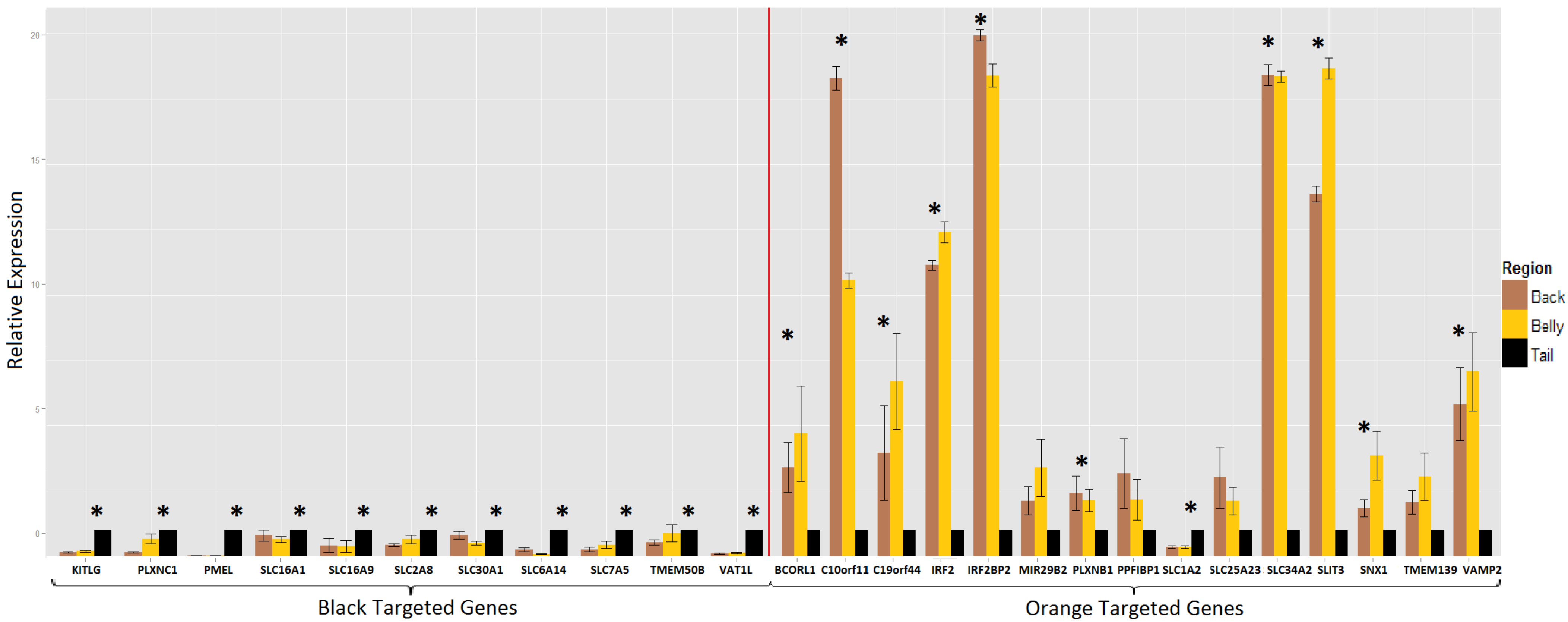

Figure 4.2: Relative gene expression fold change comparison in pigmentation genes. Both orange/belly and brown/back are set relative to the black/tail Owl Monkey samples. The error bars indicated standard error. (*) Indicates that there is a significant difference (p<0.05) in gene expression between the tail and back and belly regions. The only genes above that are NOT significant are MIR29B2, PPFIBP2, SLC25A23, and TMEM139.

4.3 qRT-PCR Analysis of Pelage Structure Genes

All samples consistently amplified the HKG, and of the 11 genes tested, 10 showed consistent qRT-PCR success rates, shown in Table 4.2 below. The only sample that did not yield consistent results is KRT73, which consistently amplified in the tail samples but not at all in the belly or back samples. Due to this, an accurate relative quantification to the tail samples could not be performed. KRT73 has been shown to be specifically expressed in the inner root sheath cuticle [60] in the lowermost bulb region of the hair follicle. One possible explanation as to why KRT73 is only expressed in the tail hairs could be that any expression of KRT73 in the back and belly regions was so low that it fell below the detection limits of the ABI 7500 during qRT-PCR. Because the data showed consistent results in the tail samples, another possibility is that it is not expressed in thinner samples at all and is only expressed in the inner root sheath of larger, thicker hair.

Table 4.2: Genes that amplified successfully and were assessed for relative gene expression in hair thickness

KRT32	**KRT78**	**CASP14**	**SLC7A11**	**TCHH**
RAB29	**CKAP4**	**KRT8**	**SERPINB7**	**CNN1**

In comparing the back, belly, and tail hair tufts for hair thickness, it has been found that of the 10 successful genes, 6 genes showed significant difference in gene expression. As was done with the pigmentation gene expression data, all qRT-PCR data was analyzed using a Kruskal-Wallis non-parametric test as well as a Dunn's Post-Hoc test with a Bonferroni correction. Table G.1 in Appendix G shows the difference in gene expression among the 10 successful genes; those highlighted in orange did not show any significant difference in expression.

Like the pigmentation genes studied prior to the hair thickness genes, *TBP* was multiplexed with every gene of interest as the HKG. The average C_T was calculated for HKG for each hair region and all amplification data was normalized with the C_T of the HKG of the same region, giving the ΔC_T. Relative fold change data was generated using the $2^{-\Delta\Delta C_T}$ method. All fold change values were assessed for significant difference in comparison to the tail/black samples.

When comparing the qRT-PCR data in the back, belly, and tail samples provided, 6 of the 10 successfully amplified genes had a significant difference in expression. Figure 4.3 below shows the expression levels of the gene successful genes with an (*) denoting those that have a significant difference in expression levels. The overall P value and significance in expression between each region was done using a Kruskal-Wallis non-parametric test as well as a Dunn's Post-Hoc test with a Bonferroni correction. As observed in the table, the back and belly regions did not show significant differences between each other. However, when looking at back-to-tail and belly-to-tail comparisons, significant difference in expression can be seen.

Of the 6 genes that had a significant difference in expression, *KRT32, KRT78, CASP14*, *SLC7A11*, and *TCHH* were all upregulated in the dark/tail samples. *TCHH* is expressed in the inner root sheath of the hair follicle and parallels the distribution of the EDAR variant in Asian populations. It functions as an intermediate filament protein between the inner root sheath and cortex of the hair shaft during the anagen phase, and is known to help with keratin intermediate filament (KIFs) assembly to regulate cellular mechanical strength [54]. Because it forms multiple crosslinks with itself, it could be postulated that this increased strength in the inner root sheath causes the hair to be thicker. Because it also helps with the assembly of KIFs with the inner root sheath it may also have a direct association with *KRT32* and *KRT8* because they are known type I hair keratins. *TCHH* may be involved in the regulation, assembly, and movement of *KRT32* and *KRT8* from the inner root sheath of the hair during anagen. *KRT32* is a known type I hair keratins that is also expressed in the inner root sheath [60]. If TCHH has a high expression and in turn upregulates the expression of *KRT32*, it could lead to more crosslinks and more keratins being moved into the hair which could cause thicker, stronger hair. This hypothesis would agree with the results of the owl monkey analysis, since the thickest hair showed the most expression of *TCHH* and *KRT32*. *KRT78* is a type II epithelial keratin that help maintain the intracellular matrix and therefore cell structure [60], however any functional value for hair structure and growth is unknown. Just like *KRT32* and *KRT8*, it could be associated with *TCHH* since its expression was also highest within the thickest hairs. *CASP14* has been found in keratinocytes but its functional purpose is still unknown, however, its increased expression has been associated with tumor growth [73]. *SLC7A11* is a known regulator of pheomelanin production. Samples that have a high expression of *SLC7A11* are shown to not only have darker pigmentation, but thicker hair shafts as well. Because *SLC7A11* negatively regulates pheomelanin, high expression of this gene could slow or stop the creation of pheomelanin. This would leave more room for the production of eumelanin which are larger, darker melanin granules. This corroborates with the results that show *SLC7A11* having a higher level of expression in darker, thicker hairs. This gene should be further investigated in future pigmentation and hair thickness studies. The only gene that showed a significant higher expression in the belly and back hairs compared to the tail is *CNN1*. *CNN1* is a known actin filament-associated regulatory protein in smooth- muscle, though any functional analysis in hair has not been studied. However, *CNN1* has been associated with tyrosine, and that tyrosine phosphorylation regulates the amount of *CNN1* available to bind to F-actin [74]. It could be possible that the downregulation in *TYR*, which in turn would leave more tyrosine, not converted into melanin, to phosphorylate *CNN1*. In turn *CNN1* would not be able to bind to F-actin, leaving the cellular structure around the hairs weaker and thinner.

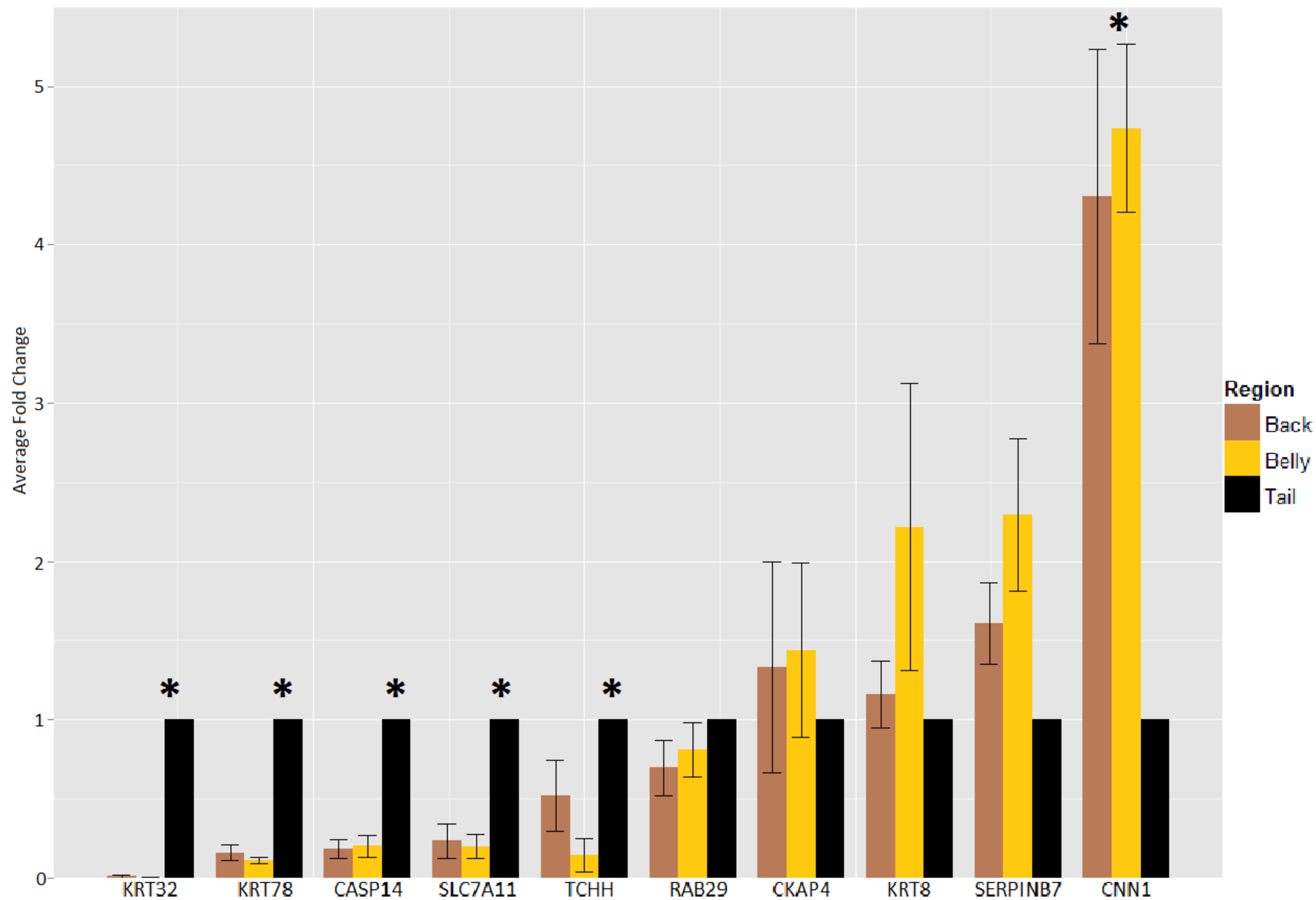

Figure 4.3: Relative gene expression fold change comparison in hair thickness genes. Both orange/belly and brown/back are set relative to the black/tail Owl Monkey samples. The bars indicated standard error. * Indicates significant difference ($p<0.05$) in gene expression between the tail, back, and belly regions.

4.4 Microscopic Owl Monkey Hair Observations

4.4.1 Pelage Thickness Measurements

To get an accurate average measurement of hair shaft thickness for each body region, three different hairs from each hair tuft had their diameter measured in the center of the shaft and then averaged. Table 4.3 below shows the results from measuring the diameter of all hair samples available.

Table 4.3: The measured diameters of the hair shafts for each owl monkey hair sample

Monkey	Region	1st Hair (µm)	2nd Hair (µm)	3rd Hair (µm)	Ave Diam. (µm)	Ave Diam/Region (µm)
11	Belly	30	27	37	31.3333	
12	Belly	25	27	31	27.6666	**Belly**
13	Belly	35	25	30	30.0000	29.4166 ± .7978
16	Belly	30	20	36	28.6666	
11	Back	42	50	45	46.3333	
12	Back	55	47	46	49.3333	**Back**
13	Back	43	50	50	47.6666	48.2500 ± 2.0654
16	Back	46	56	50	50.6666	
11	Tail	70	70	65	68.3333	
12	Tail	72	65	62	66.3333	**Tail**
13	Tail	70	72	75	72.3333	68.9166 ± 1.2500
16	Tail	65	66	75	68.6666	

Using the observed diameters from table 2.4, the data was submitted to the Levene's test to check for homogeneity with the data. Because the data passed Levene's test and appears to be homogenous, a One-Way ANOVA statistical analysis test was performed with a Tukey HSD post-hoc test to check significant difference in hair thickness between each region. Figure 4.4 shows the average differences in diameter between regions and coordinating *p*-values.

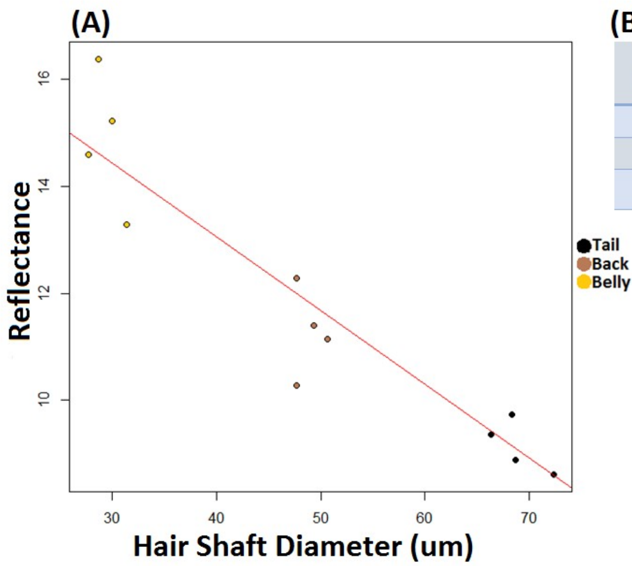

(B)

Comparison	Difference in Diameter	P-Value
Back-Belly	18.8333 µm	< 0.005
Back-Tail	20.6666 µm	< 0.005
Tail-Belly	39.5000 µm	< 0.005

Figure 4.4A: Pearson's R for hair shaft diameter vs reflectance. The red line is the trend line for all reflectance values vs shaft diameter.

Table 4.4B: Table of Tukey HSD pairwise comparison results for hair thickness between all three body regions of the Owl Monkey. All three regions have a significant difference in thickness. Belly being the finest hairs and Tail being the thickest

As shown in the above figure and table all three regions have a significant difference in hair shaft diameter, tail being the thickest among the hairs, and belly being the finest. As well as testing significance among the hair shaft thickness between regions, a Pearson's R correlation test was also performed to test the correlation between each region's hair thickness and its spectral reflectance measurements. The observations resulted in a high negative correlation (tau=-7.99, df = 10, p<0.05) with a Pearson's R of -0.928 and an R^2 of 0.863. The correlation statistics show that a major difference in hair thickness can be due to the major difference in pigmentation in the hair shafts [8]. The belly hairs were consistently lighter in pigmentation as well as smaller in shaft diameter, while the tail hairs were the opposite extreme. This is further supported by the fact that the thickness of the intermediate colored hairs (the back) were almost exactly in between the tail and belly hairs (difference in diameter seen in fig 4.4B). Another possibility as to why the hairs are different in thickness is the location on the body at which the hairs were plucked from.

4.4.2 Pelage Pigmentation and Other Physical Observations

All belly hairs observed shared phenotypic similarities that were not seen in the other two body regions. As seen in Figure 4.5, not only were the pigment granules hard to see due to the light nature of the hair shaft color, but the medullas are very fragmented throughout the entire shaft. When present, the medulla is unilateral in shape. The hairs were also uniformly monochromatic along the shaft with no noticeable changes in pigmentation or color banding in each hair. The average shaft thickness is 29.4166 ± 0.7978 µm, which as seen above are the thinnest/finest hairs.

Figure 4.5: Belly/Light hairs under Leica compound light microscope at 20x magnification.

The black tail hairs had the darkest pigmentation among the hairs analyzed. All tail hairs had a solid, dark coloring with no noticeable banding. Due to the darkness of the color, the medulla was difficult to see in some of the individuals, however, when visible the medulla is unilateral in shape like the belly hairs. The pigment in the hairs seemed to be most condensed towards the middle of the shaft. The tail hairs were consistently the thickest of all three regions for all monkeys observed, having an average diameter of 68.9166 ± 1.2500 µm. Examples of hair from each monkey is shown in Figure 4.6.

Figure 4.6: Tail/Dark hairs under Leica compound light microscope at 20x magnification.

Although the belly and tail hairs were found to be a single solid color throughout the shaft of the hair, the back hairs were observed to have a banding coloration, switching between a darker brown to a lighter orange or white color. Figure 4.7 shows two examples of this banding, exemplifying the change from darker brown pigment on the right side to a lighter pigment on the left. Another notable similarity found within the back hair, which was not seen at all in the belly or tail hairs, was the presence of a bilateral or “stacked” medulla. Figure 4.8 best shows the bilateral medullas found within the shaft of the back hairs. The medulla was also continuous and uniform throughout the darker regions of the shaft. All back hairs observed had a consistent shaft thickness with an average diameter of 48.2500 ± 2.0654 µm. Of all three regions, the back hairs were consistently thicker than the belly hair but thinner than the tail hair.

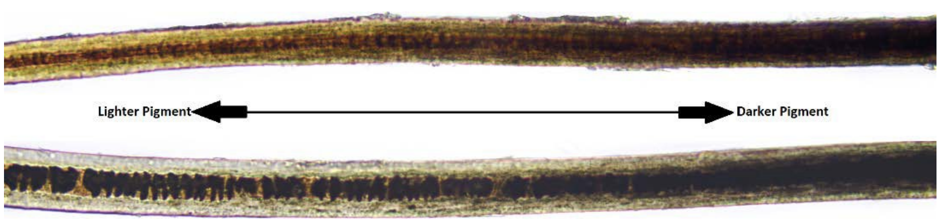

Figure 4.7: Example of color banding seen in the back hairs

Figure 4.8: Back/Intermediate hairs under a Leica compound light microscope at 20x magnification

Aside from the pigmentation being different in each region test, one interesting major difference between regions is the medulla. When visible, the tail hairs had a single, unilateral medulla along the entire shaft while the back hairs had a “stacked” bilateral medulla that takes over most of the inside of the hair shaft. The belly hairs barely had a unilateral medulla at all, and when it did it was very fragmented at best. The medulla’s function in both human and animal species is still unknown and widely debated [20]. In the instance of the Owl Monkey samples, it may have more to do with the hair’s placing on the body and structure than with pigmentation. Judging by the location of each hair, it could be hypothesized that the medulla plays a role in the hair’s overall strength and structure. For example, it could help hairs on the back stand up farther away from the body as a stress response of for better protection against the elements. The belly hairs and distal tail hairs may not need this kind of function; therefore, they do not possess a thick/wide medulla to give the hair in that region more strength. This could be studied further in the future to gain better knowledge of the functional purpose of the medulla. It could also explain why the medulla is always present in animal hair, while almost never present in human hair. It would be interesting to elucidate which gene, or set of genes, controls the creation and maintenance of the medulla in hair.

CHAPTER 5. RESULTS AND DISCUSSION: HUMAN SCALP HAIR STRUCTURAL MORPHOLOGY

5.1 Microscopic vs Photo Hair Width Correlation Results

ICY© measurements were shown to be consistent with the initial microscopic measurements of the hair samples. The one sample t-test did not show any significant difference between the two measurements (tau=.99, df=36, p=0.1468). This shows that the two measurements between ICY© and microscopic analysis were close and that any difference between them is negligible.

The test set proved to be successful in figuring out a way to find accurate, quantitative measurements in 2D photos when physical samples are not available for analysis. The difference between the width measurements taken microscopically and through photo-analysis showed to be negligible, which gives confidence when only 2D imagery is available for a study and quantitative values are needed for analysis. With that said, the current database in our laboratory houses 2,196 individuals with 2D hair photos, but no physical sample available. While these images are perfect to test out the ICY© photo-analysis software to measure the average hair width of each individual, it is important to note that the photos in the test set were taken with slightly differently parameters than the rest of the photos in the database. Both types of images were taken under the same lighting, with the same camera equipment, settings, and at the same distance; however, the images in the database (not a part of the test set) do not have the sticker label with the known width/length to set a scale to measure the hair shafts. An example of this can be seen in fig 5.1.

Figure 5.1: On the left is the hair photo for the training set with the label sticker in it to set a scale for measurement. On the right is the same person, but their database photo does not contain the label sticker

To address this issue was to go through each test set image and find the average distance in pixels/µm. Because both sets of images were taken with the same equipment, settings, and at the same distance, setting the measuring scale on the 2,196 pictures in the database to a specific scale is possible. However, because there was a small difference in pixels/unit in some of the photos in the test set, it is important to recognize the amount of deviation between photos when measuring. The average pixels/unit set for the 2,196 other individuals is 0.0405 pixels/unit ± 0.0096.

With the ability to confidently set the same scale to all hair photos in the database, almost all photos were measured for average hair width. One of the biggest obstacles with the photos, both in the test set and with the 2,196 individuals in the database, is ensuring that the photo was properly taken for reliable readings to be made. Some issues that were encountered while assessing the pictures were that the camera took the picture before fully focusing, flash not going off, the surrounding light being too bright, or the individual moving while the picture is being taken.

These are a few problems that need to be address at the time the photos are taken, because once it gets to the analysis step, it is too late to get a proper photo of the individual. Of the 2,196 individuals used for this study, people whose hair pictures were not taken do to being bald or religious reasons, were not included for assessment. About 9% of the pictures in the database had one or more of these issues, so their hair shaft width cannot be included in future studies. However, for the rest in the database, future studies can reliably use the measurements taken with the ICY© photo-analysis software, and any future individuals who get added to the growing database can be measured using the same parameters as the others.

With a reliable way to properly measure the hair shaft diameter in the hair photos in the database, the next step could be to run a correlation between the spectral reflectance values of each of the individuals in the database and the corresponding hair shaft diameter. This can perhaps strengthen (or weaken) the idea that hair thickness correlates with hair pigmentation. This was performed on the owl monkey samples, and therefore it would also be interesting to measure in human samples. Looking at the reflectance values as a form of pigmentation analysis can also show the varying levels of pigmentation in each of the hair color categories. Many people claim to have blond or light brown hair, but how accurate are they? Within the test set of 45 individuals alone, there was variation in the actual pigmentation within each category of hair color (Appendix J). A future study could be done to put a more quantitative value on hair color rather than categories like blond, brown, and black. Just like finding a reliable quantitative value for hair curliness (rather than using categories like straight, wavy, curly) measuring pigmentation either by spectral reflectance or red-blue-green (RGB) ratio values on color corrected photos will create better data for comparison in either a GWAS or another gene related study. All measurements performed on the test set, both microscopically and via photo analysis, can be seen in Appendix I.

5.2 Micro vs Photo Curly Hair Correlation Results

For the first correlation test between the ICY© and CD meter, the observations resulted in a high negative correlation (tau=-7.53, df = 13, p=4.337e^{-6}) with a Pearson's R coefficient of -0.901 and an R^2 of 0.813. Because the CD meter was ranked 1-8 (1 being the straightest and 8 being the curliest) and the curl diameter length in the photographs was smaller the tighter the curl was, it makes sense that the correlation is negative. What is important to note is that the correlation is very high and that the p- value is less than the set alpha level of 0.05.

Using the CD meter as a correlation between hair curliness in physical samples and 2D imagery will allow a better ranking system for curliness that just straight, wavy, curly. The CD meter ranks curly hair 1-8, 1 being straight and 8 being very curly/kinky. In the past, when analyzing photos with different hair morphology the ranking was stuck to straight, wavy, and curly, but that can be a very ambiguous description. Tight, kinky curls were lumped in the same category as someone with loose falling curls. An example of this can be seen in figure 3.4. Although the hair structure of both individuals is vastly different, under this ranking they would be put in the same category. Now that it is possible to measure the amount of curl in the individual's hair and put a more stringent rank on it, the two individuals in the figure will not be put in different categories for analysis. For example, under the CD meter ranking, the person on the left has a CD curl rank of 4, while the person on the right has a CD curl rank of 7.

For the second correlation test between the ICY and curl index, it resulted in a high positive correlation (tau=6.46, df=13, p=2.171e^{-5}) with a Pearson's R coefficient of 0.873 and an R^2 of 0.763. In the microscopic observations, the smaller the curl index, the tighter the curl for the individual was. The same could be said of the photographic ICY observations. The smaller the diameter of the curl, the tighter the curl the individual had. Figure 5.2 below shows a correlation graph between these two variables. Again, just as the correlation between ICY and the CD meter, the correlation is quite high. This gives confidence in being able to give a quantifiable measurement to an individual's hair photo when a physical sample is not available.

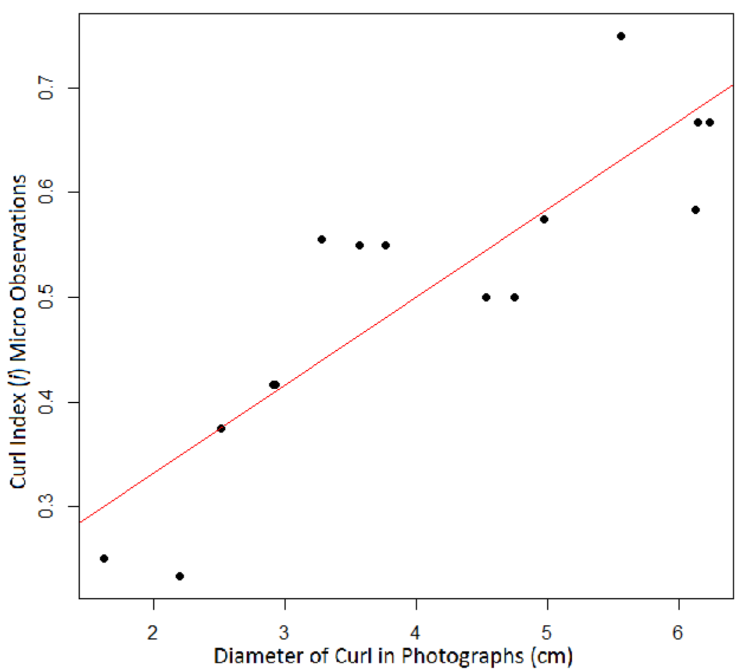

Figure 5.2: Curl Index vs Curl Diameter

Using the curl index (*i*) as a correlation between hair curliness in physical samples and 2D imagery can also give a second quantitative value to 2D photos that isn't base on a rank, but a ratio. For (*i*), the closer the ratio is to 0, the curlier the hair is, and the closer it is to 1 the straighter the hair of the individual is. For example, one individual in the training set who claimed to have curly hair was measured for curl diameter during photo-analysis and resulted in 3.2 cm in length, and their (*i*) was 0.55. However, another individual in the training set claiming to have curly hair was measured for curl diameter during photo-analysis and resulted in 1.6 cm in length, and their (*i*) was 0.25. The second individual has much curlier hair according to the curl index ratio, but when analyzing both people just as "curly" then this difference would go unnoticed. With this ratio, the difference in straight, wavy, and curly hair will have a lot more discrimination and genetic analysis further down the road could be more accurate.

While both the CD meter ranking and the (*i*) ratio proved to be successful on the test set of 45 individuals, using either of these measurement types in a real-world application will need a little more work. A larger set of individuals with both a physical hair sample and a 2D image of their hair will be needed to really narrow down which 2D photo measurement falls into which CD meter ranking. With enough individuals, giving parameters for each CD ranking (1-8) will be possible, and the need for physical samples will no longer be required. For example, CD rank 5 (which is fairly curly hair but not tight/kinky) could have a possible range in photo-analysis lengths between 1.5-2.5 cm, and CD rank 7 (very curly/tight) could have a range in photo-analysis lengths between 0.5-1.0 cm. While the test set had people ranging from straight to curly, it did not have anyone with tight/kinky curls, which is needed to fully establish a proper ranking system that could better describe the hair structure of the individuals in a GWAS for hair structure. The same goes for the (*i*) ratio system; more individuals with curly hair are needed to create a confident ratio system of hair curliness. The smaller the photo-analysis length is with the 2D images, the curlier the individual's hair is.

CHAPTER 6. CONCLUSIONS

The first goal of this study was to look at a list of candidate pigmentation genes generated using RNA-sequencing bioinformatics data, and assess the differential gene expression in different hair color follicles. Of the 26 genes that gave expression data, 22 showed significant difference in expression levels between light and dark pigmented samples. The four that did not show statistical significance are *MIR29B2 (p=0.1877), PPFIBP2 (p=0.7691), SLC25A23 (p=0.3792)*, and *TMEM139 (p=0.198).* The goal was also to look at candidate hair thickness/morphology genes generated from the same RNA-sequencing data, and assess their expression data as well. Of the 10 genes that gave reliable expression results, six had a significant difference in gene expression between the three regions studied in the Owl monkey. Having a parallel study on humans with the pigmentation genes in tandem with this study with non- human primates also helped us gain a better understanding on the similarities and differences between the species on a molecular level. Gaining a better understanding of these candidate genes and their functional value to hair structure within humans will be invaluable in genetics research and practical applications such as forensic science. With FDP emerging as a useful tool in the criminal justice system, knowing as many genes (and their causal SNPs) that control a person's physical appearance is paramount. The more information that can be gathered from DNA found at a crime scene, the better the prediction of physical appearance will be. As of now, hair, skin, and eye pigmentation can be predicted with high confidence, but adding natural hair morphology/curliness will only add to the phenotypes that can be predicted. The more information that can be given to authorities about DNA found at a crime scene, the better possibility of helping them in criminal cases, missing person cases, and other situations where DNA of an unknown source is available.

The second goal of this study was to obtain the ability to accurately assign quantitative morphological phenotypes to hair structure in humans using both microscopy techniques and 2D imagery. Three distinct types of quantitative measurements were correlated between the physical samples and 2D photographs: Hair width from both analyses, CD meter vs hair curl diameter, and Curl index vs hair curl diameter. This will be very useful in the future, when GWAS studies or other genetic analyses only have 2D images of the individuals in the study and do not have physical samples to gather quantitative observations. If either or both measurements can be studied further to create a more confident curliness reading, future GWAS studies will be able to properly phenotype hair curliness using only 2D imagery, which will help narrow down which genes may be responsible for differing hair morphologies. This could also help further along the genetic analysis that was performed in part one with the owl monkey samples. In turn, an even better candidate list of genes for hair structure analysis can be created. The more genes shown to have a significant effect on hair structure, the more can be understood about human DNA and the genes that control physical characteristics. This research will only strengthen the ability to predict an individual's appearance, when only a sample of DNA is available and the source is unknown.

REFERENCES

1. Ruitberg, C.M., D.J. Reeder, and J.M. Butler, *STRBase: a short tandem repeat DNA database for the human identity testing community.* Nucleic Acids Res, 2001. 29(1): p. 320-2.
2. Butler, J.M., *The future of forensic DNA analysis.* Philos Trans R Soc Lond B Biol Sci, 2015. 370(1674).
3. Walsh, S., et al., *Developmental validation of the IrisPlex system: determination of blue and brown iris colour for forensic intelligence.* Forensic Sci Int Genet, 2011. 5(5): p. 464-71.
4. Walsh, S., et al., *Developmental validation of the HIrisPlex system: DNA-based eye and hair colour prediction for forensic and anthropological usage.* Forensic Sci Int Genet, 2014. 9: p. 150-61.
5. Menezes, A.N., C.R. Bonvicino, and H.N. Seuanez, *Identification, classification and evolution of owl monkeys (Aotus, Illiger 1811).* BMC Evol Biol, 2010. 10: p. 248.
6. Rogers, J. and R.A. Gibbs, *Comparative primate genomics: emerging patterns of genome content and dynamics.* Nat Rev Genet, 2014. 15(5): p. 347-59.
7. Bradley, B., Gerald, M., Widdig, A., Mundy, N. , *Coat Color Variation and Pigmentation Gene Expression.* J Mammal Evol, 2013. 20: p. 263-271.
8. Vaughn, M.R., et al., *A comparison of macroscopic and microscopic hair color measurements and a quantification of the relationship between hair color and thickness.* Microsc Microanal, 2009. 15(3): p. 189-93.
9. Loussouarn, G., et al., *Worldwide diversity of hair curliness: a new method of assessment.* Int J Dermatol, 2007. 46 Suppl 1: p. 2-6.
10. Rylands, A., *An Assessment of the Diversity of New World Primates.* Primates, 2000. 8(2): p. 61-93.
11. Groves, C., *Order Primates.* Mammal Species of the World: A Taxonomic and Geographic Reference, 2001. 3: p. 139-141.
12. Ford, S., *Taxonomy and Distribution of the Owl Monkey.* Academics Pr, 1994: p. 1-57.

13. D'Mello, S.A., et al., *Signaling Pathways in Melanogenesis.* Int J Mol Sci, 2016. 17(7).

14. Sitaram, A. and M.S. Marks, *Mechanisms of protein delivery to melanosomes in pigment cells.* Physiology (Bethesda), 2012. 27(2): p. 85-99.

15. Videira, I.F., D.F. Moura, and S. Magina, *Mechanisms regulating melanogenesis.*An Bras Dermatol, 2013. 88(1): p. 76-83.

16. Zafarina, Z. and S. Panneerchelvam, *Analysis of hair samples using microscopical and molecular techniques to ascertain claims of rare animal species.* Malays J Med Sci, 2009. 16(3): p. 35-40.

17. Schlake, T., *Determination of hair structure and shape.* Semin Cell Dev Biol, 2007. 18(2): p. 267-73.

18. Kshirsagar, S.J., M.R. Bhalekar, and R.P. Pawar, *In vitro drug release and in vivo human X-ray studies of ileo-cecal targeting budesonide fast disintegrating tablet.* Drug Dev Ind Pharm, 2009. 35(7): p. 788-95.

19. Bryson, W.G., et al., *Cortical cell types and intermediate filament arrangements correlate with fiber curvature in Japanese human hair.* J Struct Biol, 2009. 166(1): p. 46-58.

20. Cichorek, M., et al., *Skin melanocytes: biology and development.* Postepy Dermatol Alergol, 2013. 30(1): p. 30-41.

21. Tobin, D.J., et al., *The fate of hair follicle melanocytes during the hair growth cycle.* J Investig Dermatol Symp Proc, 1999. 4(3): p. 323-32.

22. Manceau, M., et al., *The developmental role of Agouti in color pattern evolution.* Science, 2011. 331(6020): p. 1062-5.

23. Steiner, C.C., J.N. Weber, and H.E. Hoekstra, *Adaptive variation in beach mice produced by two interacting pigmentation genes.* PLoS Biol, 2007. 5(9): p. e219.

24. Suzuki, I., Cone, R., et al, *Binding of Melanotropic Hormones to the Melanocortin Receptor MC1R on Human Melanocytes Stimulates Proliferation and Melanogenesis.* Endocrinology, 1996. 137(5): p. 1627-1633.

25. Yamaguchi, Y., Brenner, M., Hearing, V, *The Regulation of Skin Pigmentation.* J Biol Chem, 2007. 282(38): p. 27557-27561.

26. Xiong, W.H., et al., *Serum TRPM1 autoantibodies from melanoma associated retinopathy patients enter retinal on-bipolar cells and attenuate the electroretinogram in mice.* PLoS One, 2013. 8(8): p. e69506.

27. McKay, B.S., et al., *A role for myocilin in receptor-mediated endocytosis.* PLoS One, 2013. 8(12): p. e82301.

28. Kwon, B.S., et al., *A melanocyte-specific gene, Pmel 17, maps near the silver coat color locus on mouse chromosome 10 and is in a syntenic region on human chromosome 12.* Proc Natl Acad Sci U S A, 1991. 88(20): p. 9228-32.

29. Ray, P., et al., *Ectopic expression of a c-kitW42 minigene in transgenic mice: recapitulation of W phenotypes and evidence for c-kit function in melanoblast progenitors.* Genes Dev, 1991. 5(12A): p. 2265-73.

30. Miller, C.T., et al., *cis-Regulatory changes in Kit ligand expression and parallel evolution of pigmentation in sticklebacks and humans.* Cell, 2007. 131(6): p. 1179-89.

31. Picardo, M. and G. Cardinali, *The genetic determination of skin pigmentation: KITLG and the KITLG/c-Kit pathway as key players in the onset of human familial pigmentary diseases.* J Invest Dermatol, 2011. 131(6): p. 1182-5.

32. Weiner, L., et al., *Skin as a living coloring book: how epithelial cells create patterns of pigmentation.* Pigment Cell Melanoma Res, 2014. 27(6): p. 1014-31.

33. Peters, E.M., et al., *Profiling mRNA of the graying human hair follicle constitutes a promising state-of-the-art tool to assess its aging: an exemplary report.* J Invest Dermatol, 2013. 133(5): p. 1150-60.

34. Zhang, J., et al., *Skin transcriptome profiles associated with skin color in chickens.* PLoS One, 2015. 10(6): p. e0127301.

35. Hoashi, T., et al., *MART-1 is required for the function of the melanosomal matrix protein PMEL17/GP100 and the maturation of melanosomes.* J Biol Chem, 2005. 280(14): p. 14006-16.

36. Doege, H., et al., *GLUT8, a novel member of the sugar transport facilitator family with glucose transport activity.* J Biol Chem, 2000. 275(21): p. 16275-80.

37. He, L., K. Vasiliou, and D.W. Nebert, *Analysis and update of the human solute carrier (SLC) gene superfamily.* Hum Genomics, 2009. 3(2): p. 195-206.

38. Murphy, T.M., et al., *Risk and protective genetic variants in suicidal behaviour: association with SLC1A2, SLC1A3, 5-HTR1B &NTRK2 polymorphisms.* Behav Brain Funct, 2011. 7: p. 22.

39. Nuiplot, N.O., et al., *Transmembrane protein 139 (TMEM139) interacts with human kidney isoform of anion exchanger 1 (kAE1).* Biochem Biophys Res Commun, 2015. 463(4): p. 706-11.

40. Gronskov, K., et al., *Mutations in c10orf11, a melanocyte-differentiation gene, cause autosomal-recessive albinism.* Am J Hum Genet, 2013. 92(3): p. 415-21.

41. Praetorius, C., et al., *A polymorphism in IRF4 affects human pigmentation through a tyrosinase-dependent MITF/TFAP2A pathway.* Cell, 2013. 155(5): p. 1022-33.

42. Yuan, W., et al., *A genetic model for a central (septum transversum) congenital diaphragmatic hernia in mice lacking Slit3.* Proc Natl Acad Sci U S A, 2003. 100(9): p. 5217-22.

43. Gullapalli, A., et al., *An essential role for SNX1 in lysosomal sorting of protease-activated receptor-1: evidence for retromer-, Hrs-, and Tsg101-independent functions of sorting nexins.* Mol Biol Cell, 2006. 17(3): p. 1228-38.

44. Garzon, R., et al., *MicroRNA 29b functions in acute myeloid leukemia.* Blood, 2009. 114(26): p. 5331-41.

45. Moldrich, R.X., et al., *Transmembrane protein 50b (C21orf4), a candidate for Down syndrome neurophenotypes, encodes an intracellular membrane protein expressed in the rodent brain.* Neuroscience, 2008. 154(4): p. 1255-66.

46. Dastani, Z., et al., *Fine mapping and association studies of a high-density lipoprotein cholesterol linkage region on chromosome 16 in French-Canadian subjects.* Eur J Hum Genet, 2010. 18(3): p. 342-7.

47. Bassi, M.T., et al., *Cellular expression and alternative splicing of SLC25A23, a member of the mitochondrial Ca2+-dependent solute carrier gene family.* Gene, 2005. 345(2): p. 173-82.

48. Pagan, J.K., et al., *A novel corepressor, BCoR-L1, represses transcription through an interaction with CtBP.* J Biol Chem, 2007. 282(20): p. 15248-57.

49. Childs, K.S. and S. Goodbourn, *Identification of novel co-repressor molecules for Interferon Regulatory Factor-2.* Nucleic Acids Res, 2003. 31(12): p. 3016-26.

50. Bisbing, R., *Human Hair in a Forensic Perspective.* Proceedings of the International Symposium on Forensic Hair Comparisons, 1989: p. 35-44.

51. Fujimoto, A., et al., *A scan for genetic determinants of human hair morphology: EDAR is associated with Asian hair thickness.* Hum Mol Genet, 2008. 17(6): p. 835-43.

52. Franbourg, A., et al., *Current research on ethnic hair.* J Am Acad Dermatol, 2003. 48(6 Suppl): p. S115-9.

53. Khumalo, N.P., et al., *What is normal black African hair? A light and scanning electron-microscopic study.* J Am Acad Dermatol, 2000. 43(5 Pt 1): p. 814-20.

54. Lee, S.C., et al., *Human trichohyalin gene is clustered with the genes for other epidermal structural proteins and calcium-binding proteins at chromosomal locus 1q21.* J Invest Dermatol, 1993. 100(1): p. 65-8.

55. Yamamoto, S., et al., *Molecular elements of the regulatory control of keratin filament modulator AHF/trichohyalin in the hair follicle.* Exp Dermatol, 2009. 18(2): p. 152-9.

56. Medland, S.E., et al., *Common variants in the trichohyalin gene are associated with straight hair in Europeans.* Am J Hum Genet, 2009. 85(5): p. 750-5.

57. Mikolajczyk, J., et al., *Activation and substrate specificity of caspase-14.* Biochemistry, 2004. 43(32): p. 10560-9.

58. Tuffy, K.P., S. , *Cytoskeleton-Associated Protein 4: Functions Beyond the Endoplasmic Reticulum in Physiology and Disease.* Cell, 2012.

59. Hossain, M.M., et al., *Developmentally regulated expression of calponin isoforms and the effect of h2-calponin on cell proliferation.* Am J Physiol Cell Physiol, 2003. 284(1): p. C156-67.

60. Nanashima, N., et al., *Damage of hair follicle stem cells and alteration of keratin expression in external radiation-induced acute alopecia.* Int J Mol Med, 2012. 30(3): p. 579-84.

61. Schweizer, J., et al., *Hair follicle-specific keratins and their diseases.* Exp Cell Res, 2007. 313(10): p. 2010-20.

62. Gomez, P.F., et al., *Identification of rab7 as a melanosome-associated protein involved in the intracellular transport of tyrosinase-related protein 1.* J Invest Dermatol, 2001. 117(1): p. 81-90.

63. Gerber, P.A., et al., *Systematic identification and characterization of novel human skin-associated genes encoding membrane and secreted proteins.* PLoS One, 2013. 8(6): p. e63949.

64. Chintala, S., et al., *Slc7a11 gene controls production of pheomelanin pigment and proliferation of cultured cells.* Proc Natl Acad Sci U S A, 2005. 102(31): p. 10964-9.

65. Bailey, J., Schliebe, S. , *The Precision of Average Curvature Measurement in Human Hair.* Proceedings of the International Symposium on Forensic Hair Comparisons, 1989: p. 147-148.

66. Bernard, B., *Hair Shape of Curly Hair.* Proceedings of the International Symposium on Forensic Hair Comparisons, 1989: p. 120-126.

67. De la Mettrie, R., et al., *Shape variability and classification of human hair: a worldwide approach.* Hum Biol, 2007. 79(3): p. 265-81.

68. Schmittgen, T.D. and K.J. Livak, *Analyzing real-time PCR data by the comparative C(T) method.* Nat Protoc, 2008. 3(6): p. 1101-8.

69. Heckman, K.L., et al., *Incongruence between genetic and morphological diversity in Microcebus griseorufus of Beza Mahafaly.* BMC Evol Biol, 2006. 6: p. 98.

70. Beaumont, K.A., et al., *Altered cell surface expression of human MC1R variant receptor alleles associated with red hair and skin cancer risk.* Hum Mol Genet, 2005. 14(15): p. 2145-54.

71. Tang, A., et al., *E-cadherin is the major mediator of human melanocyte adhesion to keratinocytes in vitro.* J Cell Sci, 1994. 107 (Pt 4): p. 983-92.

72. Chen, D.R., et al., *SLC34A2 as a novel marker for diagnosis and targeted therapy of breast cancer.* Anticancer Res, 2010. 30(10): p. 4135-40.

73. Fang, H.Y., et al., *Caspase-14 is an anti-apoptotic protein targeting apoptosis-inducing factor in lung adenocarcinomas.* Oncol Rep, 2011. 26(2): p. 359-69.

74. Abouzaglou, J., et al., *Tyrosine phosphorylation of calponins. Inhibition of the interaction with F-actin.* Eur J Biochem, 2004. 271(13): p. 2615-23.

APPENDIX A: PIGMENTATION qRT-PCR PRIMER DESIGN

Black/Brown Genes				
Gene Symbol	**Gene Name**	**Primers**	**qPCR Target Size**	**Probes**
GPR143	G protein-coupled receptor 143	F: CTTCTGGTGGCTGTTTTGCT R: ATGGTGCTCAGTCCTGCC	70	GPR143 Probe: Forward ACGCGGTGGATGCTTATTTGG
TRPM1	transient receptor potential cation channel subfamily M, member 1	F: ATCGCCATGAAACTCCTGAC R: GCAATGAAGTCCCGGTGTTT	95	TRPM1 Probe: Forward CAACTCGACCTGCCTCAAACTGG
KIT	v-kit Hardy-Zuckerman 4 feline sarcoma viral oncogene homolog	F: ATGGCACCTGAGAGCATTT R: GGATAGGGGCTGCTTCCTAA	106	KIT Probe: Forward AAGCGACGTCTGGTCCTATGGG
KITLG	KIT ligand	F: TCTGCAGGAATCGTGTGACT R: TGACTTGGCAAAACATCCATCC	118	KITLG Prove: Forward TCACTAAATTGGTGGCAAATCTTCCGA
MLANA	melan-A	F: GATCCTGGGAGTCTTACTGCTC R: CAGCATGAAGACTTTTGTCCATCAA	88	MLANA Probe: Reverse TCGTCTTCTGCAATACCAACAGCCA
PLXNC1	plexin C1	F: AGGAGAATTCGTGTTGCAAACT R: TGCACCTTTGTAGCGAATGG	103	PLXNC1 Probe: Reverse TAACAGCCACAGACCCTCACTGC
TMEM50B	transmembrane protein 50B	F: TTGAGGAAGGCTGGGATACA R: CAGACGCCACAGCATTTCTT	137	TMEM50B Probe: Reverse TCGATACATTCACATTCTGGCCAACGA
SLC2A8	solute carrier family 2 (facilitated glucose transporter), member 8	F: CATCTACAAGCCCTTCGTCA R: CTGCTGTCCTTGAACTTGGC	120	SLC2A8 Probe: Forward GCGTCTCCCTGATGGCCTTCC
VAT1L	vesicle amine transport 1-like	F: CTCTGGAGGAGGTCAAAGAG R: GGTCTCTGTGCTGTCATTGG	119	VAT1L Probe: Reverse CCCTCGGTCATGAATCCGCT
SLC16A9	solute carrier family 16, member 9	F: TCAACAGGTTCAAGCGTTGG R: CAGCAAGCATCCATCCAGTC	87	SLC16A9 Probe: Forward GCAGAGGATGCTGGTTGAGTTCT
SLC30A1	solute carrier family 30 (zinc transporter), member 1	F: GGAGGAGACCAACACCCTT R: GGGTTTTCTGGGTCTGCG	78	SLC30A1 Probe: Forward CCAGCAACTCCAACGGGCTTAAAC
SLC7A5	solute carrier fam 7 (amino acid transporter light chain, L system), mem 5	F: GGGTCCAGGATGCCTTCG R: ACATCACCCTTCCCAATCTG	87	SLC7A5 Probe: Forward CCTGATCATCCTGCTGGGCTTCG
SLC6A14	solute carrier family 6 (amino acid transporter), member 14	F: CGATCAAGTGGAATGGATGA R: TATACCACCTTGCCAGAAGA	125	SLC6A14 Probe: Reverse TGCTCCAACTATGAGCCAAGCCA
SLC16A1	solute carrier family 16 (monocarboxylate transporter), member 1	F: GACCTTGTTGGACCCCAGAG R: TGAGCTTACCTAAAAGTGGTGG	98	SLC16A1 Probe: Forward GAATGCTGTCCTGTCCTCCTGG
PMEL	Premelanosome Protein	F: GAAGACCTGGGGCCAATACT R: CACTTCCATGGTGTGTGTGC	100	PMEL Probe: Forward CCAGTGTCTGGGCTGAGCATTGG
TYR	Tyrosinase	F: TTTGCCTGAGTTTGACCCAA R: ACTAGCAAATCCTTCCAGTGTAT	89	TYR Probe: Forward TGGTTCCATGGATAAAGCTGCCA
TYRP1	Tyrosinase Related Protein 1	F: CCGAAACACAGTGGAAGGTT R: AGCCAAATTGTGAAGACTTCGA	76	TYRP1 Probe: Forward CCACGGGAAAGTATGACCCTGC

Orange Genes

Gene Symbol	Gene Name	Primers	qPCR Target Size	Probes
MIR29B2	microRNA 29b-2	F: TGGAAGCTGGTTTCACATGG R: AACACTGATTTCAAATGGTGCT	70	MIR29B2 Probe: Forward TGGCTTAGATTTTTCCATCTTTGTATC
TMEM139	transmembrane protein 139	F: CTGGTCCGGTTTCTGGAATG R: ATTGTCCCGTGCATTGCCT	90	TMEM139 Probe: Forward TCGGTTCCAGCTCCAATCAATGC
C19orf44	Chromosome 19 open reading frame 44	F: CTGCATGCCTCCCTCCTG R: TGTACTCTTTGGCTTCCTCCA	76	C19orf44 Probe: Forward ACGCAGACTCCTTCCACTACC
SLC25A23	solute carrier fam 25 (mitochondrial carrier; phosphate carrier), mem 23	F: CAAAGCAGGAGAAGCTGACG R: ATGGACCTGCATGAAGACCT	122	SLC25A23 Probe: Reverse TGTCCGTGACACGGCACCTG
BCORL1	BCL6 corepressor-like 1	F: GAAAGCAAAGAGCAGTTTCC R: AGATGCTTCCAGACTGACTT	77	BCORL1 Probe: Forward TTATCCCTGTGGTTCTGAGCAC
SLC34A2	solute carrier fam 34 (type II sodium/phosphate Co-transporter), mem 2	F: CATCAACACTGATTTCCCCTTTCC R: CTGCTCTGCACGATGAAGGTC	93	SLC34A2 Probe: Forward TACCTGGCCATCCTCGTTGGAGC
PPFIBP1	PTPRF interacting protein, binding protein 1 (liprin beta 1)	F: GGGTCACTAGATGGTTGGATG R: ACCATCAACCCGTCCTTCAT	75	PPFIBP1 Probe: Forward TGGCCTCCCTCAATATAAGACCCAGT
****IRF2**	interferon regulatory factor 2	F: GCTCAAGTGGCTTAACAAGGA R: GCTTTCCTGTGTGGATTGCC	125	IRF2 Probe: Reverse CGTCCCACCCATGTCTAGCAGCA
SLIT3	slit guidance ligand 3	F: CTCCGAGTCTTGCATCTGG R: ATTCTTGTTCAGGCGCAGTC	99	SLIT3 Probe: Forward CAACCAGGTCAGCGTCATTGAGA
SNX1	Sorting Nexin 1	F: CCATAGGAAAGAGCTAGCG R: CAATGCCGTGTTGTCCTC	85	SNX1 Probe: Forward GAGTCTAGCCATGCTTGGGAGC
****IRF2BP2**	interferon regulatory factor 2 binding protein 2	F: CTGAAGCGGCCCAGAATG R: CCTGGTTGGCATCTTTTGAGG	96	IRF2BP2 Probe: Forward CCCATGGCAGCCCTGATCTTAG
****C10orf11**	Chrome 10 open reading frame 11	F: GAAATTCCAGAGCACCTTGG R: TCCTTCCAGTGACCTCAGAA	87	C10orf11 Probe: Reverse TTGCGAAATGTCCACAGTCCCTG
PLXNB1	Plexin B1	F: CGGGACTCCCCGATCAACAA R: TCTGCATAGTACCTTTCCACCA	78	PLXNB1 Probe: Forward GGGACATTCCCCGGTACAAGCG
VAMP2	vesicle-associated membrane protein 2	F: TGGATGAGGTGGTGGACATC R: CGGTCATCCAGCTCAGATAG	82	VAMP2 Probe: Forward CAAGGTCCTGGAGCGAGACCA
SLC1A2	solute carrier family 1 member 2	F: CCTGACGGTGTTTGGTGTC R: ATCAGGGTGGATGGGAGATG	76	SLC1A2 Probe: Forward GCAGTGTGTGGAGGGCTTCTTC

House Keeping Gene

Gene Symbol	Gene Name	Primers	qPCR Target Size	Probes
TBP	TATA Box Binding Protein	F: CCTAAAGACCATTGCACTTCG R: CTTCACTCTTGGCTCCTGTG	145	TBP Probe: Forward CACGAACCACGGCACTGATTTTCA

APPENDIX B: SEQUENCES THE cDNA PRIMERS MAKE

Black/Brown Genes

1. GPR143
    a. CTTCTGGTGGCTGTTTTGCTATGCGGTGGATGCTTATTTGGTGATCCGGAGATCGGCAGGACTGAGCACCAT
2. TPMP1
    a. ATCGCCATGAAACTCCTGACCTATGAGCTGAAAAACTGGAGCAACTCGACCTGCCTCAAACTGGCCGTGGCAGCCAAACACCGGGACTTCATTGC
3. KIT
    a. CCTGAGAGCATCTTCAATTGTGTATACACATTTGAAAGTGACGTCTGGTCCTATGGGATTTTTCTTTGGGAGCTGTTCTCTTTAGGAAGCAGCC
4. KITLG
    a. TCTGCAGGAATCGTGTGACTAATAATGTAAAAGACGTCACTAAATTGGTGGCAAATCTTCCGAAAGACTATATGATAACCCTCAAATATGTCCCCGGGATGGATGTTTTGCCAAGTCA
5. MLANA
    a. GTGATCCTGGGAATCATACTGCTCATTGGCTGTTGGTATTGCAGAAGACGAAATGGATACAGAGCCTTGATGGACAAAAGTCTTCATGC
6. PLXNC1
    a. AGGAGAATTCGTGTTGCAAACTGCAATAAACATAAATCCTGTTCGGAGTGTTTAACAGCCACAGACCCTCACTGCGGTTGGTGCCATTCGCTACAAAGGTGCA
7. TMEM50B
    a. TTGAGGAAGGCTGGGATACAGCATTTAATGAAAAATTTATGCTTAAGAAGTAAAAATGGCAGGCTTCCTAGATAATTTTCGTTGGCCAGAATGTGAATGTATCGACTGGAGTGAGAGAAGAAATGCTGTGGCGTCTG
8. SLC2A8
    a. CATCTACAAGCCCTTCGTCATCGGCGTCTCCCTGATGGCCTTCCAGCAGCTGTCGGGGGTCAACGCCATTATGTTCTATGCACAGACCATCTTTGAAGAGGCCAAGTTCAAGGACAGCAG
9. VAT1L
    a. CTCTGGAGGAGGTCAAAGAGGCCATGCAGCGGATCCATGACCGAGGGAACATTGGCAAGTTAATTCTGGATGTAGAAAAGACTCCAACTCCTCTGATGGCCAATGACAGCACAGAGACC
10. SLC16A9
    a. TCAACAGGTTCAAGCGTTGGCCTTTTCATATATGCTGCTCTGCAGAGGATGCTGGTTGAGTTCTATGGACTGGATGGATGCTTGCTG
11. SLC30A1
    a. GGAGGAGACCAACACCCTTGTGGCCAATACCAGCAACTCCAACGGGCTTAAACTGGACCCCGCAGACCCAGAAAAACCC

12. SLC7A5
    a. GGGTCCAGGATGCCTTCGCCGCCGCCAAGCTCCTGGCCCTGGCCCTGA TCATCCTGCTGGGCTTCGTCCAGATTGGGAAGGGTGATGT
13. SLC6A14
    a. CGATCAAGTGGAATGGATGAGACTGGAGTAATTGTGTGGTATTTAGC ACTTTGTCTTCTTCTGGCTTGGCTCATAGTTGGAGCAGCACTTTTTAAA GGAATCAAGTCTTCTGGCAAGGTGGTATA
14. SLC16A1
    a. GACCTTGTTGGACCCCAGAGGTTCTCCAGCGCTGTGGGATTGGTGACC ATTGTGGAATGCTGTCCTGTCCTCCTGGGGCCACCACTTTTAGGTCGG CTCA
15. PMEL
    a. GAAGACCTGGGGCCAATACTGGCAAGTTCTAGGGGGCCCAGTGTCTG GGCTGAGCATTGGGACAGGCAGGGCAATGCTGGGCACACACACCATG GAAGTG
16. TYR
    a. TTTGCCTGAGTTTGACCCAATATGAATCTGGTTCCATGGATAAAGCTG CCAATTTCAGCTTTAGAAATACACTGGAAGGATTTGCTAGT
17. TYRP1
    a. CCGAAACACAGTGGAAGGTTACAGTGACCCCACGGGAAAGTATGACC CTGCTGTTCGAAGTCTTCACAATTTGGCT

Orange Genes

1. MIR29B2
    a. TGGAAGCTGGTTTCACATGGTGGCTTAGATTTTTCCATCTTTGTATCTA GCACCATTTGAAATCAGTGTT

2. TMEM139
    a. CTGGTCCGGTTTCTGGAATGGGGGCTTCGGTTCCAGCTCCAATCAATG CAGACTGAGAGCCCAAGGCCGTCAGGCAATGCACGGGACAAT
3. C19orf44
    a. CTGCATGCCTCCCTCCTGCACTCCCTGGACGCAGACTCCTTCCACTAC CACACCCTGGAGGAAGCCAAAGAGTACA
4. SLC25A23
    a. CAAAGCAGGAGAAGCTGACGGGCATGTGGTGGAAGCAACTGGTGGCT GGCGCAGTGGCAGGTGCCGTGTCACGGACAGGCACAGCCCCTCTGGA CCGCCTCAAGGTCTTCATGCAGGTCCAT
5. BCORL1
    a. GAAAGCAAAGAGCAGTTTCCGTGACTTTATCCCTGTGGTTCTGAGCAC CCGCACGCGAAGTCAGTCTGGAAGCATCT
6. SLC34A2
    a. CATCAACACTGATTTCCCCTTTCCCTTTGCGTGGCTGACTGGCTACCTG GCCATCCTCGTTGGAGCAGGCATGACCTTCATCGTGCAGAGCAG
7. PPFIBP1
    a. ACTGGGTCACTAGATGGTTGGATGACATTGGCCTCCCTCAATATAAGA CCCAGTTTGATGAAGGACGGGTTGATGGTCGAATGCTAC

8. IRF2
   a. GCTCAAGTGGCTTAACAAGGAGAAGAAGATTTTTCAGATCCCCTGGATGCATGCTGCTAGACATGGGTGGGACGTGGAGAAAGATGCACCACTCTTTAGAAACTGGGCAATCCACACAGGAAAGC
9. SLIT3
   a. CTCCGAGTCTTGCATCTGGAAGACAACCAGGTCAGCGTCATTGAGAGAGGCGCCTTCCAGGACCTGAAGCAGCTGGAGCGACTGCGCCTGAACAAGAAT
10. SNX1
   a. CCATAGGAAAGAGCTAGCGCTGAACACAGCCCAGTTTGCAAAGAGTCTAGCCATGCTTGGGAGCTCCGAGGACAACACGGCATTG
11. IRF2BP2
   a. CTGAAGCGGCCCAGAATGGCCAGTCCCCCATGGCAGCCCTGATCTTAGTAGCAGACAATGCAGGGGGCAGTCATGCCTCAAAAGATGCCAACCAGG
12. C10orf11
   a. GAAATTCCAGAGCACCTTGGCAGGGACTGTGGACATTTCGCAAAGAGGCTTGATCTGAGCTTTAACCTTCTGAGGTCACTGGAAGGA
13. PLXNB1
   a. CGGGACTCCCCGATCAACAAACTTCTGTATGCACGGGACATTCCCCGGTACAAGCGGATGGTGGAAAGGTACTATGCAGA
14. VAMP2
   a. TGGATGAGGTGGTGGACATCATGAGGGTGAACGTGGACAAGGTCCTGGAGCGAGACCAGAAGCTATCTGAGCTGGATGACCG
15. SLC1A2
   a. CCTGACGGTGTTTGGTGTCATCCTGGGGGCAGTATGTGGAGGGCTTCTTCGCTTGGCATCTCCCATCCACCCTGATGTGGTTATGC

Housekeeping Gene

1. TBP
   a. CTAAAGACCATTGCACTTCGTGCCCGAAACGCCGAATATAATCCCAAGCGGTTTGCTGCGGTAATCATGAGGATAAGAGAGCCACGAACCACGGCACTGATTTTCAGTTCTGGGAAAATGGTGTGCACAGGAGCCAAGAGTGA

APPENDIX C: STATISTICAL BREAKDOWN OF PIGMENTATION EXPRESSION DATA

Table C.1: The P-values using Kruskal Wallis with a Bonferroni Correction.

Gene	Chi^2	KW P Value	Back/Belly		Back/Tail		Belly/Tail	
BCORL1	10.812	.004489	-.983419	.4881	2.2256	.0391	3.2081	.0020
C10orf11	20.224	4.06e-5	-.3623	1	3.7007	.0003	4.0630	.0001
C19orf44	15.27	.0004832	-1.5527	.181	2.3292	.0298	3.88	.0002
IRF2	20.103	4.132e-5	.103517	1	3.93367	.0001	3.830158	.0002
IRF2BP2	20.224	4.06e-5	-.362	1	3.701	.0003	4.063	.0001
KITLG	20.417	3.68e-5	-.569	.85	-4.116	.00001	-3.597	.0005
MIR29B2	3.3461	.1877	-.362	1	1.372	.2553	1.734	.1244
PLXNB1	7.619	.02216	-.6211	.802	2.0185	.065	2.6396	.0124
PLXNC1	19.032	7.368e-5	-2.4844	.0195	-4.348	.00001	-1.8633	.094
PMEL	20.695	3.207e-5	.7764	.6563	-3.49	.0007	-4.2701	.00001
PPFIBP1	.52508	.7691	.569347	.8537	.672865	.7515	.103517	1
SLC1A2	20.092	4.335e-5	0.00001	1	-3.882	.0002	-3.8819	.0002
SLC2A8	13.545	.001145	-.8281	.6114	-3.5196	.0006	-2.6915	.0107
SLC6A14	20.867	2.994e-5	.8799	.5684	-3.4419	.0009	-4.3219	.00001
SLC7A5	13.931	.000944	-1.03	.4509	-3.623	.0004	-2.587	.0145
SLC16A1	7.2574	.02655	.1552	1	-2.2515	.0365	-2.4067	.0241
SLC16A9	7.3297	.02561	-.310553	1	-2.4844	.0195	-2.1739	.0446
SLC25A23	1.9396	.3792	.362312	1	1.3457	.2676	0.9834	.4881
SLC30A1	10.515	.005208	1.8115	.11	-1.4233	.2319	-3.234	.0018
SLC34A2	20.189	4.131e-5	-.310553	1	3.7266	.0003	4.0371	.0001
SLIT3	20.695	3.207e-5	-.7764	.6563	3.494	.0007	4.2701	.00001
SNX1	10.151	.006249	-1.708	.1314	1.4751	0.2103	3.1831	.0022
TMEM50B	7.836	.01988	-.77638	.6563	-2.71734	.0099	-1.9409	.0784
TMEM139	3.2389	.198	.1553	1	1.6304	0.1545	1.4751	0.2103
VAMP2	16.661	.0002411	-.6211	.8018	3.1831	.0022	3.8042	.0002
VAT1L	20.189	4.131e-5	-.31055	1	-4.037	.0001	-3.7266	.0003
			Z-Value	**P-Value**	**Z-Value**	**P-Value**	**Z-Value**	**P-Value**

Orange = NO statistical significance between all three regions

Green = Statistical significance in gene expression when comparing the hair regions

APPENDIX D: FULL qRT-PCR DATA FOR PIGMENTATION ANALYSIS

Monkey 7 Pigmentation Analysis

Monkey	Region	Target	Ave Delta C_T	SD of Delta C_T	Ddelta C_T	Fold Change	SE of Delta C_T	Ave Fold Change
7	Back	KITLG	2.371147	0.472976242	2.823249963	0.141291838	0.334444708	0.103435463
7	Back	KITLG			3.930620339	0.065579089		
7	Back	PLXNC1	4.237997328	0.434633131	3.723554235	0.075700454	0.307332035	0.095790077
7	Back	PLXNC1			3.109300232	0.115879701		
7	Back	TMEM50B	-1.051180041	0.308484462	1.790857461	0.289000229	0.218131455	0.258165984
7	Back	TMEM50B			2.137128976	0.227331739		
7	Back	SLC2A8	4.620068395	0.335744069	1.950731423	0.258685049	0.237406908	0.20085022
7	Back	SLC2A8			2.805757668	0.143015392		
7	Back	VAT1L	2.437008702	0.616550321	1.677259591	0.312676004	0.435966913	0.215836729
7	Back	VAT1L			3.070997384	0.118997454		
7	Back	SLC16A9	3.680094563	0.439698723	7.040723947	0.007595055	0.310913948	0.008258293
7	Back	SLC16A9			6.808492806	0.008921532		
7	Back	SLC30A1	-1.282589114	0.322047703	1.679559853	0.312177864	0.227722115	0.261617861
7	Back	SLC30A1			2.244289544	0.211057859		
7	Back	SLC7A5	4.730021321	0.402240402	4.267381814	0.051926622	0.284426916	0.054206516
7	Back	SLC7A5			4.145952371	0.05648641		
7	Back	SLC6A14	-0.546599544	0.254694725	2.283695367	0.205371036	0.180096368	0.216172701
7	Back	SLC6A14			2.139398721	0.226974366		
7	Back	SLC16A1	2.034470403	0.265511462	1.25721946	0.418349478	0.187744955	0.427024981
7	Back	SLC16A1			1.198591378	0.435700484		
7	Back	PMEL	2.989468419	0.588865991	9.58641639	0.001300772	0.416391136	0.001555697
7	Back	PMEL			9.109298852	0.001810622		
7	Back	MIR29B2	2.784336888	0.253276073	-2.377050254	5.194735358	0.179093229	3.866631604
7	Back	MIR29B2			-1.343992087	2.538527849		
7	Back	TMEM139	2.814667546	0.772224433	-0.476949546	1.391797717	0.546045133	1.538264643

7	Back	BCORL1	-3.294316447	0.444641037	-3.288116309	9.768359589	0.314408693	7.541807352
7	Back	BCORL1			-2.410138938	5.315255115		
7	Back	SLC34A2	-3.450764812	0.281523619	-3.073728416	8.419464141	0.19906726	9.61132793
7	Back	SLC34A2			-3.433385703	10.80319172		
7	Back	PPFIBP1	0.811640584	0.260921371	-1.002874229	2.003988499	0.184499271	1.857661359
7	Back	PPFIBP1			-0.775121543	1.71133422		
7	Back	IRF2	-1.955782092	0.348690378	-0.417524192	1.335633507	0.246561331	1.492663694
7	Back	IRF2			-0.72219834	1.64969388		
7	Back	SLIT3	-2.156636394	0.297178811	-2.123472068	4.357413628	0.210137152	4.028865982
7	Back	SLIT3			-1.88764939	3.700318336		
7	Back	SNX1	1.591248357	0.251389306	-1.216775748	2.324266904	0.177759083	1.948688488
7	Back	SNX1			-0.65361962	1.573110071		
7	Back	IRF2BP2	-4.498409427	0.250625406	-2.318944785	4.989671319	0.177218924	5.309832688
7	Back	IRF2BP2			-2.493133399	5.629994056		
7	Back	C10ORF11	0.603142583	0.253825821	-1.365878913	2.577332933	0.179481959	2.440912303
7	Back	C10ORF11			-1.204448554	2.304491672		
7	Back	PLXNB1	-1.059714473	0.290386463	-0.716161582	1.642805386	0.205334237	1.662658187
7	Back	PLXNB1			-0.750615928	1.682510989		
7	Back	VAMP2	-5.331178821	0.422971308	-2.717513892	6.577383965	0.29908588	6.371189185
7	Back	VAMP2			-2.624099586	6.164994406		
7	Back	SLC1A2	5.012493932	0.736246703	1.211092141	0.431941506	0.520605036	0.572161382
7	Back	SLC1A2			0.489278532	0.712381259		
7	Belly	KITLG	1.380373752	0.576552553	2.229862311	0.213179067	0.40768422	0.19241434
7	Belly	KITLG			2.542461493	0.171649613		
7	Belly	PLXNC1	3.617759573	0.706552135	2.541833671	0.171724326	0.499607806	0.14621037
7	Belly	PLXNC1			3.050545286	0.120696414		
7	Belly	TMEM50B	-1.75164243	0.55416299	1.200819114	0.435028217	0.391852408	0.416916892
7	Belly	TMEM50B			1.326242545	0.398805567		
7	Belly	SLC2A8	3.196659839	0.674184428	0.641363242	0.641106863	0.476720381	0.528126512
7	Belly	SLC2A8			1.268308738	0.415146161		
7	Belly	VAT1L	2.590291507	0.605888972	2.054845908	0.240674315	0.4284282	0.182838168
7	Belly	VAT1L			2.999976677	0.125002021		

7	Belly	SLC16A9	5.579663074	0.557641285	8.731886008	0.002352017	0.394311934	0.002210783
7	Belly	SLC16A9			8.916467765	0.002069549		
7	Belly	SLC30A1	-2.467066014	0.581574642	0.763982871	0.588868386	0.411235373	0.583423351
7	Belly	SLC30A1			0.790912726	0.577978316		
7	Belly	SLC7A5	5.313603198	0.564011704	4.552415946	0.042617331	0.398816501	0.036632467
7	Belly	SLC7A5			5.028081992	0.030647602		
7	Belly	SLC6A14	0.606851375	0.625134687	3.67449961	0.078318687	0.442036977	0.099300803
7	Belly	SLC6A14			3.055496314	0.120282919		
7	Belly	SLC16A1	2.293906009	0.553680884	1.458398917	0.363896753	0.391511508	0.35674108
7	Belly	SLC16A1			1.516283133	0.349585407		
7	Belly	PMEL	5.114191806	0.678520856	11.05698214	0.000469371	0.479786699	0.000366594
7	Belly	PMEL			11.88817988	0.000263816		
7	Belly	MIR29B2	1.120499408	0.579896587	-3.944818399	15.39957252	0.410048809	11.99848171
7	Belly	MIR29B2			-3.103898904	8.597390904		
7	Belly	TMEM139	2.588545596	0.5924307	-1.070497415	2.100157338	0.418911765	1.813851113
7	Belly	TMEM139			-0.611214775	1.527544887		
7	Belly	C19ORF44	-1.121274198	0.595038423	-3.368923089	10.33110803	0.420755704	11.07778048
7	Belly	C19ORF44			-3.563701531	11.82445292		
7	Belly	SLC25A23	-3.473372663	0.583057686	-1.518184564	2.864303889	0.412284043	4.014321221
7	Belly	SLC25A23			-2.368583581	5.164338553		
7	Belly	BCORL1	-4.401647771	0.566996372	-4.049280068	16.55597498	0.400926979	15.55647066
7	Belly	BCORL1			-3.863637826	14.55696635		
7	Belly	SLC34A2	-4.540783132	0.553661341	-4.252645394	19.06223524	0.391497689	20.34269684
7	Belly	SLC34A2			-4.434505364	21.62315844		
7	Belly	PPFIBP1	2.413197314	0.560003625	0.590566733	0.664081985	0.395982361	0.612419767
7	Belly	PPFIBP1			0.834550956	0.56075755		
7	Belly	IRF2	-2.950631345	0.597350668	-1.425226113	2.685565881	0.422390708	2.97201818
7	Belly	IRF2			-1.704194924	3.258470479		
7	Belly	SLIT3	-3.164018834	0.554855819	-2.992132089	7.956489788	0.392342312	8.072934945
7	Belly	SLIT3			-3.033754251	8.189380101		
7	Belly	SNX1	0.198691165	0.567188116	-2.536172769	5.800481921	0.401062563	5.072712058
7	Belly	SNX1			-2.119336984	4.344942195		

7	Belly	IRF2BP2	-5.192763532	0.571749888	-2.91386976	7.536369809	0.404288223	8.648304942
7	Belly	IRF2BP2			-3.286916635	9.760240075		
7	Belly	C10ORF11	-0.29236337	0.738185589	-2.5781764	5.971843674	0.521976036	4.706821487
7	Belly	C10ORF11			-1.783162973	3.4417993		
7	Belly	PLXNB1	-0.611284459	0.562157989	-0.440324685	1.356909672	0.397505726	1.225447275
7	Belly	PLXNB1			-0.129592797	1.093984879		
7	Belly	VAMP2	-6.420476163	0.571219771	-3.466487786	11.05393237	0.403913374	13.83047081
7	Belly	VAMP2			-4.053720376	16.60700924		
7	Belly	SLC1A2	5.787489688	0.555779049	1.530893424	0.346062993	0.392995135	0.324861755
7	Belly	SLC1A2			1.719468761	0.303660516		
7	Tail	KITLG	-1.005788151	0.565207228	0	1	0.399661864	1
7	Tail	KITLG			0	1		
7	Tail	PLXNC1	0.821570095	0.424127768	0	1	0.299903621	1
7	Tail	PLXNC1			0	1		
7	Tail	TMEM50B	-3.01517326	0.421695886	0	1	0.298184021	1
7	Tail	TMEM50B			0	1		
7	Tail	SLC2A8	2.241823849	0.926935524	0	1	0.655442394	1
7	Tail	SLC2A8			0	1		
7	Tail	VAT1L	0.062880215	0.59317966	0	1	0.41944136	1
7	Tail	VAT1L			0	1		
7	Tail	SLC16A9	-3.244513813	0.460914846	0	1	0.325916013	1
7	Tail	SLC16A9			0	1		
7	Tail	SLC30A1	-3.244513813	0.460914846	0	1	0.325916013	1
7	Tail	SLC30A1			0	1		
7	Tail	SLC7A5	0.523354229	0.475328021	0	1	0.336107667	1
7	Tail	SLC7A5			0	1		
7	Tail	SLC6A14	-2.758146587	0.441972925	0	1	0.312522052	1
7	Tail	SLC6A14			0	1		
7	Tail	SLC16A1	0.806564983	0.419215557	0	1	0.296430163	1
7	Tail	SLC16A1			0	1		
7	Tail	PMEL	-6.358389202	0.460245229	0	1	0.325442523	1
7	Tail	PMEL			0	1		

7	Tail	MIR29B2	4.644858059	0.872943539	0	1	0.617264296	1
7	Tail	MIR29B2			0	1		
7	Tail	TMEM139	3.429401691	0.678556736	0	1	0.47981207	1
7	Tail	TMEM139			0	1		
7	Tail	C19ORF44	2.345038113	0.424326594	0	1	0.300044212	1
7	Tail	C19ORF44			0	1		
7	Tail	SLC25A23	-1.52998859	0.59055317	0	1	0.417584151	1
7	Tail	SLC25A23			0	1		
7	Tail	BCORL1	-0.445188824	0.487737626	0	1	0.344882583	1
7	Tail	BCORL1			0	1		
7	Tail	SLC34A2	-0.197207752	0.435314887	0	1	0.307814108	1
7	Tail	SLC34A2			0	1		
7	Tail	PPFIBP1	1.70063847	0.425942711	0	1	0.301186979	1
7	Tail	PPFIBP1			0	1		
7	Tail	IRF2	-1.385920826	0.417533477	0	1	0.295240753	1
7	Tail	IRF2			0	1		
7	Tail	SLIT3	-0.151075664	0.41671906	0	1	0.294664873	1
7	Tail	SLIT3			0	1		
7	Tail	SNX1	2.526446041	0.590127044	0	1	0.417282834	1
7	Tail	SNX1			0	1		
7	Tail	IRF2BP2	-2.092370335	0.433896727	0	1	0.306811318	1
7	Tail	IRF2BP2			0	1		
7	Tail	C10ORF11	1.888306316	0.423164801	0	1	0.2992227	1
7	Tail	C10ORF11			0	1		
7	Tail	PLXNB1	-0.326325718	0.434243102	0	1	0.307056242	1
7	Tail	PLXNB1			0	1		
7	Tail	VAMP2	-2.660372082	0.499050454	0	1	0.35288196	1
7	Tail	VAMP2			0	1		
7	Tail	SLC1A2	4.162308595	0.45462671	0	1	0.32146963	1
7	Tail	SLC1A2			0	1		

Monkey 11 Pigmentation Analysis

Monkey	Region	Target	Ave Delta C_T	SD of Delta C_T	Ddelta C_T	Fold Change	SE of Delta C_T	Ave Fold Change
11	Back	KITLG	2.667712056	0.32091158	4.048163	0.060447957	0.226918755	0.067602964
11	Back	KITLG			3.741629	0.07475797		
11	Back	PLXNC1	4.331374013	0.447693922	1.56663	0.337596171	0.316567408	0.248929872
11	Back	PLXNC1			2.641482	0.160263573		
11	Back	TMEM50B	-1.793124354	0.302533973	1.245333	0.421810565	0.213923824	0.607234156
11	Back	TMEM50B			0.33523	0.792657747		
11	Back	SLC2A8	4.208073461	0.318691485	1.321776	0.400042288	0.22534891	0.386046607
11	Back	SLC2A8			1.426428	0.372050926		
11	Back	VAT1L	2.767433435	0.332536938	3.020487	0.123237483	0.235139124	0.105444695
11	Back	VAT1L			3.512071	0.087651908		
11	Back	SLC16A9	5.428031917	0.368367155	6.043753	0.015158252	0.260474913	0.01331488
11	Back	SLC16A9			6.445801	0.011471507		
11	Back	SLC30A1	-0.036846316	0.623504177	2.0959	0.233922132	0.440884032	0.326158483
11	Back	SLC30A1			1.257063	0.418394834		
11	Back	SLC7A5	4.204647402	1.04559967	1.240423	0.423248439	0.739350617	0.61186144
11	Back	SLC7A5			0.321073	0.800474441		
11	Back	SLC6A14	1.480208241	0.505060526	4.596058	0.041347444	0.357131723	0.036895919
11	Back	SLC6A14			4.945887	0.032444394		
11	Back	SLC16A1	2.409532399	0.667564922	0.90386	0.534454769	0.472039683	0.732608384
11	Back	SLC16A1			0.103516	0.930761999		
11	Back	PMEL	3.779978597	0.250616721	8.221594	0.003350068	0.177212783	0.00275103
11	Back	PMEL			8.860111	0.002151992		
11	Back	MIR29B2	5.172358357	0.883862516	2.181479	0.22044969	0.624985178	0.67926616
11	Back	MIR29B2			-0.18661	1.13808263		
11	Back	TMEM139	3.764365193	0.337651805	-0.35354	1.277695531	0.238755881	1.20321383
11	Back	TMEM139			-0.1747	1.12873213		
11	Back	C19ORF44	2.373896962	0.614861927	0.734549	0.601005994	0.434773038	0.583943677
11	Back	C19ORF44			0.818881	0.56688136		
11	Back	SLC25A23	2.431048238	0.352306172	3.365107	0.097051429	0.249118083	0.079223113
11	Back	SLC25A23			4.02574	0.061394796		

11	Back	BCORL1	2.61045345	0.312558777	2.169302	0.222318185	0.221012431	0.236087213
11	Back	BCORL1			2.00083	0.249856241		
11	Back	SLC34A2	-2.134146846	0.399854474	-2.54195	5.82374898	0.28273981	6.044182724
11	Back	SLC34A2			-2.64723	6.264616468		
11	Back	PPFIBP1	1.222229802	0.263812789	0.237906	0.84797542	0.186543812	0.933098103
11	Back	PPFIBP1			-0.02605	1.018220786		
11	Back	IRF2	-1.485695041	0.257200729	-2.45	5.464148916	0.181868379	5.440087586
11	Back	IRF2			-2.43723	5.416026255		
11	Back	SLIT3	-1.298961795	0.321858059	-2.7712	6.826764296	0.227588016	7.413915897
11	Back	SLIT3			-3.00019	8.001067498		
11	Back	SNX1	1.327800595	0.335224936	-1.95917	3.888395492	0.237039826	3.4169031
11	Back	SNX1			-1.55847	2.945410708		
11	Back	IRF2BP2	-1.090204394	0.254275314	-0.17102	1.125855965	0.179799799	1.067764179
11	Back	IRF2BP2			-0.01389	1.009672393		
11	Back	C10ORF11	1.502629125	0.491796489	-2.11516	4.332391615	0.347752633	3.433343786
11	Back	C10ORF11			-1.34159	2.534295957		
11	Back	PLXNB1	0.74458965	0.264760557	1.151716	0.45008944	0.187213985	0.415459536
11	Back	PLXNB1			1.392782	0.380829632		
11	Back	VAMP2	-2.242511905	0.279302988	-0.23354	1.175714302	0.197497037	0.883723794
11	Back	VAMP2			0.756981	0.591733287		
11	Back	SLC1A2	5.534135228	0.530319909	2.004552	0.24921252	0.374992804	0.1959492
11	Back	SLC1A2			2.809086	0.14268588		
11	Belly	KITLG	1.917839801	0.57787582	2.609257	0.163883584	0.408619911	0.186807885
11	Belly	KITLG			2.25338	0.209732185		
11	Belly	PLXNC1	4.434277331	0.597714893	1.058884	0.480003334	0.422648254	0.371432553
11	Belly	PLXNC1			1.927624	0.262861772		
11	Belly	TMEM50B	-3.021887982	0.770532712	-0.43803	1.354751586	0.544848906	2.500415973
11	Belly	TMEM50B			-1.86635	3.646080361		
11	Belly	SLC2A8	4.625534808	0.56208407	0.954899	0.515877763	0.397453457	0.475453293
11	Belly	SLC2A8			1.200817	0.435028822		
11	Belly	VAT1L	2.511596687	0.622062703	2.096928	0.233755523	0.439864756	0.205477963
11	Belly	VAT1L			2.496546	0.177200403		

11	Belly	SLC16A9	5.800665652	0.55759474	5.846798	0.017375545	0.394279022	0.016716498
11	Belly	SLC16A9			5.960613	0.016057452		
11	Belly	SLC30A1	-0.748272145	0.558947441	0.321325	0.800334329	0.395235526	0.841098067
11	Belly	SLC30A1			0.181376	0.881861805		
11	Belly	SLC7A5	3.881713443	0.577964489	-0.39674	1.316526064	0.408682609	1.19976784
11	Belly	SLC7A5			-0.11505	1.083009615		
11	Belly	SLC6A14	0.527383116	1.012172972	3.838739	0.06989149	0.715714372	0.131658834
11	Belly	SLC6A14			2.370145	0.193426179		
11	Belly	SLC16A1	2.905784268	0.597289492	0.407356	0.75400382	0.42234745	0.822931186
11	Belly	SLC16A1			0.165113	0.891858552		
11	Belly	PMEL	5.103249347	0.872950468	9.308395	0.001577225	0.617269195	0.001770305
11	Belly	PMEL			8.992441	0.001963385		
11	Belly	MIR29B2	4.108649051	0.71501144	0.124657	0.917222292	0.505589438	2.065881114
11	Belly	MIR29B2			-1.68461	3.214539936		
11	Belly	TMEM139	2.596440112	0.623118268	-1.87301	3.662956906	0.440611152	4.504551
11	Belly	TMEM139			-2.4185	5.346145095		
11	Belly	C19ORF44	1.678671634	0.619037492	-0.8756	1.83477445	0.437725609	1.572052008
11	Belly	C19ORF44			-0.38883	1.309329566		
11	Belly	SLC25A23	-0.285925115	0.74445728	0.461426	0.72626815	0.526410791	0.840092779
11	Belly	SLC25A23			0.068064	0.953917407		
11	Belly	BCORL1	0.324039256	0.650979879	-1.205	2.30537562	0.460312287	1.923849295
11	Belly	BCORL1			-0.6251	1.54232297		
11	Belly	SLC34A2	-3.860302175	0.647421969	-5.43942	43.39385321	0.457796464	34.07295535
11	Belly	SLC34A2			-4.62948	24.75205748		
11	Belly	PPFIBP1	0.621733462	0.656303824	-0.88536	1.847221542	0.464076885	2.36873235
11	Belly	PPFIBP1			-1.53119	2.890243157		
11	Belly	IRF2	-2.591806615	0.573858192	-4.41742	21.36861267	0.405779019	19.31480347
11	Belly	IRF2			-4.10944	17.26099428		
11	Belly	SLIT3	-2.963096822	0.566537227	-5.2069	36.93461285	0.400602315	38.44299409
11	Belly	SLIT3			-5.32017	39.95137532		
11	Belly	SNX1	0.724433696	0.620679161	-3.3172	9.967265786	0.438886444	8.550333459
11	Belly	SNX1			-2.83459	7.133401132		

11	Belly	IRF2BP2	-4.341612065	0.865913635	-3.63496	12.42317548	0.612293403	17.37087601
11	Belly	IRF2BP2			-4.48017	22.31857654		
11	Belly	C10ORF11	-0.143820966	0.848913308	-3.72107	13.18722712	0.600272357	17.56740257
11	Belly	C10ORF11			-4.45599	21.94757802		
11	Belly	PLXNB1	-0.038994992	0.912323154	0.106792	0.928650441	0.645109889	1.199864005
11	Belly	PLXNB1			-0.55687	1.47107757		
11	Belly	VAMP2	-4.391598905	0.588931132	-2.86719	7.296413542	0.416437197	6.170879942
11	Belly	VAMP2			-2.33495	5.045346343		
11	Belly	SLC1A2	5.959836662	1.016557224	2.649874	0.159333971	0.718814507	0.246011315
11	Belly	SLC1A2			1.587755	0.332688658		
11	Tail	KITLG	-1.227183643	0.589621058	0	1	0.416925049	1
11	Tail	KITLG			0	1		
11	Tail	PLXNC1	2.227318462	0.570065214	0	1	0.403096978	1
11	Tail	PLXNC1			0	1		
11	Tail	TMEM50B	-2.583405796	0.631152168	0	1	0.446291978	1
11	Tail	TMEM50B			0	1		
11	Tail	SLC2A8	2.833971676	0.49696359	0	1	0.351406324	1
11	Tail	SLC2A8			0	1		
11	Tail	VAT1L	-0.498845402	0.702960948	0	1	0.497068453	1
11	Tail	VAT1L			0	1		
11	Tail	SLC16A9	-0.816745106	0.416905448	0	1	0.294796669	1
11	Tail	SLC16A9			0	1		
11	Tail	SLC30A1	-1.713327709	0.417252002	0	1	0.29504172	1
11	Tail	SLC30A1			0	1		
11	Tail	SLC7A5	3.423899349	0.553949935	0	1	0.391701755	1
11	Tail	SLC7A5			0	1		
11	Tail	SLC6A14	-3.290764255	0.458404941	0	1	0.324141242	1
11	Tail	SLC6A14			0	1		
11	Tail	SLC16A1	1.905844387	0.419992534	0	1	0.296979569	1
11	Tail	SLC16A1			0	1		
11	Tail	PMEL	-4.760874096	0.614375598	0	1	0.434429151	1
11	Tail	PMEL			0	1		

11	Tail	MIR29B2	4.174921688	0.925942932	0	1	0.654740526	1
11	Tail	MIR29B2			0	1		
11	Tail	TMEM139	4.028488812	0.428448472	0	1	0.30295882	1
11	Tail	TMEM139			0	1		
11	Tail	C19ORF44	1.597181973	0.747910861	0	1	0.528852842	1
11	Tail	C19ORF44			0	1		
11	Tail	SLC25A23	-1.264375034	0.470953916	0	1	0.333014708	1
11	Tail	SLC25A23			0	1		
11	Tail	BCORL1	0.525387463	0.422114969	0	1	0.298480357	1
11	Tail	BCORL1			0	1		
11	Tail	SLC34A2	0.460440334	0.479409739	0	1	0.338993877	1
11	Tail	SLC34A2			0	1		
11	Tail	PPFIBP1	1.116302189	0.429504204	0	1	0.303705335	1
11	Tail	PPFIBP1			0	1		
11	Tail	IRF2	0.957920727	0.421987754	0	1	0.298390402	1
11	Tail	IRF2			0	1		
11	Tail	SLIT3	1.586735424	0.418577956	0	1	0.295979311	1
11	Tail	SLIT3			0	1		
11	Tail	SNX1	3.086622486	0.421058563	0	1	0.297733365	1
11	Tail	SNX1			0	1		
11	Tail	IRF2BP2	-0.99774963	0.422193267	0	1	0.298535722	1
11	Tail	IRF2BP2			0	1		
11	Tail	C10ORF11	3.23100346	0.434677929	0	1	0.307363711	1
11	Tail	C10ORF11			0	1		
11	Tail	PLXNB1	-0.527659718	0.488935526	0	1	0.345729626	1
11	Tail	PLXNB1			0	1		
11	Tail	VAMP2	-2.504233662	0.711799986	0	1	0.503318597	1
11	Tail	VAMP2			0	1		
11	Tail	SLC1A2	3.127316695	0.428850413	0	1	0.303243035	1
11	Tail	SLC1A2			0	1		

Monkey 12 Pigmentation Analysis								
Monkey	Region	Target	Ave Delta C_T	SD of Delta C_T	Ddelta C_T	Fold Change	SE of Delta C_T	Ave Fold Change
12	Back	KITLG	2.668347203	0.392301912	2.909044412	0.133134427	0.277399342	0.212808169
12	Back	KITLG			1.773580697	0.29248191		
12	Back	PLXNC1	3.149712209	0.347777574	2.927824166	0.131412629	0.245915881	0.133003754
12	Back	PLXNC1			2.893304574	0.134594879		
12	Back	TMEM50B	-0.231379664	0.262599822	2.263830331	0.208218429	0.185686115	0.182262302
12	Back	TMEM50B			2.677553323	0.156306175		
12	Back	SLC2A8	3.622860753	0.369694559	1.318998483	0.400813086	0.261413529	0.358387626
12	Back	SLC2A8			1.662176278	0.315962166		
12	Back	VAT1L	2.853788168	0.576200639	3.412689406	0.093902709	0.407435379	0.134982264
12	Back	VAT1L			2.505846013	0.176061819		
12	Back	SLC16A9	4.701784932	0.334806963	6.910791543	0.008310831	0.236744274	0.009646396
12	Back	SLC16A9			6.508720544	0.010981961		
12	Back	SLC30A1	-2.263835109	0.454010263	0.563097146	0.676847561	0.321033735	0.914303775
12	Back	SLC30A1			-0.20384011	1.151759989		
12	Back	SLC7A5	3.712851369	0.256669056	3.403646615	0.094493139	0.18149243	0.099124609
12	Back	SLC7A5			3.268732217	0.10375608		
12	Back	SLC6A14	1.561165422	0.652162771	4.91583645	0.03312728	0.461148718	0.025577115
12	Back	SLC6A14			5.793700883	0.01802695		
12	Back	SLC16A1	-0.917281184	0.331099292	-1.052030418	2.073445918	0.234122555	1.985615102
12	Back	SLC16A1			-0.924316016	1.897784286		
12	Back	PMEL	4.225644017	1.025226971	8.935987618	0.002041736	0.724944943	0.001350708
12	Back	PMEL			10.56594685	0.00065968		
12	Back	MIR29B2	4.519972646	0.742029913	-0.355539176	1.279463664	0.524694383	2.239059219
12	Back	MIR29B2			-1.677465293	3.198654774		
12	Back	TMEM139	1.728661382	0.250934322	-1.360273215	2.567337948	0.177437361	3.018838023
12	Back	TMEM139			-1.795076224	3.470338098		
12	Back	C19ORF44	-0.720935023	0.706159195	-2.617666099	6.137563725	0.499329955	12.91448093
12	Back	C19ORF44			-4.299493644	19.69139813		
12	Back	SLC25A23	-1.36702267	0.269883203	-0.144021842	1.104981214	0.190836243	1.034448621
12	Back	SLC25A23			0.053020623	0.963916029		

12	Back	BCORL1	0.53540405	0.549857538	-0.192003104	1.142348705	0.388807994	0.838650572
12	Back	BCORL1			0.902517465	0.534952439		
12	Back	SLC34A2	-5.120376742	0.255421085	-6.059823844	66.70966281	0.180609981	66.49222415
12	Back	SLC34A2			-6.05038819	66.27478548		
12	Back	PPFIBP1	-1.72545544	0.285267387	-3.1188086	8.686702326	0.201714504	10.78229762
12	Back	PPFIBP1			-3.686824653	12.87789291		
12	Back	IRF2	-3.586328662	0.261173874	-5.380956504	41.67055771	0.184677818	46.09481271
12	Back	IRF2			-5.65875611	50.5190677		
12	Back	SLIT3	-2.666658557	0.346254018	-4.947723243	30.86122112	0.244838564	27.03004039
12	Back	SLIT3			-4.535981986	23.19885966		
12	Back	SNX1	3.955780827	0.334683578	0.241609719	0.845801064	0.236657027	0.797877154
12	Back	SNX1			0.415127442	0.749953244		
12	Back	IRF2BP2	-5.837145961	0.254278734	-5.651445243	50.26370953	0.179802217	49.83846511
12	Back	IRF2BP2			-5.626825187	49.41322069		
12	Back	C10ORF11	-2.21701847	0.339039046	-6.034299705	65.53981542	0.239736809	74.84164338
12	Back	C10ORF11			-6.394779433	84.14347135		
12	Back	PLXNB1	-1.825672305	0.251965847	-1.503770682	2.835829278	0.178166759	3.310838003
12	Back	PLXNB1			-1.920616004	3.785846728		
12	Back	VAMP2	-5.990882075	0.264308149	-3.648032996	12.53624171	0.186894084	13.2595696
12	Back	VAMP2			-3.805591437	13.98289749		
12	Back	SLC1A2	4.523409688	0.351299087	1.849359401	0.277515566	0.248405967	0.365031851
12	Back	SLC1A2			1.143856842	0.452548135		
12	Belly	KITLG	1.643505847	0.557591221	1.624025443	0.32442897	0.394276533	0.41067406
12	Belly	KITLG			1.008916953	0.49691915		
12	Belly	PLXNC1	3.279597079	0.624911261	3.09212313	0.117267641	0.44187899	0.121621988
12	Belly	PLXNC1			2.988775351	0.125976335		
12	Belly	TMEM50B	0.389065539	0.555481391	2.971548179	0.127489631	0.392784658	0.117751213
12	Belly	TMEM50B			3.210725882	0.108012794		
12	Belly	SLC2A8	4.366860187	0.935716165	2.788576224	0.144728783	0.661651245	0.228341109
12	Belly	SLC2A8			1.680597403	0.311953434		
12	Belly	VAT1L	3.678812999	0.566704968	3.785338014	0.072527	0.400720926	0.072579596
12	Belly	VAT1L			3.783247066	0.072632192		

12	Belly	SLC16A9	6.565705096	0.594732542	8.77130709	0.002288619	0.420539414	0.002649284
12	Belly	SLC16A9			8.376045325	0.003009949		
12	Belly	SLC30A1	-1.235396588	0.564565139	1.245744803	0.421690141	0.399207838	0.432995791
12	Belly	SLC30A1			1.170389274	0.444301441		
12	Belly	SLC7A5	2.258047854	0.55365559	1.909662345	0.26615483	0.391493622	0.271474988
12	Belly	SLC7A5			1.853109458	0.276795145		
12	Belly	SLC6A14	1.398232257	0.55871977	5.125570395	0.028645049	0.395074538	0.027387963
12	Belly	SLC6A14			5.258100608	0.026130878		
12	Belly	SLC16A1	0.096042468	0.628279009	0.324293235	0.798689562	0.444260347	1.003919419
12	Belly	SLC16A1			-0.273992364	1.209149276		
12	Belly	PMEL	4.699534213	0.902160318	10.61649523	0.000636966	0.637923678	0.000866604
12	Belly	PMEL			9.833219626	0.001096241		
12	Belly	MIR29B2	3.55226401	0.580770483	-1.941125772	3.840051798	0.410666747	3.958226385
12	Belly	MIR29B2			-2.027295968	4.076400972		
12	Belly	TMEM139	0.436419284	0.558216413	-2.593236825	6.034510818	0.394718611	7.445076132
12	Belly	TMEM139			-3.14659681	8.855641446		
12	Belly	C19ORF44	-1.078302587	0.553716532	-3.436050317	10.82316332	0.391536715	14.57473748
12	Belly	C19ORF44			-4.195844552	18.32631163		
12	Belly	SLC25A23	-0.498486722	0.594696102	0.948831656	0.518051828	0.420513646	0.567401612
12	Belly	SLC25A23			0.69723902	0.616751395		
12	Belly	BCORL1	-0.563154424	0.591537483	-0.797208688	1.737735718	0.418280166	1.675170805
12	Belly	BCORL1			-0.689393899	1.612605893		
12	Belly	SLC34A2	-3.917453969	0.559973488	-4.832454583	28.49139949	0.395961051	28.8863924
12	Belly	SLC34A2			-4.871911904	29.28138531		
12	Belly	PPFIBP1	-0.9224064	0.632008416	-2.196592233	4.583952939	0.446897437	6.300144362
12	Belly	PPFIBP1			-3.002942941	8.016335785		
12	Belly	IRF2	-2.71265241	0.564901396	-4.638563058	24.90844507	0.399445608	25.04065096
12	Belly	IRF2			-4.653797051	25.17285686		
12	Belly	SLIT3	-1.94892999	0.553834743	-4.05109205	16.57678185	0.391620303	16.27263622
12	Belly	SLIT3			-3.997156045	15.9684906		
12	Belly	SNX1	2.87576369	0.554551428	-0.659276864	1.579290822	0.392127075	1.687168059
12	Belly	SNX1			-0.84402025	1.795045297		

12	Belly	IRF2BP2	-5.035231793	0.554090373	-4.834644219	28.53467487	0.39180106	28.58573239
12	Belly	IRF2BP2			-4.839797875	28.63678992		
12	Belly	C10ORF11	-0.654868329	0.554220319	-4.651296517	25.12926409	0.391892946	25.14831514
12	Belly	C10ORF11			-4.653482339	25.1673662		
12	Belly	PLXNB1	-1.37609216	0.555730332	-1.038679025	2.054345771	0.392960686	2.428260691
12	Belly	PLXNB1			-1.486547372	2.802175612		
12	Belly	VAMP2	-5.364867414	0.860610396	-2.615495584	6.128336786	0.608543447	9.068899014
12	Belly	VAMP2			-3.586099526	12.00946124		
12	Belly	SLC1A2	4.253489596	0.618534165	1.210367044	0.432158654	0.437369702	0.427324603
12	Belly	SLC1A2			1.243009016	0.422490552		
12	Tail	KITLG	0.327034649	0.651679229	0	1	0.460806802	1
12	Tail	KITLG			0	1		
12	Tail	PLXNC1	0.239147839	0.469649096	0	1	0.33209206	1
12	Tail	PLXNC1			0	1		
12	Tail	TMEM50B	-2.702071491	0.468459832	0	1	0.331251124	1
12	Tail	TMEM50B			0	1		
12	Tail	SLC2A8	2.132273373	0.417675754	0	1	0.295341358	1
12	Tail	SLC2A8			0	1		
12	Tail	VAT1L	-0.105479542	0.434263622	0	1	0.307070752	1
12	Tail	VAT1L			0	1		
12	Tail	SLC16A9	-2.007971111	0.421291467	0	1	0.297898053	1
12	Tail	SLC16A9			0	1		
12	Tail	SLC30A1	-2.443463627	0.447676479	0	1	0.316555074	1
12	Tail	SLC30A1			0	1		
12	Tail	SLC7A5	0.376661953	0.418574089	0	1	0.295976576	1
12	Tail	SLC7A5			0	1		
12	Tail	SLC6A14	-7.793603245	0.417077056	0	1	0.294918014	1
12	Tail	SLC6A14			0	1		
12	Tail	SLC16A1	0.070892033	0.435313715	0	1	0.30781328	1
12	Tail	SLC16A1			0	1		
12	Tail	PMEL	-5.525323215	0.445764235	0	1	0.315202913	1
12	Tail	PMEL			0	1		

12	Tail	MIR29B2	5.53647488	0.479009999	0	1	0.338711218	1
12	Tail	MIR29B2			0	1		
12	Tail	TMEM139	3.306336102	0.525406566	0	1	0.371518546	1
12	Tail	TMEM139			0	1		
12	Tail	C19ORF44	2.737644848	0.673416102	0	1	0.476177092	1
12	Tail	C19ORF44			0	1		
12	Tail	SLC25A23	-1.32152206	0.418498438	0	1	0.295923083	1
12	Tail	SLC25A23			0	1		
12	Tail	BCORL1	0.18014687	0.504536333	0	1	0.356761062	1
12	Tail	BCORL1			0	1		
12	Tail	SLC34A2	0.934729275	0.420403156	0	1	0.297269922	1
12	Tail	SLC34A2			0	1		
12	Tail	PPFIBP1	1.677361187	0.493996094	0	1	0.349307988	1
12	Tail	PPFIBP1			0	1		
12	Tail	IRF2	1.933527645	0.434415213	0	1	0.307177943	1
12	Tail	IRF2			0	1		
12	Tail	SLIT3	2.075194057	0.419919675	0	1	0.29692805	1
12	Tail	SLIT3			0	1		
12	Tail	SNX1	3.627412247	0.428288357	0	1	0.302845602	1
12	Tail	SNX1			0	1		
12	Tail	IRF2BP2	-0.198010746	0.417444622	0	1	0.295177923	1
12	Tail	IRF2BP2			0	1		
12	Tail	C10ORF11	3.997521099	0.417505104	0	1	0.29522069	1
12	Tail	C10ORF11			0	1		
12	Tail	PLXNB1	-0.113478962	0.495795126	0	1	0.350580096	1
12	Tail	PLXNB1			0	1		
12	Tail	VAMP2	-2.264069859	0.417562495	0	1	0.295261272	1
12	Tail	VAMP2			0	1		
12	Tail	SLC1A2	3.026801566	0.487296145	0	1	0.344570409	1
12	Tail	SLC1A2			0	1		

Monkey 13 Pigmentation Analysis								
Monkey	Region	Target	Ave Delta C_T	SD of Delta C_T	Ddelta C_T	Fold Change	SE of Delta C_T	Ave Fold Change
13	Back	KITLG	2.793360555	0.291994708	3.267904427	0.10381563	0.206471438	0.11212597
13	Back	KITLG			3.053657678	0.12043631		
13	Back	PLXNC1	4.254187428	0.585136463	3.756151345	0.074009211	0.413753961	0.129798218
13	Back	PLXNC1			2.429830697	0.185587224		
13	Back	TMEM50B	-1.719863093	0.340221259	0.760913995	0.59012235	0.240572759	0.848920846
13	Back	TMEM50B			-0.147592399	1.107719342		
13	Back	SLC2A8	3.542071187	0.292948575	1.519971993	0.348692686	0.207145924	0.295893216
13	Back	SLC2A8			2.040415309	0.243093747		
13	Back	VAT1L	3.124874913	0.825427464	3.818775323	0.070865374	0.583665357	0.046670764
13	Back	VAT1L			5.475461002	0.022476154		
13	Back	SLC16A9	-1.820314563	0.251725784	-0.805335853	1.747552567	0.177997009	1.755450312
13	Back	SLC16A9			-0.818317267	1.763348056		
13	Back	SLC30A1	-1.668435252	0.790115633	-0.620965812	1.537904386	0.558696122	1.184431079
13	Back	SLC30A1			0.267152932	0.830957772		
13	Back	SLC7A5	4.284331166	0.425728117	3.455328134	0.091168033	0.301035238	0.099322329
13	Back	SLC7A5			3.21790519	0.107476624		
13	Back	SLC6A14	0.24009689	0.720722342	2.262552569	0.208402925	0.509627656	0.270335908
13	Back	SLC6A14			1.589576867	0.332268892		
13	Back	SLC16A1	2.802175929	0.354131327	1.728498605	0.301765838	0.250408662	0.626430178
13	Back	SLC16A1			0.072339375	0.951094518		
13	Back	PMEL	2.577760541	0.361798562	6.749458459	0.009294169	0.255830217	0.008634339
13	Back	PMEL			6.970388558	0.007974509		
13	Back	MIR29B2	1.50571655	0.682861533	-1.913095328	3.766162705	0.48285602	2.80094356
13	Back	MIR29B2			-0.876349493	1.835724416		
13	Back	TMEM139	2.575030171	0.259541976	1.236608651	0.424369051	0.183523891	0.426591697
13	Back	TMEM139			1.221574929	0.428814344		
13	Back	C19ORF44	0.92396053	0.35192722	-0.641622397	1.56008258	0.248850124	1.494251824
13	Back	C19ORF44			-0.514421317	1.428421067		
13	Back	SLC25A23	-1.556673205	0.533949204	-1.767585609	3.404836705	0.377559103	2.475822927
13	Back	SLC25A23			-0.629295203	1.54680915		

13	Back	BCORL1	-0.549868739	0.567059636	-2.189042899	4.560028683	0.400971714	4.736861478
13	Back	BCORL1			-2.296808097	4.913694273		
13	Back	SLC34A2	-1.86163441	0.250966433	-1.324315879	2.50414114	0.177460067	2.380335956
13	Back	SLC34A2			-1.174106452	2.256530771		
13	Back	PPFIBP1	0.869568669	0.252053779	1.552704003	0.340870581	0.178228936	0.338097741
13	Back	PPFIBP1			1.576368478	0.3353249		
13	Back	IRF2	-0.540101207	0.255074605	-1.451474998	2.734875195	0.180364983	2.759842666
13	Back	IRF2			-1.477578971	2.784810137		
13	Back	SLIT3	-0.740358508	0.525264054	-1.554220054	2.936749179	0.371417775	2.134972286
13	Back	SLIT3			-0.414888236	1.333195392		
13	Back	SNX1	3.17247852	0.257575945	0.060384896	0.959008232	0.182133697	1.203530259
13	Back	SNX1			-0.534113695	1.448052285		
13	Back	IRF2BP2	-2.972479976	0.361906549	-2.947110984	7.712031712	0.255906575	8.828591466
13	Back	IRF2BP2			-3.313993308	9.945151221		
13	Back	C10ORF11	1.324299657	0.653844346	-0.406926963	1.325858636	0.462337771	2.289214717
13	Back	C10ORF11			-1.70158046	3.252570798		
13	Back	PLXNB1	0.947255933	0.252692353	-0.122236106	1.088420554	0.178680476	1.006825903
13	Back	PLXNB1			0.112114098	0.925231251		
13	Back	VAMP2	-3.813150561	0.345117003	-1.459920737	2.750932494	0.244034573	3.406600098
13	Back	VAMP2			-2.022285316	4.062267701		
13	Back	SLC1A2	4.759804406	0.918174176	2.615030435	0.16322903	0.649247186	0.198189213
13	Back	SLC1A2			2.100673408	0.233149395		
13	Belly	KITLG	3.61508826	0.605515547	3.810308555	0.071282485	0.428164149	0.063713542
13	Belly	KITLG			4.15470896	0.056144598		
13	Belly	PLXNC1	2.263682162	0.704121074	1.699377158	0.30791901	0.497888786	0.506144573
13	Belly	PLXNC1			0.505594352	0.704370136		
13	Belly	TMEM50B	-1.774563993	0.55453784	0.521404365	0.69669332	0.392117467	0.854443218
13	Belly	TMEM50B			-0.017484567	1.012193115		
13	Belly	SLC2A8	1.430346286	0.926985876	0.041231254	0.971825199	0.655477999	1.300586025
13	Belly	SLC2A8			-0.704293754	1.629346851		
13	Belly	VAT1L	2.720024859	0.677815211	3.693542579	0.077291706	0.479287732	0.056706662
13	Belly	VAT1L			4.790993639	0.036121619		

13	Belly	SLC16A9	-1.993122304	0.578265579	-1.07947149	2.113261777	0.408895513	1.983088653
13	Belly	SLC16A9			-0.889797113	1.852915528		
13	Belly	SLC30A1	2.301003253	0.839335506	4.324384788	0.04991493	0.593499828	0.077125889
13	Belly	SLC30A1			3.260679343	0.104336848		
13	Belly	SLC7A5	3.831017291	0.910319886	3.269620994	0.10369218	0.643693365	0.140419374
13	Belly	SLC7A5			2.49698458	0.177146568		
13	Belly	SLC6A14	2.694092547	1.051818881	4.871095917	0.034170711	0.743748263	0.050834042
13	Belly	SLC6A14			3.889024833	0.067497373		
13	Belly	SLC16A1	2.199412124	0.644423193	0.715635398	0.608936882	0.45567601	0.847958303
13	Belly	SLC16A1			-0.120325028	1.086979723		
13	Belly	PMEL	3.884855991	0.580576949	8.364627936	0.003033864	0.410529898	0.003511912
13	Belly	PMEL			7.96940998	0.00398996		
13	Belly	MIR29B2	3.418720996	0.765561741	0.822935203	0.565290673	0.541333899	0.713828016
13	Belly	MIR29B2			0.213628867	0.86236536		
13	Belly	TMEM139	2.347021853	0.599831859	0.797693351	0.575268209	0.424145175	0.504597927
13	Belly	TMEM139			1.204473594	0.433927645		
13	Belly	C19ORF44	0.434308803	0.694486685	-0.660108468	1.580201426	0.491076244	2.180248921
13	Belly	C19ORF44			-1.475238702	2.780296417		
13	Belly	SLC25A23	-1.888073171	0.91405317	-2.279874703	4.85635775	0.646333195	3.28662889
13	Belly	SLC25A23			-0.779806039	1.716900031		
13	Belly	BCORL1	0.275598323	0.626620247	-1.930768869	3.812583325	0.443087426	2.842011149
13	Belly	BCORL1			-0.904148004	1.871438974		
13	Belly	SLC34A2	-2.599319661	0.566085291	-1.987945458	3.966716957	0.400282748	3.963834694
13	Belly	SLC34A2			-1.985847375	3.96095243		
13	Belly	PPFIBP1	-0.956160749	0.650906822	-0.534047982	1.44798633	0.460260628	1.219967843
13	Belly	PPFIBP1			0.011661628	0.991949357		
13	Belly	IRF2	-1.525857175	0.556740849	-2.512191674	5.704860758	0.393675229	5.470265492
13	Belly	IRF2			-2.38837423	5.235670226		
13	Belly	SLIT3	-1.941374982	0.568130579	-2.338716409	5.058523715	0.401728985	4.574721154
13	Belly	SLIT3			-2.032424829	4.090918593		
13	Belly	SNX1	2.369354999	0.599110996	-0.622926614	1.539996011	0.423635448	2.142729277
13	Belly	SNX1			-1.457049229	2.745462544		

13	Belly	IRF2BP2	-4.287792409	0.616471733	-4.255334756	19.09780274	0.435911343	21.98441681
13	Belly	IRF2BP2			-4.636394403	24.87103089		
13	Belly	C10ORF11	0.717084681	0.563495111	-1.515304467	2.858591495	0.398451214	3.179632977
13	Belly	C10ORF11			-1.807632907	3.50067446		
13	Belly	PLXNB1	0.469835078	0.555716036	-0.588704965	1.503896169	0.392950577	1.400933855
13	Belly	PLXNB1			-0.376258752	1.297971541		
13	Belly	VAMP2	-4.112929547	0.564201893	-1.850698373	3.606747365	0.398950984	4.150776859
13	Belly	VAMP2			-2.231065652	4.694806352		
13	Belly	SLC1A2	4.988719644	0.635414461	2.439825156	0.184305987	0.449305874	0.167322474
13	Belly	SLC1A2			2.733709161	0.15033896		
13	Tail	KITLG	-0.367420498	0.416662803	0	1	0.294625094	1
13	Tail	KITLG			0	1		
13	Tail	PLXNC1	1.161196407	0.583925261	0	1	0.412897512	1
13	Tail	PLXNC1			0	1		
13	Tail	TMEM50B	-2.026523891	0.586185251	0	1	0.414495566	1
13	Tail	TMEM50B			0	1		
13	Tail	SLC2A8	1.761877536	0.469466374	0	1	0.331962857	1
13	Tail	SLC2A8			0	1		
13	Tail	VAT1L	-1.522243249	0.567295424	0	1	0.401138441	1
13	Tail	VAT1L			0	1		
13	Tail	SLC16A9	-1.008488003	0.417947206	0	1	0.295533304	1
13	Tail	SLC16A9			0	1		
13	Tail	SLC30A1	-1.491528812	0.433963028	0	1	0.3068582	1
13	Tail	SLC30A1			0	1		
13	Tail	SLC7A5	0.947714504	0.452408297	0	1	0.319900974	1
13	Tail	SLC7A5			0	1		
13	Tail	SLC6A14	-1.685967828	0.462122372	0	1	0.326769863	1
13	Tail	SLC6A14			0	1		
13	Tail	SLC16A1	1.901756939	1.010755635	0	1	0.714712164	1
13	Tail	SLC16A1			0	1		
13	Tail	PMEL	-4.282162968	0.429617383	0	1	0.303785365	1
13	Tail	PMEL			0	1		

13	Tail	MIR29B2	2.900438961	0.428002037	0	1	0.302643143	1
13	Tail	MIR29B2			0	1		
13	Tail	TMEM139	1.345938381	0.420519691	0	1	0.297352325	1
13	Tail	TMEM139			0	1		
13	Tail	C19ORF44	1.501982388	0.445301897	0	1	0.314875991	1
13	Tail	C19ORF44			0	1		
13	Tail	SLC25A23	-0.358232799	0.533638041	0	1	0.377339078	1
13	Tail	SLC25A23			0	1		
13	Tail	BCORL1	1.693056759	0.600530156	0	1	0.424638946	1
13	Tail	BCORL1			0	1		
13	Tail	SLC34A2	-0.612423244	0.433446012	0	1	0.306492615	1
13	Tail	SLC34A2			0	1		
13	Tail	PPFIBP1	-0.694967571	0.418935558	0	1	0.296232174	1
13	Tail	PPFIBP1			0	1		
13	Tail	IRF2	0.924425777	0.417668995	0	1	0.295336579	1
13	Tail	IRF2			0	1		
13	Tail	SLIT3	0.244195637	0.540321295	0	1	0.382064852	1
13	Tail	SLIT3			0	1		
13	Tail	SNX1	3.40934292	0.551232412	0	1	0.389780176	1
13	Tail	SNX1			0	1		
13	Tail	IRF2BP2	0.15807217	0.416662841	0	1	0.29462512	1
13	Tail	IRF2BP2			0	1		
13	Tail	C10ORF11	2.378553368	0.52025891	0	1	0.367878603	1
13	Tail	C10ORF11			0	1		
13	Tail	PLXNB1	0.952316937	0.461326244	0	1	0.326206915	1
13	Tail	PLXNB1			0	1		
13	Tail	VAMP2	-2.072047535	0.446461095	0	1	0.315695668	1
13	Tail	VAMP2			0	1		
13	Tail	SLC1A2	2.401952485	0.66602799	0	1	0.470952908	1
	Tail	SLC1A2			0	1		

Monkey 16 Pigmentation Analysis

Monkey	Region	Target	Ave Delta Cт	SD of Delta Cт	Ddelta Cт	Fold Change	SE of Delta Cт	Ave Fold Change
16	Back	KITLG	1.745400273	0.256710469	2.220640328	0.214546113	0.181521713	0.190955346
16	Back	KITLG		0.250616721	2.578933862	0.16736458		
16	Back	PLXNC1	5.368378484	0.450072747	3.867464211	0.068513675	0.318249492	0.070249908
16	Back	PLXNC1		0.250616721	3.796137002	0.071986141		
16	Back	TMEM50B	-1.745672381	0.268838802	0.436418679	0.738966732	0.19009774	0.768897831
16	Back	TMEM50B		0.250616721	0.324041512	0.79882893		
16	Back	SLC2A8	3.983090245	1.047400846	1.283010629	0.410937066	0.740624241	0.560554141
16	Back	SLC2A8		0.250616721	0.493761208	0.710171215		
16	Back	VAT1L	3.37554438	0.617923367	5.669403242	0.01964896	0.436937803	0.027289914
16	Back	VAT1L		0.250616721	4.839353682	0.034930868		
16	Back	SLC16A9	3.983973348	0.477297127	5.231870797	0.026610311	0.337500035	0.02965456
16	Back	SLC16A9		0.250616721	4.934618142	0.032698808		
16	Back	SLC30A1	-1.746388591	0.31171943	-0.555225226	1.469398011	0.220418922	1.311907573
16	Back	SLC30A1		0.250616721	-0.207164619	1.154417135		
16	Back	SLC7A5	4.633786046	0.439736401	1.310934213	0.403059795	0.310940591	0.434992917
16	Back	SLC7A5		0.250616721	1.098734048	0.46692604		
16	Back	SLC6A14	-0.21692673	0.549084582	0.96466842	0.512396164	0.388261432	0.695276751
16	Back	SLC6A14		0.250616721	0.187448647	0.878157338		
16	Back	SLC16A1	3.693590962	0.257865885	2.644510415	0.159927461	0.182338716	0.222770534
16	Back	SLC16A1		0.250616721	1.807863381	0.285613607		
16	Back	PMEL	4.438584172	0.771816223	8.359577325	0.003044503	0.545756485	0.00459002
16	Back	PMEL		0.250616721	7.348594811	0.006135536		
16	Back	MIR29B2	2.261319005	0.475693507	-0.325616691	1.253200014	0.336366104	1.356810682
16	Back	MIR29B2		0.250616721	-0.546384666	1.460421351		
16	Back	TMEM139	0.983326756	0.33538532	-1.887914512	3.700998399	0.237153234	4.139756124
16	Back	TMEM139		0.250616721	-2.194879386	4.578513848		
16	Back	C19ORF44	-0.013772166	0.254289233	-1.3034533	2.468189731	0.179809641	2.468134259
16	Back	C19ORF44		0.250616721	-1.30338845	2.468078787		
16	Back	SLC25A23	-2.94262997	0.295393328	-3.153169486	8.8960783	0.208874625	9.709710059
16	Back	SLC25A23		0.250616721	-3.395521018	10.52334182		

16	Back	BCORL1	-0.096704639	0.380436508	-1.816411826	3.522041299	0.269009234	3.623007405
16	Back	BCORL1		0.250616721	-1.896842811	3.72397351		
16	Back	SLC34A2	-3.153777278	0.345749096	-3.137479636	8.799854295	0.24448153	7.568848341
16	Back	SLC34A2		0.250616721	-2.663991782	6.337842386		
16	Back	PPFIBP1	-1.254538692	0.667896208	0.366205361	0.775820412	0.472273938	1.955705074
16	Back	PPFIBP1		0.250616721	-1.648736808	3.135589736		
16	Back	IRF2	-1.534917033	0.266286511	-2.391940925	5.248630094	0.188292998	5.414583158
16	Back	IRF2		0.250616721	-2.480403754	5.580536222		
16	Back	SLIT3	-3.649051108	0.612469647	-4.235290381	18.83429833	0.433081441	28.75293271
16	Back	SLIT3		0.250616721	-5.273201323	38.6715671		
16	Back	SNX1	2.394018971	0.26005223	-1.280984733	2.430047868	0.183884695	1.798988501
16	Back	SNX1		0.250616721	-0.223952739	1.167929134		
16	Back	IRF2BP2	-5.553297198	0.373787508	-5.237237784	37.71947745	0.264307682	34.69096397
16	Back	IRF2BP2		0.250616721	-4.984701011	31.66245049		
16	Back	C10ORF11	-0.917239345	0.295479028	-3.49144921	11.24685098	0.208935225	8.474230882
16	Back	C10ORF11		0.250616721	-2.511369559	5.701610789		
16	Back	PLXNB1	-0.509626544	0.488130856	-2.213180396	4.636963582	0.345160639	5.636745512
16	Back	PLXNB1		0.250616721	-2.73042855	6.636527442		
16	Back	VAMP2	-4.141455806	0.327844181	-2.607164237	6.093048555	0.231820844	5.154988746
16	Back	VAMP2		0.250616721	-2.07619271	4.216928938		
16	Back	SLC1A2	4.203615987	0.542871861	1.308759835	0.40366773	0.383868374	0.405014067
16	Back	SLC1A2		0.250616721	1.29916826	0.406360405		
16	Belly	KITLG	2.718735492	0.575834668	3.042741874	0.121351019	0.407176598	0.099055476
16	Belly	KITLG		0.55365559	3.703502753	0.076759932		
16	Belly	PLXNC1	2.316715991	0.704319439	0.243616202	0.844625552	0.498029051	0.62304442
16	Belly	PLXNC1		0.55365559	1.316660026	0.401463289		
16	Belly	TMEM50B	-1.198769773	0.628487625	1.124837974	0.458553518	0.444407861	0.530848377
16	Belly	TMEM50B		0.55365559	0.729427436	0.603143237		
16	Belly	SLC2A8	3.220270572	0.575286896	-0.309419534	1.239209006	0.406789265	0.958625839
16	Belly	SLC2A8		0.55365559	0.560552024	0.678042672		
16	Belly	VAT1L	2.572193723	0.586127054	4.330631374	0.049699275	0.414454414	0.045879391
16	Belly	VAT1L		0.55365559	4.571424236	0.042059507		

16	Belly	SLC16A9	3.184057986	0.596813406	3.987161735	0.063058657	0.422010807	0.052441744
16	Belly	SLC16A9		0.55365559	4.579496482	0.041824831		
16	Belly	SLC30A1	-0.476308072	0.554648962	0.822465995	0.565474552	0.392196042	0.540603514
16	Belly	SLC30A1		0.55365559	0.955305198	0.515732477		
16	Belly	SLC7A5	4.346365725	0.61978494	0.964990714	0.512281709	0.438254134	0.529745209
16	Belly	SLC7A5		0.55365559	0.869836905	0.547208708		
16	Belly	SLC6A14	2.889656817	0.847544132	4.179552176	0.055186065	0.599304203	0.082543212
16	Belly	SLC6A14		0.55365559	3.185731986	0.10990036		
16	Belly	SLC16A1	4.051333224	0.553677691	2.962820151	0.128263257	0.39150925	0.172571095
16	Belly	SLC16A1		0.55365559	2.205038169	0.216878934		
16	Belly	PMEL	3.556326663	0.579814017	6.839378455	0.008732567	0.409990423	0.008000151
16	Belly	PMEL		0.55365559	7.104278663	0.007267734		
16	Belly	MIR29B2	4.368908679	0.663166563	1.237951377	0.423974271	0.468929573	0.328194498
16	Belly	MIR29B2		0.55365559	2.105226615	0.232414726		
16	Belly	TMEM139	3.115313327	0.559804709	0.027963736	0.980803657	0.395841706	0.940023816
16	Belly	TMEM139		0.55365559	0.153215506	0.899243975		
16	Belly	C19ORF44	-0.674857343	0.816817045	-1.50943937	2.846993837	0.577576871	4.098559665
16	Belly	C19ORF44		0.55365559	-2.419572732	5.350125494		
16	Belly	SLC25A23	-0.534851277	0.555220534	-0.605371377	1.521370332	0.392600204	1.853282451
16	Belly	SLC25A23		0.55365559	-1.127761743	2.185194569		
16	Belly	BCORL1	1.231177127	0.569794915	-0.786134622	1.724447995	0.402905849	1.465695055
16	Belly	BCORL1		0.55365559	-0.271356484	1.206942114		
16	Belly	SLC34A2	-2.440942014	0.555722422	-2.222360513	4.666563454	0.392955093	4.557718939
16	Belly	SLC34A2		0.55365559	-2.153440377	4.448874425		
16	Belly	PPFIBP1	1.554333484	0.574903961	2.846811393	0.139003066	0.40651849	0.247705145
16	Belly	PPFIBP1		0.55365559	1.488401511	0.356407225		
16	Belly	IRF2	-1.327573026	0.567826602	-2.33737745	5.0538311	0.401514041	4.700805961
16	Belly	IRF2		0.55365559	-2.120279214	4.347780822		
16	Belly	SLIT3	-3.571982587	0.594946552	-4.399394891	21.10327338	0.420690741	26.05984131
16	Belly	SLIT3		0.55365559	-4.954959771	31.01640925		
16	Belly	SNX1	2.65231589	0.8087187	-1.488599679	2.806164686	0.571850477	1.756572991
16	Belly	SNX1		0.55365559	0.500256045	0.706981297		

16	Belly	IRF2BP2	-4.388411725	0.5548623	-3.850393197	14.42393802	0.392346895	15.44700327
16	Belly	IRF2BP2		0.55365559	-4.041774652	16.47006852		
16	Belly	C10ORF11	1.092207705	0.565032707	-1.672452828	3.187560729	0.399538458	2.214266914
16	Belly	C10ORF11		0.55365559	-0.311471841	1.240973098		
16	Belly	PLXNB1	-0.178041661	0.561069489	-2.242072961	4.730763242	0.39673604	4.419282017
16	Belly	PLXNB1		0.55365559	-2.03836622	4.107800791		
16	Belly	VAMP2	-2.856435979	0.564738098	-1.251413247	2.380745238	0.399330139	2.099090295
16	Belly	VAMP2		0.55365559	-0.861904046	1.817435351		
16	Belly	SLC1A2	3.784640109	0.554803123	0.524049857	0.695416953	0.39230505	0.558526997
16	Belly	SLC1A2		0.55365559	1.245926482	0.421637041		
16	Tail	KITLG	-0.654386822	0.518707306	0	1	0.366781453	1
16	Tail	KITLG		0.416659517	0	1		
16	Tail	PLXNC1	1.536577877	0.527442574	0	1	0.372958221	1
16	Tail	PLXNC1		0.416659517	0	1		
16	Tail	TMEM50B	-2.125902477	0.417040774	0	1	0.294892359	1
16	Tail	TMEM50B		0.416659517	0	1		
16	Tail	SLC2A8	3.094704327	0.619828359	0	1	0.438284836	1
16	Tail	SLC2A8		0.416659517	0	1		
16	Tail	VAT1L	-1.878834082	0.417245983	0	1	0.295037464	1
16	Tail	VAT1L		0.416659517	0	1		
16	Tail	SLC16A9	-1.099271122	0.460464885	0	1	0.325597843	1
16	Tail	SLC16A9		0.416659517	0	1		
16	Tail	SLC30A1	-1.365193668	0.421065094	0	1	0.297737983	1
16	Tail	SLC30A1		0.416659517	0	1		
16	Tail	SLC7A5	3.428951916	0.467167163	0	1	0.330337069	1
16	Tail	SLC7A5		0.416659517	0	1		
16	Tail	SLC6A14	-0.792985264	0.421104487	0	1	0.297765839	1
16	Tail	SLC6A14		0.416659517	0	1		
16	Tail	SLC16A1	1.467404064	0.674866529	0	1	0.477202699	1
16	Tail	SLC16A1		0.416659517	0	1		
16	Tail	PMEL	-3.415501896	0.416933827	0	1	0.294816737	1
16	Tail	PMEL		0.416659517	0	1		

16	Tail	MIR29B2	2.697319683	0.484990347	0	1	0.342939963	1
16	Tail	MIR29B2		0.416659517	0	1		
16	Tail	TMEM139	3.024723705	0.416700176	0	1	0.29465152	1
16	Tail	TMEM139		0.416659517	0	1		
16	Tail	C19ORF44	1.289648708	0.418874061	0	1	0.296188689	1
16	Tail	C19ORF44		0.416659517	0	1		
16	Tail	SLC25A23	0.331715282	0.530104822	0	1	0.374840714	1
16	Tail	SLC25A23		0.416659517	0	1		
16	Tail	BCORL1	1.75992268	0.475611303	0	1	0.336307978	1
16	Tail	BCORL1		0.416659517	0	1		
16	Tail	SLC34A2	-0.253041569	0.427715106	0	1	0.302440252	1
16	Tail	SLC34A2		0.416659517	0	1		
16	Tail	PPFIBP1	-0.613272968	0.907047365	0	1	0.641379343	1
16	Tail	PPFIBP1		0.416659517	0	1		
16	Tail	IRF2	0.901255306	0.417562495	0	1	0.295261272	1
16	Tail	IRF2		0.416659517	0	1		
16	Tail	SLIT3	1.105194744	0.451944076	0	1	0.319572721	1
16	Tail	SLIT3		0.416659517	0	1		
16	Tail	SNX1	3.146487707	0.916977642	0	1	0.648401109	1
16	Tail	SNX1		0.416659517	0	1		
16	Tail	IRF2BP2	-0.442327801	0.428202438	0	1	0.302784848	1
16	Tail	IRF2BP2		0.416659517	0	1		
16	Tail	C10ORF11	2.08417004	0.946217887	0	1	0.669077084	1
16	Tail	C10ORF11		0.416659517	0	1		
16	Tail	PLXNB1	1.962177929	0.420033696	0	1	0.297008675	1
16	Tail	PLXNB1		0.416659517	0	1		
16	Tail	VAMP2	-1.799777332	0.447807815	0	1	0.316647943	1
16	Tail	VAMP2		0.416659517	0	1		
16	Tail	SLC1A2	2.899651939	0.63168039	0	1	0.446665488	1
16	Tail	SLC1A2		0.416659517	0	1		

APPENDIX E: HAIR STRUCTURE qRT-PCR PRIMER DESIGN

Hair Thickness Genes				
Gene Symbol	**Gene Name**	**Primers**	**bp Size**	**Probes**
CASP14	Caspase 14	AGAAGATGGGGAGATGGTCA CCTTTGTTCTCCTCGACAGG	121	GGAGAACCTCTTTGAGGCCCTG
CKAP4	Cytoskeleton Ass. Protein 4	AACAGAAGGTGCAGTCTTTGC CCCTTGCTTCACAGCTTTCT	104	GTCCATCTTGAGAAGCTCCCAGCA
CNN1	Calponon 1	GAGCTGAGAGAGTGGATC CTTATTGATGAATTCGCAAAG	103	CGGCCTCAAAGATGGCATTAT
KRT8	Keratin 8	ATCGACAAGGTGCGGTTC TGTTGTCCATGTTGCTCCG	100	GCAGCAGAACAAGATGCTGGAGAC
KRT32	Keratin 32	CAGCAGAAGATTCTGTGTACC TCGTACTTGGCCCTGAAG	98	ACTCCAGGATGGTCGTGAACATTG
KRT73	Keratin 73	GAGGTATGAAGAAGAAATAAACAAG AGCTCCACTTTGCTCATGTA	100	AAGGACGTGGATGCGGCAG
KRT78	Keratin 78	AGTCCAAGTACCAGGAGGAG CCATCTTGCTCAGGAAAACC	99	GTGGTCCTCAAGAAGGATGTGGAT
RAB29	RAB29, member RAS oncogene	GGATATTGCAGGGCAGGAG GGTAGTGGCATTGGTAACATCA	100	TTACCGTGATGCCTCTGCCTGTG
SERPINB7	Serpin Family B Member 7	TGAAACACATGGCAAAATCAAG TGCCACTTGCCTTTGAAGTA	102	GATTGGTGACGGGAGCATAAGC
SLC7A11	solute carrier fam 7 mem 11	TTGGTCCATTACCAGCTTTTGT AGTAGCTGCAGGGCGTATT	65	CGAGTCTGGGTGGAACTGCTCG
TCHH	Trichohyalin	GTACTTAAGAGACCACATGACC TCGACATGCCCGTTACAG	79	CTGATCCTGGAACTTTTGGATCGTG

APPENDIX F: SEQUENCES THE cDNA PRIMERS MAKE FOR STRUCTURE GENES

1. CASP14
    a. AGAAGATGGGGAGATGGTCAAGCTGGAGAACCTCTTTGAGGCCCTGAACAACAA GAACTGCCA GGCCCTGCGAGCCAAGCCCAAGGTGTACATCATACAGGCCTGTCGAGGAGA ACAAAGG
2. CKAP4
    a. AACAGAAGGTGCAGTCTTTGCAAGCCACATTTGGAACTTTTGAGTCCATCTTGAG AAGCTCCCA GCATAAACAAGACCTCACAGAGAAAGCTGTGAAGCAAGGG
3. CNN1
    a. GAGCTGAGAGAGTGGATCGAGGGGGTGACGGGCCGTCGCATCGGCAACAACTTC ATGGACGG CCTCAAAGATGGCATTATTCTTTGCGAATTCATCAATAAG
4. KRT8
    a. ATCGACAAGGTGCGGTTCCTGGAGCAGCAGAACAAGATGCTGGAGACCAAGTGG AGCCTCCTG CAGCAGCAGAAAACGGCTCGGAGCAACATGGACAACA
5. KRT32
    a. CAGCAGAAGATTCTGTGTACCAAGGCAGAGAACTCCAGGATGGTCGTGAACATT GATAACGCC AAGCTAGCTGCCGACGACTTCAGGGCCAAGTACGA
6. KRT73
    a. GAGGTATGAAGAAGAAATAAACAAGCGCACAACTGCTGAGAATGAATTTGTGGT GCTAAAAAA GGACGTGGATGCAGCATACATGAGCAAAGTGGAGCT
7. KRT78
    a. AGTCCAAGTACCAGGAGGAGGCCCACAGGCGCACCACACTTGAAAATGACTTTG TGGTCCTCA AGAAGGATGTGGATGGGGTTTTCCTGAGCAAGATGG
8. RAB29
    a. GGATATTGCAGGGCAGGAGCGTTTCACCTCCATGACACGACTGTATTACCGTGAT GCCTCTGCC TGTGTTATTATGTTTGATGTTACCAATGCCACTACC
9. SERPINB7
    a. TGAAACACATGGCAAAATCAAGAACATGATTGGTGACGGGAGCATAAGCTCATC TGCTGTAAT GGTGCTGGTGAACGCTGTGTACTTCAAAGGCAAGTGGCA
10. SLC7A11
    a. TTGGTCCATTACCAGCTTTTGTACGAGTCTGGGTGGAACTGCTCGTAATACGCCCTGCA GCTACT
11. TCHH
    a. GTACTTAAGAGACCACATGACCCCAAGACGGTAGATCTGATCCTGGAACTTTTGG ATCGTGACT GTAACGGGCATGTCGA

Purple is the Probe, Yellow are the Primers

APPENDIX G: STATISTICAL BREAKDOWN OF PIGMENTATION GENE EXPRESSION

Table G.1: Breakdown of Structure Gene Statistics of Significance Using Kruskal Wallis and Dunn's Pairwise with Bonferroni Correction.

Gene	Chi^2	KW P Value	Back/Belly		Back/Tail		Belly/Tail	
CASP14	15.963	0.0003417	0.1440	1.0000	-3.3858	0.0011	-3.5298	0.0006
CKAP4	0.50338	0.7775	-0.5042	0.9211	-0.6843	0.7406	-0.1800	1.000
CNN1	15.989	0.0003373	-0.2161	1.000	3.3497	0.0012	3.5659	0.0005
KRT8	1.5153	0.4688	-0.7203	0.7069	0.5042	0.9211	1.2246	0.3311
KRT32	16.819	0.0002227	0.9364	0.5235	-2.9895	0.0042	-3.9260	0.0001
KRT78	16.197	0.0003041	0.5042	0.9211	-3.2057	0.0020	-3.7099	0.0003
RAB29	2.7608	0.2515	-0.7203	0.7069	-1.6568	0.1463	-0.9364	0.5235
SERPINB7	4.7329	0.09382	-0.8644	0.5810	1.2966	0.2921	2.1611	0.0560
SLC7A11	16.025	0.0003313	0.2881	1.0000	-3.3137	0.0014	-3.6019	0.0005
TCHH	12.211	0.002231	1.8009	0.1076	-1.6929	0.1357	-3.4938	0.0007
			Z-Value	**P-Value**	**Z-Value**	**P-Value**	**Z-Value**	**P-Value**

Orange = NO statistical significance between all three regions

Green = Statistical significance in gene expression when comparing the hair regions

APPENDIX H: FULL qRT-PCR DATA FOR STUCTURE ANALYSIS

Monkey 11 Structure Analysis								
Monkey	Region	Target	Ave Delta C_T	SD of Delta C_T	Ddelta C_T	Fold Change	SE of Delta C_T	Aver Fold Change
11	Back	CASP14	0.612671509	0.7313675	1.782344	0.290710703	0.517154919	0.348323565
11	Back	CASP14			1.300674	0.405936427		
11	Back	CKAP4	-2.697974548	0.763459334	0.525828	0.694560175	0.539847272	0.638288038
11	Back	CKAP4			0.78087	0.582015901		
11	Back	CNN1	0.470944825	0.685324705	-2.82958	7.108670147	0.484597746	6.255327806
11	Back	CNN1			-2.43349	5.401985465		
11	Back	KRT8	1.458910599	0.816263563	1.266868	0.415561043	0.5771855	0.549679947
11	Back	KRT8			0.548356	0.68379885		
11	Back	KRT32	4.844145432	0.682233526	7.828828	0.004398332	0.482411953	0.003888275
11	Back	KRT32			8.209521	0.003378219		
11	Back	KRT78	6.529533718	0.818990144	1.407089	0.377071775	0.579113485	0.297772706
11	Back	KRT78			2.194469	0.218473636		
11	Back	RAB29	-0.967350349	0.735529046	1.47639	0.359386986	0.520097576	0.409227907
11	Back	RAB29			1.123218	0.459068827		
11	Back	SERPINB7	-1.02127777	0.701985034	0.062966	0.957293761	0.496378378	1.014230239
11	Back	SERPINB7			-0.099183	1.071166718		
11	Back	SLC7A11	1.218656191	0.67631255	0.794644	0.576485251	0.47822519	0.472266794
11	Back	SLC7A11			1.442033	0.368048337		
11	Back	TCHH	-1.584432945	0.676990209	-0.052205	1.036848453	0.478704367	1.079990095
11	Back	TCHH			-0.167527	1.123131737		
11	Belly	CASP14	0.602875506	0.56567046	2.039288	0.243283815	0.399989418	0.367493833
11	Belly	CASP14			1.024138	0.491703851		
11	Belly	CKAP4	-4.127530302	1.156091808	-1.368236	2.581547889	0.817480357	1.858858355
11	Belly	CKAP4			-0.184177	1.136168821		
11	Belly	CNN1	0.677732264	0.588094452	-2.40794	5.307158847	0.415845575	5.369713774

11 Belly	KRT78	7.429389082	0.600725384	2.792966	0.144289109	0.424776992	0.154140542
11 Belly	KRT78			2.608303	0.163991976		
11 Belly	RAB29	-2.59445783	1.132072787	-0.641519	1.559971169	0.800496345	1.284542193
11 Belly	RAB29			-0.013088	1.009113217		
11 Belly	SERPINB7	-2.37233373	0.625331428	-1.353275	2.554914688	0.442176093	2.583365516
11 Belly	SERPINB7			-1.385053	2.611816344		
11 Belly	SLC7A11	2.434322153	0.581260134	2.102152	0.232910559	0.411012982	0.200899523
11 Belly	SLC7A11			2.565857	0.168888487		
11 Belly	TCHH	1.871864115	0.607236005	3.607298	0.082053115	0.429380697	0.099927567
11 Belly	TCHH			3.085564	0.117802018		
11 Tail	CASP14	-0.928837588	1.130105838	0	1	0.799105501	1
11 Tail	CASP14			0	1		
11 Tail	CKAP4	-3.351323512	0.960265764	0	1	0.679010433	1
11 Tail	CKAP4			0	1		
11 Tail	CNN1	3.10247955	0.958188667	0	1	0.677541704	1
11 Tail	CNN1			0	1		
11 Tail	KRT8	0.551298711	0.945377311	0	1	0.668482708	1
11 Tail	KRT8			0	1		
11 Tail	KRT32	-3.175029185	0.959769812	0	1	0.678659742	1
11 Tail	KRT32			0	1		
11 Tail	KRT78	4.728754804	0.948693569	0	1	0.670827656	1
11 Tail	KRT78			0	1		
11 Tail	RAB29	-2.267154124	1.088093833	0	1	0.769398528	1
11 Tail	RAB29			0	1		
11 Tail	SERPINB7	-1.003169444	0.992427758	0	1	0.701752398	1
11 Tail	SERPINB7			0	1		
11 Tail	SLC7A11	0.100317571	1.064984177	0	1	0.753057533	1
11 Tail	SLC7A11			0	1		
11 Tail	TCHH	-1.474566844	0.952695757	0	1	0.67365763	1
11 Tail	TCHH			0	1		

Monkey 12 Structure Analysis								
Monkey	Region	Target	Ave Delta C_T	SD of Delta C_T	Ddelta C_T	Fold Change	SE of Delta C_T	Ave Fold Change
12	Back	CASP14	1.972687379	0.682631673	3.074325	0.118723329	0.482693485	0.111658983
12	Back	CASP14			3.257119	0.104594637		
12	Back	CKAP4	-1.674086913	0.676104714	0.891883	0.538910299	0.478078228	0.893140609
12	Back	CKAP4			-0.318891	1.247370919		
12	Back	CNN1	-1.403569564	0.675462422	-2.389134	5.238429551	0.477624059	5.479361974
12	Back	CNN1			-2.516089	5.720294397		
12	Back	KRT8	-0.760106429	0.801672157	-0.110471	1.07958043	0.566867819	1.464488973
12	Back	KRT8			-0.887055	1.849397515		
12	Back	KRT32	5.256897767	0.814467795	9.971741	0.000995879	0.575915701	0.00139859
12	Back	KRT32			9.116745	0.001801301		
12	Back	KRT78	7.932715073	1.415417491	4.537469	0.043061162	1.000851306	0.050259163
12	Back	KRT78			4.121369	0.057457164		
12	Back	RAB29	-2.384581909	0.676849308	-0.506431	1.420531265	0.478604736	1.069729124
12	Back	RAB29			0.476083	0.718926983		
12	Back	SERPINB7	-1.523669586	0.8272933	-0.468467	1.383638169	0.584984703	1.939386264
12	Back	SERPINB7			-1.319118	2.495134359		
12	Back	SLC7A11	3.885250703	0.760690804	4.713948	0.038103087	0.537889626	0.035950524
12	Back	SLC7A11			4.88692	0.03379796		
12	Back	TCHH	0.777200356	0.699055194	7.603297	0.005142561	0.494306668	0.005738973
12	Back	TCHH			7.302352	0.006335385		
12	Belly	CASP14	1.636354243	0.851891618	2.300804	0.202949921	0.60237834	0.150241206
12	Belly	CASP14			3.357973	0.097532491		
12	Belly	CKAP4	-0.876737798	0.688708688	1.572159	0.336304737	0.486990583	0.499052634
12	Belly	CKAP4			0.595532	0.661800532		
12	Belly	CNN1	-0.791077818	0.934111848	-2.239359	4.721871305	0.660516822	3.718369177
12	Belly	CNN1			-1.440882	2.714867048		
12	Belly	KRT8	0.057888781	0.855994101	1.384762	0.382952672	0.605279234	1.030217551
12	Belly	KRT8			-0.746298	1.67748243		
12	Belly	KRT32	7.427847007	0.729455793	12.01569	0.000241501	0.515803138	0.000303899
12	Belly	KRT32			11.4147	0.000366297		

12 Belly	KRT78	6.659494196	0.715695658	2.21728	0.215046475	0.506073253	0.141129712
12 Belly	KRT78			3.895117	0.067212949		
12 Belly	RAB29	-2.057631696	0.689081363	-0.051582	1.036400887	0.487254105	0.831337285
12 Belly	RAB29			0.675135	0.626273683		
12 Belly	SERPINB7	-1.004826749	0.955620657	0.190594	0.876244932	0.675725847	1.397714076
12 Belly	SERPINB7			-0.940492	1.919183221		
12 Belly	SLC7A11	5.88500384	0.979293962	6.459749	0.011361134	0.692465401	0.009224028
12 Belly	SLC7A11			7.140625	0.007086922		
12 Belly	TCHH	2.676694666	0.779691149	9.650749	0.001244042	0.551324899	0.001562779
12 Belly	TCHH			9.053889	0.001881516		
12 Tail	CASP14	-1.193034556	0.712958035	0	1	0.504137461	1
12 Tail	CASP14			0	1		
12 Tail	CKAP4	-1.960583117	1.06644598	0	1	0.754091184	1
12 Tail	CKAP4			0	1		
12 Tail	CNN1	1.049042317	0.680203057	0	1	0.480976194	1
12 Tail	CNN1			0	1		
12 Tail	KRT8	-0.261343387	1.191017945	0	1	0.842176866	1
12 Tail	KRT8			0	1		
12 Tail	KRT32	-4.287345317	0.691725834	0	1	0.489124028	1
12 Tail	KRT32			0	1		
12 Tail	KRT78	3.603295896	1.165336791	0	1	0.824017547	1
12 Tail	KRT78			0	1		
12 Tail	RAB29	-2.369408038	0.937712913	0	1	0.663063159	1
12 Tail	RAB29			0	1		
12 Tail	SERPINB7	-0.629877475	0.686644415	0	1	0.485530922	1
12 Tail	SERPINB7			0	1		
12 Tail	SLC7A11	-0.915183452	0.712740617	0	1	0.503983723	1
12 Tail	SLC7A11			0	1		
12 Tail	TCHH	-6.675624278	0.676182334	0	1	0.478133114	1
12 Tail	TCHH			0	1		

Monkey 13 Structure Analysis								
Monkey	Region	Target	Ave Delta C_T	SD of Delta C_T	Ddelta C_T	Fold Change	SE of Delta C_T	Ave Fold Change
13	Back	CASP14	1.73587288	0.720876003	3.29165	0.102120905	0.50973631	0.184859851
13	Back	CASP14			1.901856	0.267598797		
13	Back	CKAP4	-4.395426139	1.274311786	-2.340268	5.063967317	0.901074506	3.317451265
13	Back	CKAP4			-0.651624	1.570935214		
13	Back	CNN1	0.203352585	0.67820043	-0.299237	1.230493647	0.479560123	2.344874482
13	Back	CNN1			-1.790461	3.459255317		
13	Back	KRT8	1.282532349	0.696002619	-0.475785	1.390674691	0.492148172	1.200025764
13	Back	KRT8			-0.013465	1.009376837		
13	Back	KRT32	5.837239471	0.786414469	10.64659	0.000623819	0.556079004	0.000659532
13	Back	KRT32			10.49019	0.000695246		
13	Back	KRT78	7.247795218	0.821955816	2.328948	0.19902926	0.581210531	0.145748791
13	Back	KRT78			3.434897	0.092468322		
13	Back	RAB29	-0.470900878	0.708569418	1.608186	0.328010565	0.501034241	0.39031492
13	Back	RAB29			1.14363	0.452619276		
13	Back	SERPINB7	-1.621214256	1.549047267	-1.220884	2.330895186	1.095341827	1.347708357
13	Back	SERPINB7			1.455924	0.364521528		
13	Back	SLC7A11	1.968332902	0.710891286	4.521327	0.043545666	0.502676049	0.057564826
13	Back	SLC7A11			3.804219	0.071583987		
13	Back	TCHH	-4.857561454	0.680066141	1.733954	0.300626799	0.48087938	0.39877282
13	Back	TCHH			1.008918	0.496918841		
13	Belly	CASP14	1.427949702	0.558069811	3.141939	0.113287505	0.394614948	0.241474845
13	Belly	CASP14			1.435721	0.369662185		
13	Belly	CKAP4	-1.914516309	1.195299954	0.157048	0.896858233	0.845204703	0.590740232
13	Belly	CKAP4			1.81288	0.284622231		
13	Belly	CNN1	-2.012537206	0.559063716	-2.502485	5.666606784	0.395317745	5.904909448
13	Belly	CNN1			-4.018993	6.143212111		
13	Belly	KRT8	1.829099451	0.869662974	0.423981	0.745364945	0.614944586	0.814063581
13	Belly	KRT8			0.179903	0.882762218		
13	Belly	KRT32	6.058571152	0.57592588	10.48048	0.000699939	0.407241095	0.000577926
13	Belly	KRT32			11.09895	0.000455913		

13 Belly	KRT78	8.491246978	0.588539169	3.107489	0.116025288	0.416160038	0.072160633
13 Belly	KRT78			5.143259	0.028295977		
13 Belly	RAB29	-0.895360197	0.702716409	1.334854	0.396432101	0.496895538	0.535481647
13 Belly	RAB29			0.568043	0.674531192		
13 Belly	SERPINB7	-2.227865423	1.814354644	0.379117	0.768907873	1.282942472	1.665550952
13 Belly	SERPINB7			-1.35738	2.562194031		
13 Belly	SLC7A11	0.781347071	1.883934901	4.450009	0.045752406	1.332143144	0.199461103
13 Belly	SLC7A11			1.501566	0.3531698		
13 Belly	TCHH	-0.50352403	0.561033177	6.098868	0.014590088	0.396710364	0.019536512
13 Belly	TCHH			5.35208	0.024482937		
13 Tail	CASP14	-0.860880282	1.554281859	0	1	1.099043243	1
13 Tail	CASP14			0	1		
13 Tail	CKAP4	-2.89948025	0.950863324	0	1	0.672361904	1
13 Tail	CKAP4			0	1		
13 Tail	CNN1	1.24820194	1.461761798	0	1	1.03362168	1
13 Tail	CNN1			0	1		
13 Tail	KRT8	1.527157283	1.065969461	0	1	0.753754234	1
13 Tail	KRT8			0	1		
13 Tail	KRT32	-4.73114815	0.988272184	0	1	0.698813963	1
13 Tail	KRT32			0	1		
13 Tail	KRT78	4.365872953	1.566829346	0	1	1.107915656	1
13 Tail	KRT78			0	1		
13 Tail	RAB29	-1.846808818	0.950957944	0	1	0.672428811	1
13 Tail	RAB29			0	1		
13 Tail	SERPINB7	-1.738734228	1.067712257	0	1	0.754986577	1
13 Tail	SERPINB7			0	1		
13 Tail	SLC7A11	-2.194440272	0.986227614	0	1	0.697368234	1
13 Tail	SLC7A11			0	1		
13 Tail	TCHH	-6.228997615	1.114435691	0	1	0.788025034	1
13 Tail	TCHH			0	1		

Monkey 16 Structure Analysis

Monkey	Region	Target	Ave Delta C_T	SD of Delta C_T	Ddelta C_T	Fold Change	SE of Delta C_T	Ave Fold Change
16	Back	CASP14	2.571114197	0.854059663	3.219062	0.107390487	0.603911379	0.080658685
16	Back	CASP14			4.212852	0.053926882		
16	Back	CKAP4	-1.092080459	0.681961321	0.846799	0.556017063	0.482219474	0.476219753
16	Back	CKAP4			1.334889	0.396422443		
16	Back	CNN1	-0.004955634	1.328747624	-0.632694	1.550457534	0.939566455	3.145489259
16	Back	CNN1			-2.245046	4.740520984		
16	Back	KRT8	1.075543061	1.205480203	-1.102092	2.146657084	0.852403226	1.414135386
16	Back	KRT8			0.552974	0.681613687		
16	Back	KRT32	4.99875637	1.313719974	4.739738	0.037428002	0.928940302	0.030214842
16	Back	KRT32			5.442117	0.023001683		
16	Back	KRT78	7.221642849	0.801250493	2.732747	0.150439245	0.566569657	0.143910323
16	Back	KRT78			2.863741	0.1373814		
16	Back	RAB29	-1.29590641	0.686764558	0.420749	0.747036815	0.485615876	0.919124515
16	Back	RAB29			-0.125932	1.091212214		
16	Back	SERPINB7	-1.680687632	0.77327594	-0.481051	1.395760525	0.546788661	2.127020941
16	Back	SERPINB7			-1.515148	2.858281356		
16	Back	SLC7A11	4.302803651	0.676933556	2.205293	0.216840667	0.478664308	0.367584816
16	Back	SLC7A11			0.94806	0.518328966		
16	Back	TCHH	-1.338709147	0.702704599	0.358016	0.780236797	0.496887187	0.597071229
16	Back	TCHH			1.272626	0.413905662		
16	Belly	CASP14	3.391372477	0.609109793	4.235211	0.053097561	0.430705665	0.044040071
16	Belly	CASP14			4.837219	0.034982582		
16	Belly	CKAP4	-3.664897169	0.681605732	-1.381857	2.606035502	0.481968035	2.800032349
16	Belly	CKAP4			-1.582088	2.994029196		
16	Belly	CNN1	-1.54851991	0.557556136	-2.995983	3.988877845	0.394251724	3.951766522
16	Belly	CNN1			-2.968885	3.914655199		
16	Belly	KRT8	-0.876841749	0.590916407	-2.487238	5.607033735	0.417840999	4.757813995
16	Belly	KRT8			-1.96665	3.908594255		
16	Belly	KRT32	7.081384457	0.557523309	7.628824	0.005052368	0.394228513	0.007274769
16	Belly	KRT32			6.718287	0.009497169		

16 Belly	KRT78	7.963741099	1.260875147	3.969759	0.063823911	0.891573367	0.089786556
16 Belly	KRT78			3.110926	0.115749201		
16 Belly	RAB29	-0.657177175	0.749643869	0.792965	0.577156664	0.530078263	0.579900945
16 Belly	RAB29			0.77931	0.582645225		
16 Belly	SERPINB7	-2.492082525	0.809208432	-1.97354	3.927305638	0.57219677	3.527879155
16 Belly	SERPINB7			-1.645449	3.128452671		
16 Belly	SLC7A11	4.138333588	0.792002397	1.675127	0.313138497	0.560030265	0.381993481
16 Belly	SLC7A11			1.149285	0.450848465		
16 Belly	TCHH	-0.863105978	0.568360382	0.617752	0.651685475	0.40189148	0.453992592
16 Belly	TCHH			1.964096	0.25629971		
16 Tail	CASP14	-1.144842532	0.961074257	0	1	0.679582124	1
16 Tail	CASP14			0	1		
16 Tail	CKAP4	-2.182924655	0.976808885	0	1	0.690708187	1
16 Tail	CKAP4			0	1		
16 Tail	CNN1	1.433914182	0.944080517	0	1	0.667565736	1
16 Tail	CNN1			0	1		
16 Tail	KRT8	1.35010204	0.959576049	0	1	0.678522732	1
16 Tail	KRT8			0	1		
16 Tail	KRT32	-0.0921711	1.13505926	0	1	0.8026081	1
16 Tail	KRT32			0	1		
16 Tail	KRT78	4.423398587	1.079604643	0	1	0.763395764	1
16 Tail	KRT78			0	1		
16 Tail	RAB29	-1.443314937	1.073483044	0	1	0.75906714	1
16 Tail	RAB29			0	1		
16 Tail	SERPINB7	-0.682587947	1.008493894	0	1	0.713112872	1
16 Tail	SERPINB7			0	1		
16 Tail	SLC7A11	2.72612724	1.328381091	0	1	0.939307278	1
16 Tail	SLC7A11			0	1		
16 Tail	TCHH	-2.15403023	1.264141174	0	1	0.893882797	1
16 Tail	TCHH			0	1		

APPENDIX I: ALL OBSERVATIONS ON HUMAN TEST SET FOR MICROSCOPY TO PHOTO-ANALYSIS

ICY Photo-Analysis, Microscopic Width, CD Meter, and Curl Index Measurements for Training Set

ID #	Sex	Hair Color	ICY Dia 1	ICY Dia 2	ICY Dia 3	ICY Dia 4	ICY Dia 5	ICE AVE	ICY St Dev	Diam (µm)	Hair Morph	CD Meter	Curl Index
401940	M	Blond	72.166	78.873	84.464	86.137	74.788	79.2856	6.01757545	80	Wavy	3	0.6667
106858	F	Blond	79.011	90.898	79.011	67.751	86.764	80.687	8.862173802	80	Curly	4	0.5000
78544	F	Blond	65.234	61.127	88.295	81.503	74.387	74.1092	11.21705247	70	Wavy	3	0.6250
827773	F	Blond	67.029	65.982	80.889	82.626	74.941	74.2934	7.668187941	80	Wavy	3	0.6453
938009	F	Blond	78.155	82.826	76.384	79.299	74.927	78.3182	3.022839344	87.5	Straight	1	0.9167
335400	F	Blond	53.168	59.814	56.393	85.11	79.752	66.8474	14.54252763	57.5	Wavy	3	0.6667
294611	F	Blond	100.098	76.742	80.857	103.179	84.084	88.992	11.88426895	87.5	Straight	2	0.8750
533375	F	Blond	76.351	92.64	79.644	78.7	83.986	82.2642	6.425665818	85	Straight	2	0.9167
							ICY.M.MEAN	78.099625	MIC.M.MEAN	78.4375			

ID #	Sex	Hair Color	ICY Dia 1	ICY Dia 2	ICY Dia 3	ICY Dia 4	ICY Dia 5	ICE AVE	ICY St Dev	Micro Diam (µm)	Hair Morph	CD Meter	Curl Index
631155	F	Dark Brown	68.868	67.002	66.697	60.069	68.63	66.2532	3.587769042	70	Curly	5	0.2333
403439	M	Dark Brown	83.365	71.224	83.82	77.04	96.3	82.3498	9.35117106	87.5	Straight	1	0.8500
786718	F	Dark Brown	99.744	89.856	92.743	95.987	92.743	94.2146	3.776382965	90	Curly	4	0.5000
429616	F	Dark Brown	53.868	78.964	76.181	60.226	54.129	64.6736	12.08683698	57.5	Curly	6	0.5000
284504	M	Dark Brown	73.832	83.189	92.29	73.832	92.29	83.0866	9.229177526	100	Straight	2	0.4333
181194	M	Dark Brown	65.04	69.462	82.087	73.929	68.406	71.7848	6.577175207	70	Curly	4	0.4167
420039	M	Dark Brown	60.618	63.876	58.848	68.696	77.031	65.8138	7.304218452	62.5	Straight	1	0.9714
744075	M	Dark Brown	55.988	86.068	78.208	61.828	65.579	69.5342	12.32000415	67.5	Curly	5	0.2500
496592	F	Dark Brown	95.883	71.343	80.162	79.764	80.162	81.4628	8.896946145	85	Straight	1	0.9467
264330	F	Dark Brown	74.863	55.607	57.529	69.509	87.923	69.0862	13.26303997	70	Curly	4	0.5556
377905	F	Dark Brown	72.362	85.279	73.36	76.752	72.362	76.023	5.479561753	75	Wavy	3	0.7456
418539	M	Dark Brown	52.749	52.749	66.722	94.36	58.486	65.0132	17.37512742	65	Curly	4	0.3333
596623	F	Dark Brown	101.258	101.258	75.474	80.074	101.258	91.8644	12.96512541	87.5	Curly	4	0.3750
756319	F	Dark Brown	67.424	71.906	69.499	69.499	72.745	70.2146	2.125757112	70	Wavy	3	0.7500
812834	F	Dark Brown	72.183	85.195	77.172	75.78	73.205	76.707	5.144226813	75	Wavy	3	0.6333
988246	F	Dark Brown	85.25	95.313	77.904	95.313	83.399	87.4358	7.681621684	75	Straight	1	0.9583
							ICY.M.MEAN	75.96985	MIC.M.MEAN	75.46875			

ICY Photo-Analysis, Microscopic Width, CD Meter, & Curl Index Measurements for Training Set Con

ID #	Sex	Hair Color	ICY Dia 1	ICY Dia 2	ICY Dia 3	ICY Dia 4	ICY Dia 5	ICE AVE	ICY St Dev	Micro Diam (µm)	Hair Morph	CD Meter	Curl Index
511095	F	Light Brown	71.583	82.604	97.014	110.613	93.305	91.0238	14.77887735	95	Wavy	3	0.5833
415441	M	Light Brown	73.609	75.289	75.289	81.278	75.289	76.1508	2.957068853	75	Wavy	4	0.3750
566198	M	Light Brown	81.762	66.627	87.999	68.991	80.575	77.1908	9.055336228	82.5	Straight	1	0.8583
544400	F	Light Brown	61.973	52.553	60.998	70.616	64.698	62.1676	6.550281544	60	Wavy	3	0.5833
394162	F	Light Brown	79.235	75.932	74.417	80.039	71.788	76.2822	3.414382038	70	Curly	4	0.5500
7315	M	Light Brown	43.256	30.586	68.393	44.587	61.173	49.599	15.1163808	42.5	Straight	2	0.8571
44413	F	Light Brown	57.429	57.772	68.488	83.868	92.875	72.0864	15.84031165	102.5	Straight	2	0.9583
127882	F	Light Brown	71.918	88.441	62.155	78.134	73.413	74.8122	9.582763312	50	Straight	2	0.8333
143546	F	Light Brown	62.027	81.244	93.04	63.274	58.844	71.6858	14.80138227	75	Curly	5	0.2500
206103	F	Light Brown	63.296	76.072	53.406	60.256	63.296	63.2652	8.220023309	57.5	Straight	1	0.9167
588693	F	Light Brown	56.06	50.648	44.848	46.228	61.638	51.8844	6.992903889	45	Curly	4	0.4167
705470	F	Light Brown	88.378	93.159	80.167	91.891	91.891	89.0972	5.300343781	80	Straight	1	0.9500
							ICY.M.MEAN	71.27045	MIC.M.MEAN	69.58333333			

ID #	Sex	Hair Color	ICY Dia 1	ICY Dia 2	ICY Dia 3	ICY Dia 4	ICY Dia 5	ICE AVE	ICY St Dev	Micro Diam (µm)	Hair Morph	CD Meter	Curl Index
846556	M	Red/Auburn	60.46	68.935	62.32	58.148	70.536	64.0798	5.400036685	62.5	Wavy	3	0.5417
894623	F	Red/Auburn	56.705	68.783	69.319	64.164	65.871	64.9684	5.079970945	52	Wavy	3	0.6833
							ICY.M.MEAN	64.5241	MIC.M.MEAN	57.25			

ID #	Sex	Hair Color	ICY Dia 1	ICY Dia 2	ICY Dia 3	ICY Dia 4	ICY Dia 5	ICE AVE	ICY St Dev	Micro Diam (µm)	Hair Morph	CD Meter	Curl Index
601895	F	Black	60.462	62.1564	59.1365	68.1548	59.5461	61.89116	3.688952925	60	Very Curly	8	0.0417
769934	M	Black	60.202	67.229	61.602	71.605	65.443	65.2162	4.558623992	65	Straight	1	0.9538
							ICY.M.MEAN	63.55368	MIC.M.MEAN	62.5			

APPENDIX J: MICROSCOPIC PHOTOS FOR EACH INDIVIDUAL IN TEST SET

Black Hair Samples from Test Set


601895


769934

Blond Hair Samples from Test Set

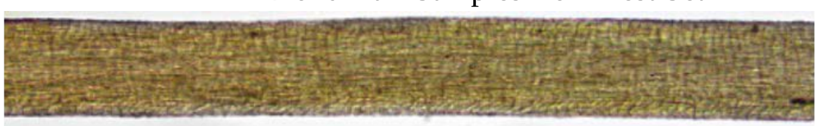
78544


106858


335400


401940


827773

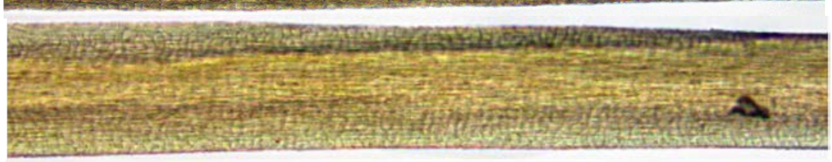
938009


533375


294611

Red Hair Samples from Test Set

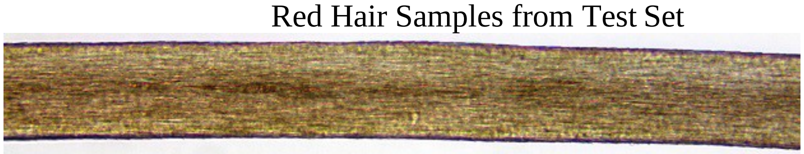
846556


894623

Light Brown Samples from Test Set

7351
394162
415441
511095
544400
566198
44413
127882
206103
496592
705470

Dark Brown Samples from Test Set

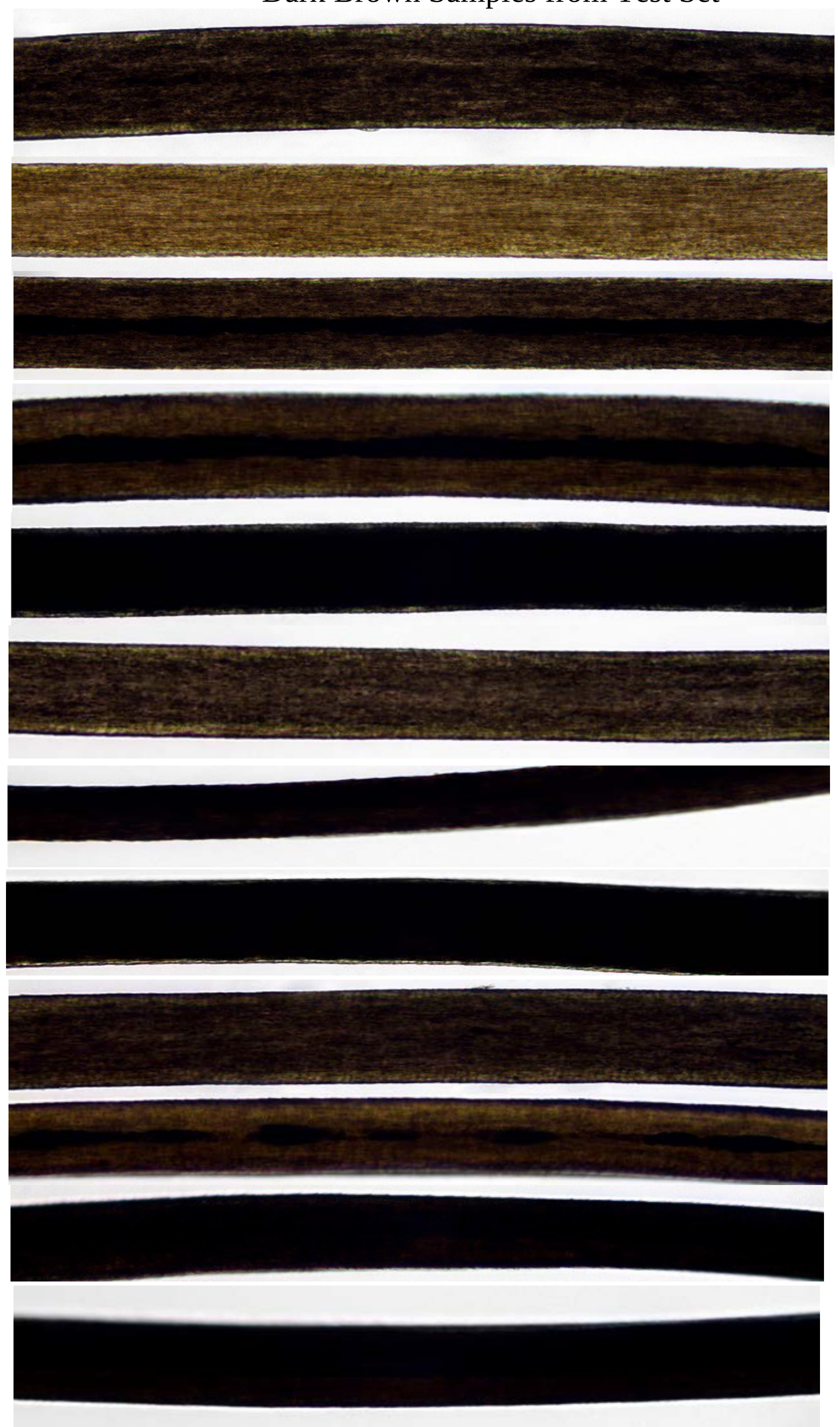

181194

264330

284504

297151

403439

420039

429626

631155

697875

744075

786718

418539

Dark Brown Samples from Test Set Continued

377905

496592

596623

756319

812834

988246